UNIVERSITÉ DU QUÉBEC À MONTRÉAL

RÉPONSE DES COMMUNAUTÉS MICROBIENNES D'EAU DOUCE FACE À UNE EXPOSITION AU CHLORURE DE SODIUM

MÉMOIRE

PRÉSENTÉ

COMME EXIGENCE PARTIELLE

À LA MAÎTRISE EN BIOLOGIE

PAR

JEAN-CHRISTOPHE GAGNON

MAI 2023

REMERCIEMENTS

Merci au laboratoire Lazar ayant constitué un pilier de mon développement scientifique et personnel au cours de ce projet. Merci à Julia Meyer, Benjamin Groult, Karine Villeneuve, Valérie Turcotte, Divya Patel, Alison Derry, Louis Astorg et Cassandre Lazar, ainsi que tous ceux que j'ai eu la chance de côtoyer au cours de ce projet. Merci également à l'ensemble des organismes et personnes ayant contribué au développement du projet, incluant l'Université de Montréal pour son accès à la station biologique des Laurentides, et le Groupe de recherche interuniversitaire en limnologie (GRIL) pour son soutien général.

DÉDICACE

Ce mémoire est dédié aux gens ayant offert leur support personnel durant cette maîtrise, notamment ma famille, Isabelle Gagnon, Jean-Charles Gagnon, Martine Tremblay et Sylvie Chiasson, mes amis, dont Isabelle Durivage, Francis Fillion, Lauri-anne Bonneau, Kris Chamie, Patrick Marois et mon chien Scotch. Merci encore à Cassandre Lazar de m'avoir pris sous son aîle.

Et un merci particulier à Lauren Aghabozorgi, sans qui je n'aurais jamais entrepris d'études supérieures.

TABLE DES MATIÈRES

REMERCIEMENTS ii

DÉDICACE iii

LISTE DES FIGURES vii

LISTE DES TABLEAUX xi

LISTE DES ABRÉVIATIONS, DES SIGLES ET DES ACRONYMES xiii

LISTE DES SYMBOLES ET DES UNITÉS xv

RÉSUMÉ xvi

ABSTRACT xvii

CHAPITRE 1 CHLORURE DE SODIUM, SEL DE VOIRIES ET PROCARYOTES 1

1.1 Chlorure de sodium 2

1.2 Sels de voiries et syndrome de salinisation des eaux douces 5

1.3 Les procaryotes et la salinité 7

1.4 Adaptations et acclimatations procaryotes. 9

1.5 Hypothèses de travail 11

1.5.1 Mise en contexte du projet et objectifs 11

1.5.2 Questions et hypothèses 11

CHAPITRE 2 RESPONSE OF PROKARYOTIC COMMUNITIES TO FRESHWATER SALINIZATION – A MESOCOSM EXPERIMENT 13

2.1 Introduction 13

2.2 Methods 15

2.2.1 Experimental setup 15

2.2.2 Sampling and physicochemical measurements 15

2.2.3 Filtration, DNA extraction and dPCR 16

2.2.4 Sequencing and sequence processing 17

2.2.5 Statistical analyses 17

2.3 Results 19
2.3.1 Archaeal absolute abundance and 16S rRNA gene diversity 20
2.3.2 Bacterial absolute abundance, alpha diversity indices, and 16S rRNA gene diversity 21
2.3.3 Correlation between bacterial taxa relative abundances and chloride levels 22
2.3.4 Correlation between bacterial beta diversity and abiotic factors 22
2.3.5 Microbial source tracking 24
2.3.6 Significantly different OTUs between bacterial sample groups 24
2.4 Discussion 25
2.4.1 Direct and indirect effect of salinity on prokaryotic communities 25
2.4.2 Influence of salinity on bacterial community transition 29
2.4.3 Microbial source tracking and overall procaryotic transitional community trends 29
2.5 Conclusions 31
2.6 Figures 33
2.7 Supplementary material 37
2.7.1 Supplementary figures 37
2.7.2 Supplementary tables 44
CHAPITRE 3 RESPONSE OF HYPOLIMNETIC MICROBIAL COMMUNITIES TO FRESHWATER SALINIZATION – A MICROCOSM EXPERIMENT 51
3.1 Introduction 51
3.2 Material et methods 53
3.2.1 Experimental setup 53
3.2.2 DNA extraction 54
3.2.3 16S and 18S rRNA gene sequencing and dPCR 54
3.2.4 Bioinformatic and statistical analyses 55
3.3 Results 57
3.3.1 Absolute abundance and correlation with salinity concentrations 57
3.3.2 Alpha diversity indices and correlation with salinity concentrations 57
3.3.3 β-diversity and correlation with environmental variables 58
3.3.3.1 Archaea 58
3.3.3.2 Bacteria 59
3.3.4 Microbial community structures (ß-diversity) 60
3.3.5 Correlations between the most abundant taxa and NaCl concentrations 60
3.3.6 Differential significance of microbial taxa 61
3.4 Discussion 62

3.4.1 Aquatic procaryotic abundance and diversity 63
3.4.2 Sediment procaryotic abundance and α-diversity 65
3.4.3 Salinity threshold for microbial community transition 67
3.4.4 Contributors to the transition 69
3.5 Conclusion 70
3.6 Figures and tables 72
3.7 Supplementary figures and tables 77
CHAPITRE 4 DISCUSSION 95
4.1 Sensibilité des différents domaines et relation avec les régulations en place 95
4.2 Alternatives au chlorure de sodium comme sel de voiries 98
4.2.1 Chlorure de calcium, magnésium et CMA 98
4.2.2 Sous-produits agriculturels 99
4.2.3 Abrasifs 100
CONCLUSION 102
ANNEXE A 106
RÉFÉRENCES 113

LISTE DES FIGURES

Figure 2.6.1. **(a)** Regression of bacterial absolute abundance and Cl^- in mesocosms at T3 and T6. (**b)** Regression of bacterial diversity (Shannon's H) and Cl^- in mesocosms after three (T3) and six weeks (T6) exposition. 33
Figure 2.6.2. **(a)** Correlation between bacterial mesocosm community composition and explanatory factors, using db-RDA. T3, 3 weeks exposure to the salinity gradient; T6, 6 weeks exposure; TP, total phosphorus; Sal, salinity; Temp, temperature; DO, dissolved oxygen; Abarc, absolute abundance of Archaea; Abbac, absolute abundance of Bacteria; Abeuk, absolute abundance of eukaryotes; EukA1, eukaryotic community composition represented by the first axis of a PCoA; EukA2, eukaryotic community composition represented by the second axis of a PCoA. **(b)** Variance partitioning analysis separating variation in bacterial mesocosm community composition between 3 explanatory variables: salinity (Sal), eukaryotic community composition represented by the first axis of a PCoA (EukA1), and absolute abundance of Eukaryotes (Abeuk). Values represent the portion of variation explained by the explanatory variables. 34
Figure 2.6.3. Linkage tree analysis showing clustering of bacterial mesocosm samples constrained by significant explanatory variables: TP, total phosphorus; Sal, salinity; Temp, temperature; Abeuk, absolute abundance of eukaryotes; EukA1, eukaryotic community composition represented by the first axis of a PCoA. For each cluster, R is the optimal ANOSIM R value (relative subgroup separation). The B% axis shows the absolute group separation which is scaled to maximum for first division. 35
Figure 2.6.4. Bacterial source tracking of bacterial samples from week 6, carried out using FEAST. The source samples are the initial freshwater lake sample used to set up the mesocosms (T0), and the samples for each bag at week 3 (T3). 36
Figure 3.6.1. Distance-based redundancy analysis (db-RDA) used to correlate archaeal communities from water and sediment samples with explanatory factors. OTUs are represented as red points. T3, samples taken after a thre-weeks incubation; T6, samples taken after a six-week incubation; Sed, sedimentary samples; Wat, Water samples Bac1, bacterial community composition represented by the first axis of a PCoA (see Table S3 for PCoA axes values); Bac2, bacterial community composition represented by the second axis of a PCoA; Euka1, eukaryotic community composition represented by the first axis of a PCoA; EukA2, eukaryotic community composition represented by the second axis of a PCoA; Diveuc, eukaryotic diversity. 73
Figure 3.6.2. Distance-based redundancy analysis (db-RDA) used to correlate bacterial communities from water and sediment samples with explanatory factors. OTUs are represented as red points. T3, samples taken after a three-weeks incubation in microcosms; T6, samples taken after a six-week incubation; Sed, sedimentary samples; Wat, water samples; arc1, archaeal community

composition represented by the first axis of a PCoA (see Table S3 for PCoA axes values); Arc2, archaeal community composition represented by the second axis of a PCoA; Euka1, eukaryotic community composition represented by the first axis of a PCoA; EukA2, eukaryotic community composition represented by the second axis of a PCoA; Diveuc, eukaryotic diversity. 74
Figure 3.6.3. Principal coordinate analysis based on dissimilarity matrices (Bray-Curtis) for the microcosm's communities. **(a)** Archaeal communities. **(b)** Bacterial communities. **(c)** Eukaryotic communities. For each PCoA, the two first axes of variance are shown. The different type of medium and sampling times are shown within the "Time" section. Treatments are shown under "Treat". The different microcosms treatment represents salinities as follow: S0 (0.01 ppt or 10 mg/L^{-1}), S5 (0.16 ppt or 160 mg/L^{-1}), S11 (0.93 ppt or 930 mg/L^{-1}), S15 (1.93 ppt or 1930 mg/L^{-1}) and S20 (3.22 ppt or 3220 mg/L^{-1}). Clusters created for further analysis are shown (circles) and identified. 76

Supplementary figure 2.7.S1. **(a)** Location of the Laurentians Biological Station, Quebec, Canada, site of the mesocosm installations. **(b)** Salinity levels in the mesocosms. 37
Supplementary figure 2.7.S2. **(a)** Regression of archaeal absolute abundance and Cl- in mesocosms at T3 and T6 **(b)** Regression of archaeal diversity indices (Shannon's H) and Cl- in mesocosms at T3 and T6. 38
Supplementary figure 2.7.S3. **(a)** Regression of archaeal absolute abundance and eukaryotic diversity (Shannon's H) in mesocosms at T3 and T6. **(b)** Regression of archaeal diversity (Shannon's H) and eukaryotic diversity (Shannon's H) in mesocosms at T3 and T6. 39
Supplementary figure 2.7.S4. Taxonomical classification of the archaeal 16S rRNA genes based on the SILVA database v.138. **(a)** Genus-level identification and ; **(b)** Phylum-level identification. 40
Supplementary figure 2.7.S5. **(a)** Regression of bacterial absolute abundance and eukaryotic diversity (Shannon's H) in mesocosms after three (T3) and six (T6) week incubation. **(b)** Regression of bacterial diversity (Shannon's H) and eukaryotic diversity (Shannon's H) in mesocosms after three (T3) and six weeks (T6) exposition. 41
Supplementary figure 2.7.S6. Composition of bacterial communities representing a total of more than 2% at the level of **(a)** Classes and ; **(b)** Orders. 42
Supplementary figure 2.7.S7. Heatmap of correlations (Spearman) between Cl- values and the most abundant **(a)** classes and ; **(b)** order, representing the 500 most abundant taxa, in the mesocosms after three (T3) weeks incubation. None of the classes present showed significance after six (T6) weeks incubation, and were therefore not shown in the figure. 43
Supplementary figure 2.7.S8. Principal coordinate analysis based on a distance matrix between bacterial mesocosm communities. Variance explained by each axis is

shown with the axis label. T3, 3 weeks exposure to the salinity gradient; T6, 6 weeks exposure. 44
Supplementary figure 3.7.S1. **(a)** Planktonic and **(b)** sedimentary archaeal absolute abundance regression analysis, with salinity as the independent variable. Values are shown through the gradient after a three- (T3) and six-week (T6) incubation. All abundance values were obtained by digital polymerase chain reactions (dPCR). R2 and *p*-values are displayed. 77
Supplementary figure 3.7.S2. **(a)** Planktonic and **(b)** sedimentary bacterial absolute abundance regression analysis, with salinity as the independent variable. Values are shown through the gradient after a three- and six-week incubation in microcosms. All abundance values were obtained by digital polymerase chain reactions (dPCR). R2 and *p*-values are displayed. 78
Supplementary figure 3.7.S3. **(a)** Regression for archaeal α diversity (Shannon's H) in water samples and salinity after a three- and six-week incubation in microcosms. **(b)** Regression for archaeal α diversity in sediment samples and salinity after a three- and six-week incubation in microcosms. All Shannon index values were calculated from raw OTU tables. R2 and *p*-values for both sampling times are shown. 79
Supplementary figure 3.7.S4. **(a)** Regression for bacterial α diversity (Shannon's H) in water samples, with salinity as the independent variable after a three- and six-week incubation in microcosms. **(b)** Regression for bacterial α diversity in sediment samples and salinity after a three- and six-week incubation in microcosms. Shannon indexes were obtained from raw OTU tables. R2 and *p*-values for both sampling times are shown. 80
Supplementary figure 3.7.S5. **(a)** Variance partitioning analysis explaining variation in archaeal communities for three explanatory factors, separately and together: salinity, bacterial abundance and the bacterial community composition's first PCoA axis (Bac1). Residual variance is shown (bottom right). **(b)** Variance partitioning analysis explaining variation in bacterial communities for three explanatory factors, separately and together: salinity, archaeal community composition's first PCoA axis (Arc1) and eukaryotic diversity. Residual variance is shown (bottom right). 81
Supplementary figure 3.7.S6. Linkage tree (LINKTREE) analysis showing the clustering of archaeal samples constrained by explanatory factors. R represents the optimal ANOSIM R value. B% represents the absolute difference (Bray-Curtis). Abbac, bacterial abundance; Divbac, bacterial diversity; Bac1, bacterial community composition represented by the first axis of a PCoA; Sal, salinity; T0, initial sampling; T3, sampling after three weeks; T6, sampling after six weeks. 82
Supplementary figure 3.7.S7. Linkage tree (LINKTREE) analysis showing the clustering of bacterial microcosm samples constrained by explanatory factors. R represents the optimal ANOSIM R value. B% represents the absolute difference (Bray-Curtis). Sal, salinity; Diveuc, eukaryotic diversity; Euka2, eukaryotic

community composition represented by the second axis of a PCoA; arc1, archaeal community composition represented by the first axis of a PCoA; Divarc, archaeal diversity; Divbac, bacterial diversity; T0, initial sampling; T3, sampling after three weeks; T6, sampling after six weeks. 83
Supplementary figure 3.7.S8. Spearman correlations between the 500 most abundant archaeal taxa present in the microcosm samples and the salinity values. Time and sampling media is shown at the base of the column. The correlation coefficients are shown on the color scale, with a positive relation being in shown in red, while negative relations are shown in blue. Absence of the taxa or absence of relation (Spearman ρ ≈ 0) is shown in white. The level of significance is shown by asterisks (0.001 ="***", 0.01="**", 0.05="*"). **(a)** Correlations of the 500 most abundant archaeal taxa, presented at the class taxonomic rank. **(b)** Correlations of the 500 most abundant archaeal taxa, presented at the order taxonomic rank. 84
Supplementary figure 3.7.S9. Spearman correlations between the 500 most abundant bacterial taxa present in the microcosm samples and the salinity values. Time and sampling media is shown at the base of the column. The correlation coefficient is shown on the color scale, with a positive relation being in shown in red, while negative relations are shown in blue. Absence of the taxa or absence of relation (Spearman ρ ≈ 0) is shown in white. The level of significance are shown by asterisks (0.001 ="***", 0.01="**", 0.05="*"). **(a)** Correlations of the 500 most abundant bacterial taxa, presented at the class taxonomic rank. **(b)** Correlations of the 500 most abundant bacterial taxa, presented at the order rank. 85
Supplementary figure 3.7.S10. **(a)** Regression for eukaryotic α diversity (Shannon's H) in water samples, with salinity as the independent variable after a three- and six-week incubation in microcosms. **(b)** Regression for eukaryotic α diversity in sediment samples and salinity after a three-and six-week incubation in microcosms. Shannon indexes were obtained from raw OTU tables. R2 and *p*-values for both sampling times are shown. 86

LISTE DES TABLEAUX

Table 3.6.1. Values associated with regression between salinity and archaeal and bacterial absolute abundance in water and sediment samples. Sampling times, R^2 and *p* values are shown. Visual representations are available in Fig. 3.7.S1 and 3.7.S2. 72
Table 3.6.2. Values associated with regression between salinity and archaeal or bacterial α diveristy (Shannon's H) in water and sediment samples. Sampling times, R^2 and *p* values are shown. Visual representations are available in Fig. 3.7.S3 and 3.7.S4. 72

Supplementary table 2.7.S1. Reaction mixture used for each chip in the context of dPCR. 44
Supplementary table 2.7.S2. Steps carried out during dPCR, depending on the primers used. The phases, temperatures, times and number of cycles are presented. 44
Supplementary table 2.7.S3. Water physico-chemical values measured using a YSI multi-parameter probe in the different mesocosms, at the beginning of the incubation, with measured Cl^- values, at T0. 45
Supplementary table 2.7.S4. Biotic and abiotic factor values used to carry out multivariate analyses, shown for every sample, composing the different mesocosms at the different incubation times. For T3 and T6 samples, Cl^- values were calculated following a linear regression using Cl^- (y) and conductivity (x) : (y= -1E-20*x^3 + 1E-16*x^2 + 0.2279*x). 46
Supplementary table 2.7.S5. First 2 axes' values of a PCoA computed using the eukaryotic OTU table (the sequence data is available in Astorg *et al.* (2022). ... 46
Supplementary table 2.7.S6. Significant explanatory variables explaining bacterial mesocosm community composition variance, tested using db-RDA. Eukaryotic community composition was represented based on the scores of axes 1 and 2 (A1, A2) of a PCoA (see Table 2.S5). 47
Supplementary table 2.7.S7. Variation in bacterial mesocosm community composition explained by exposure time (3 and 6 weeks) and salinity groups (K1, K2, K3, and K4) defined in the LINKTREE analysis, tested using PERMANOVA. 48
Supplementary table 2.7.S8. SIMPER and Kruskal-Wallis analysis table showing the OTUs that are significantly different according to the clustering established by the PCoA. The table shows the compared Clusters, the result of the SIMPER analysis, the OTU group, the initial Kruskal-Wallis *p*-value (Krusk.p.val) and corrected for false discovery rate (Fdr.krusk. p.val) and the taxonomy associated with UTO. 48

Supplementary table 3.7.S1. Reaction mixture used for each chip in the context of dPCR. 87
Supplementary table 3.7.S2. Steps carried out during dPCR, depending on the primers used. The phases, temperatures, times and number of cycles are presented. 87
Supplementary table 3.7.S3. Following a Principal coordinate analysis (PCoA) on bacterial, archaeal and eukaryotic OTU tables, the first two axes values from the computed PCoA were kept as environmental variables. 88
Supplementary table 3.7.S4. All abiotic and biotic values used for multivariate analyses, for all samples at all sampling time in microcosms. 89
Supplementary table 3.7.S5. ANOVA table for explanatory variables used in archaeal, bacterial and eukaryotic db-RDA. Bac1, bacterial community composition represented by the first axis of a PCoA (see Table 3.3 for PCoA axes values); Bac2, bacterial community composition represented by the second axis of a PCoa. Arc1, archaeal community composition represented by the first axis of a PCoA; Arc2, archaeal community composition represented by the second axis of a PCoA; Euka1, community composition represented by the first axis of a PCoA; EukA2, eukaryotic community composition represented by the second axis of a PCoA. 89
Supplementary table 3.7.S6. PERMANOVA realized on the different archaeal, bacterial and eukaryotic clusters obtained from PCoA and LINKTREE analysis, and separating the different sampling mediums (water / sediment) and salinity groups 91
Supplementary table 3.7.S7. Results of the similarity percentage (SIMPER) analysis and Kruskal-Wallis test on the different clusters obtained by the PCoA for the archaeal, bacterial and eukaryotic communities of Croche lake microcosms. Only clusters from same-mediums (water-water / sediment-sediment) were kept. 92

Tableau Annexe A1. Tableau des analyse de variance à un facteur (ANOVA) réalisé sur les regressions linéaires dans les mésocosmes. *p.values :* 0 ‘***’ 0.001 ‘**’ 0.01 ‘*’ 0.05 ‘.’ 0.1 ‘ ’ 1. 106
Tableau Annexe A2. Tableau des analyse de variance à un facteur (ANOVA) réalisé sur les régressions linéaires dans les microcosmes. *p.values* : 0 ‘***’ 0.001 ‘**’ 0.01 ‘*’ 0.05 ‘.’ 0.1 ‘ ’ 1. 108

LISTE DES ABRÉVIATIONS, DES SIGLES ET DES ACRONYMES

Abarc : Abondance archée
Abbac : Abondance bactérienne
Abeuc : Abondance eucaryote
Abond : Abondance
Arc : Archées
Bac : Bactéries
Ca^{+} : Calcium
CERMO : Center of Excellence in Research on Orphan Diseases
Cl^{-}: Chlorure
CMA : Acétate de calcium et magnésium
CO2 : Dioxyde de carbone
Div : Diversité
Divarc : Diversité archée
Divbac : Diversité bactérienne
Diveuc : Diversité eucaryote
DNA : Acide désoxyribonucléique (Deoxyribonucleic acid)
DO : Oxygène dissout
DOI : Identifiant numérique d'objet (digital object identifier)
dPCR : Réaction en chaine polymérase digitale
ETM : Élément trace métallique
Euc : Eucaryotes
Hg : Mercure
K^{+} : Potassium
KCl : Chlorure de potassium
MeHg : Methylmercure
Meso: Mésocosmes
Mg^{+} : Magnésium
Micro : Microcosmes
N : Nord
Na^{+} : Sodium
NaCl : Chlorure de sodium
NCBI: National Center for Biotechnology Information
$NH4^{+}$: Ammonium
$NO2^{-}$: Dioxyde d'azote
$NO3^{-}$: Nitrate
OTU : Unité taxonomique opérationnelle
PAST : Paleonthological statistics
PCoA : Analyse de coordonnées principales
PERMANOVA : Analyse de variance permutationnelle
pH : Potentiel hydrogène

ppt : Partie par millier
rRNA : Acide ribonucléique ribosomal
Sal : Salinité
Sed: Sédiment
SIMPER : Analyse de pourcentage de similarité
TE : Tampon à base de TRIS (tris-hydroxyméthylaminométhane) et EDTA (Ethylenediaminetetraacetic acid)
Temp : Température
TOC : Carbone organique total
TP : Phosphore total
UPGMA : Unweighted pair group method with arithmetic mean
W : Ouest
Wat: Eau (Water)

LISTE DES SYMBOLES ET DES UNITÉS

UNITÉS DE BASE

°C : Degrés
SPC : Conduction spéfique/Conductance
$: Dollars
‰ : Pour mille
*** : < 0.001
** : < 0.01
* : < 0.05

UNITÉ DE CONCENTRATION

ppt : Partie par millier
mol : Mole (unité de quantité de matière)
M : Molarité (mole/L^{-1})

UNITÉS D'AIRE ET VOLUME

km2 : Kilomètre carré (= 1 000 000 m2)
m2 : Mètre carré
L : Litre
mL : Millilitre (= 1 cm3)
µL : Microlitre

UNITÉS MÉCANIQUES

km/h : Kilomètre par heure

UNITÉS DE COORDONNÉES

° : Degrés
' : Minutes
" : Secondes

UNITÉS GÉOMÉTRIQUES

m : Mètre (unité de longueur)
cm : Centimètre
mm : Millimètre
µm : Micromètre

UNITÉS DE MASSE

t : Tonne (= 1 000 kg)
kg : Kilogramme
g : Gramme
mg : Milligramme
µg : Microgramme

RÉSUMÉ

Les bactéries et archées sont des organismes omniprésents dans les milieux d'eau douce, et font partie intégrante des réseaux trophiques. Toutefois, l'utilisation accrue de chlorure de sodium (NaCl) comme sel de voirie et son introduction dans les milieux dulcicoles ont un effet sur les procaryotes. Ce projet a donc été mis en place afin, d'une part, mieux comprendre la dynamique des communautés procaryotes exposées à différentes salinités, par l'entremise d'une revue littéraire de différentes études existantes, mais également à travers la réalisation d'un projet expérimental permettant d'aborder et élucider des aspects de l'effet de la salinisation des eaux douces sur les communauté microbiennes lacustres. À l'aide d'un ensemble de mésocosmes et de microcosmes comportant un gradient de salinité variant entre 0.01 et 3.22 ppt NaCl, ainsi que l'utilisation du séquençage des gènes ARNr 16S et 18S et de PCRd, nous avons pu investiguer l'effet du NaCl sur la diversité et l'abondance procaryote dans l'épilimnion, l'hypolimnion et dans les sédiments d'un lac des Laurentides. Une relation positive entre la salinité et l'abondance absolue bactérienne a été observée après trois semaines d'exposition dans l'épilimnion du lac (mésocosmes). Des processus tels que la décomposition d'organismes eucaryotes seraient en jeu dans les variations rencontrées. Aussi, il nous a été possible d'observer une transition de dominance des Betaproteobacteries et Actinobacteries vers les Bacteroidia et Alphaproteobacteries, laquelle est similaire à celle observée en estuaires. Dans l'hypolimnion (microcosmes), un impact négatif du NaCl sur la diversité α était présent après six semaines, et la composition de la communauté archée s'est démontré être un facteur d'influence dans les variations rencontrées au sein des commuanutés bactériennes. Dans les sédiments (microcosmes), malgré l'absence de linéarité avec le NaCl, des variations au niveau de l'abondance absolue archée après trois semaines et de la diversité α archée après six semaines étaient présentes, et ce, malgré le faible potentiel de pénétration du NaCl dans les sédiments.Nos résultats suggèrent toutefois l'implication d'autres facteurs tel que l'interdépendance des espèces,la possibilité d'endosymbiose, ainsi que les fluctuations potentielle en nutriments tel que l'acétate, dans l'établissement d'espèces comme Methanosarcina et Methanosaeta. Également, la transition des communautés microbiennes et les niveaux de salinité auxquels ceux-ci sont associés ont pu être examinés, en considération des régulations en place. Un ordre de sensibilité eucaryote > archée > bactérie a pu être établie. En vue de la plus grande sensibilité des communautés eucaryotes, ayant mené à une siscion dès ≈0.4 ppt NaCl (>185 mg/L^{-1} Cl^{-}), et que les recommandations canadiennes d'exposition chronique au Cl^{-} s'élèvent à 120 mg/L^{-1} Cl^{-}, le respect de ces normes permettrait de limiter l'impact du NaCl sur les habitats dulcicoles. Néanmoins, le développement de pratiques nécessitant moins de sel de voiries (e.g., utilisation d'abrasifs, routes blanches) constitue une alternative plus écologique qui pourrait permettre de pallier au développement de problématiques comme le syndrome de salinisation des eaux douces, et favoriserait donc la protection des communautés microbiennes à long terme.

Mots clés : Chlorure de sodium, eau douce, mésocosme, microcosme, procaryotes, archées, bactéries, diversité, ARNr 16S, abondance, dPCR, hypolimnion, sédiment, épilimnion

ABSTRACT

Bacteria and archaea are ubiquitous organisms in freshwater environments, and are an integral part of food webs. However, the increased use of sodium chloride (NaCl) as road salt and its introduction into freshwater environments may not be without consequences for prokaryotes. This project was therefore set up in order, on the one hand, to better understand the dynamics of prokaryotic communities exposed to different salinities (e.g., estuaries), through a literary review of different existing studies, but also to through the realization of an experimental project to address and elucidate aspects of the effect of freshwater salinization on lacustrine microbial communities. Using a set of mesocosms and microcosms with a salinity gradient varying between 0.01 and 3.22 ppt NaCl, as well as the use of 16S and 18S rRNA gene sequencing and dPCR, we investigated the effect carried out by NaCl on prokaryotic diversity and abundance in the epilimnion, the hypolimnion and in the sediments. A positive relationship between salinity and absolute bacterial abundance was present after three weeks in the epilimnion (mesocosms). Processes such as the decomposition of eukaryotic organisms would be at play in the variations encountered. Also, we observed a transition from dominance of Betaproteobacteria and Actinobacteria to Bacteroidia and Alphaproteobacteria, which is similar to that observed in estuaries. In the hypolimnion (microcosms), a negative impact of NaCl on α-diversity was present after six weeks, and the composition of the archaeal community was shown to be an influential factor in the variations encountered within bacterial communities. In the sediments (microcosms), despite the absence of linearity with NaCl, variations in absolute archaeal abundance after three weeks and archaeal α diversity after six weeks were present, despite the low penetration potential of NaCl into the sediments. Our results, however, suggest the involvement of other factors such as the interdependence of species, the possibility of endosymbiosis, as well as potential nutrients fluctuations, such as acetate, in the establishment of species like Methanosarcina and Methanosaeta.Also, the transition of microbial communities and the salinity levels with which they are associated was examined, in consideration of the regulations in place. A eukaryotic > archaeal > bacterium order of sensitivity was established. In view of the greater sensitivity of eukaryotic communities, having led to a siscion from ≈0.4 ppt NaCl (>185 mg/L^{-1} Cl^-), and that the Canadian recommendations for chronic exposure to Cl^- amount to 120 mg/L^{-1} Cl^-, compliance with these standards would limit the impact of NaCl on freshwater habitats. Nevertheless, the development of practices requiring less road salt (e.g., use of abrasives, white roads) constitutes a more ecological alternative which could make it possible to alleviate the development of problems such as the freshwater salinization syndrome, and would therefore promote the long-term protection of microbial communities.

Keywords : Sodium chloride, freshwater, mesocosm, microcosm, prokaryotes, archaea, bacteria, diversity, 16S rRNA, abundance, dPCR, hypolimnion, sediment, epilimnion.

CHAPITRE 1

CHLORURE DE SODIUM, SEL DE VOIRIES ET PROCARYOTES

L'état de santé des milieux d'eau douce dépend d'un équilibre entre les différentes fractions de la chaîne trophique, mais également des facteurs biogéochimiques et physico-chimiques, ainsi que des dynamiques interstratigraphiques, aussi bien dans les milieux dulcicoles que salins. Comme chaque environnement constitue une niche écologique pour les micro-organismes l'y habitant, il va de soi qu'un changement dans l'équilibre des caractéristiques du milieu exercera une influence importante, directe ou indirecte, sur l'ensemble des communautés aquatiques. Parmi les facteurs pouvant causer des perturbations, l'introduction de chlorure de sodium (NaCl) constitue un impact du développement humain soulevant de plus en plus de préoccupation, car semblant influencer à divers niveaux une multitude de composantes, biologique ou non, des milieux aquatiques. Bien que le NaCl soit présent naturellement dans les environnements dulcicoles à faibles concentrations, et à concentration modérée dans les milieux marins, son introduction anthropique dans les cours d'eau douce pourrait avoir des répercussions, notamment sur les communautés microbiennes.

Ce projet de maîtrise a donc pour objectif de mettre en lumière, en premier lieu, l'effet de la salinité sur la diversité et l'abondance des communautés bactériennes et archées en environnement lacustre dulcicole, en été, afin de déterminer si un effet direct est observable, et ce, en milieu peu ou pas exploité, à différents niveaux de salinité, après une exposition de trois et six semaines. Également, en jumelant l'étude de l'effet de l'introduction du NaCl sur les communautés procaryotes à l'effet engendré sur les microorganismes eucaryotes, un regard plus général pourra être porté afin de mieux comprendre la dynamique des chaînes trophiques lors de perturbations telles que dans le cas de la salinisation des eaux douces. Finalement, une comparaison entre l'effet réalisé sur le microbiote de l'épilimnion, l'hypolimnion et les sédiments permettra de déterminer si l'une de ces niches abrite un domaine (archées, bactéries ou eucaryotes) possédant un niveau de sensibilité au NaCl supérieur aux autres. Si une attention est présentement portée par bon nombre de chercheurs sur cette problématique d'actualité, comprendre de façon plus spécifique l'effet du sel sur les

communautés microbiennes, lesquelles jouent une variété de rôles dans les écosystèmes, de la production à la décomposition, ne devrait pas être négligé.

Ainsi, deux études présentées dans ce mémoire permettront d'éclaircir certains questionnements portés vers les communautés procaryotes d'eaux douces exposées à différentes concentrations en NaCl. Un premier projet, intitulé «Response of prokaryotic communities to freshwater salinization – A mesocosm experiment» (Chapitre 2) a pour objectif d'établir l'effet possible du NaCl sur la diversité et l'abondance procaryote dans l'épilimnion. Pour mieux comprendre son effet dans l'hypolimnion et dans les sédiments, nous présentons un second projet intitulé « Response of hypolimnetic microbial communities to freshwater salinization » (Chapitre 3). Finalement, les projets seront tous deux comparés afin de déterminer le niveau de sensibilité de ces constituants des réseaux trophiques, la relation des niveaux de sensibilité face aux règlementations en place, et les voies alternatives au NaCl comme sel de voirie seront visitées (Chapitre 4).

À tous les niveaux, cette étude permettra de voir si les milieux affectés par la salinisation demeurent adéquats pour l'établissement des communautés microbiennes, ou si la présence de sel constitue un élément impossible à outrepasser pour celles-ci.

1.1 Chlorure de sodium

Le chlorure de sodium, communément appelé sel, possède pour formule NaCl. Celui-ci est composé d'ions halogénure de chlore (60.66 %), un anion, ainsi que du monocation de sodium (39.34%) (Lide, 1995), composant donc ensemble un sel inorganique. Le sodium (Na^+) est le plus abondant des métaux alcalins, en plus d'être le 6^e élément le plus abondant de la croute terrestre, composant approximativement 2.6% de celle-ci (Lide, 1995). Il est un élément très présent dans le fonctionnement cellulaire, jouant un rôle entre autres dans la balance de la pression osmotique intracellulaire et de la distribution des liquides, sans compter l'équilibre des électrolytes et du pH. Ce sodium est généralement accompagné de sa contrepartie anionique la plus commune, le chlorure, ou Cl^-. Constituant également un électrolyte essentiel au fonctionnement cellulaire, il possède des fonctions similaires au sodium, contrebalançant ce dernier dans le maintien du pH, et autres fonctions énumérées précédemment.

Alors que le chlorure et le sodium s'assemblent en cristaux lorsque sous forme solide, le NaCl est soluble (Marriott, 2010), et bien que cette propriété soit à la base de sa polyvalence d'utilisation, celle-ci rend sa gestion plus critique. Le NaCl constitue l'élément principal composant le sel de déglaçage épandu sur les routes (Environnement Canada, 2001), et est favorisé pour son faible coût, son effet corrosif modéré, ainsi qu'une température de service atteignant -20°C (Robitaille, 2011). Alors que son impact environnemental est considéré comme modéré par rapport à d'autres alternatives de déglaçage, l'utilisation du NaCl comme sel de route est de plus en plus reconnue comme constituant un apport important de la charge anthropique de sel contribuant au syndrome de salinisation des eaux douces (Kaushal *et al.*, 2018 ; Dugan *et al.*, 2017). Mais pour comprendre réellement l'influence que le sel d'épandage possède dans le développement de ce syndrome, il est important de comprendre le devenir du NaCl suite à son épandage, et la dynamique de ses composantes dans les sols et dans les eaux avoisinantes. Utilisé, car il permet d'abaisser la température de congélation de l'eau à des températures inférieures à 0°C (Kimbrough, 2006), le sel s'y retrouve rapidement en solution, où il se retrouve séparé sous forme ionique. Généralement propagés sur des surfaces imperméables comme l'asphalte des routes, les eaux de fonte vont ensuite s'écouler pour atteindre les surfaces perméables avoisinantes. Lorsqu'introduit dans les sols, le sodium peut être retenu par les plantes avoisinantes, être retenu à la surface des particules du sol (Robitaille, 2011), où il participera à des échanges cationiques pouvant mener à la libération de cations de base et d'éléments traces métalliques (ETM ; Daley *et al.*, 2009), ou encore s'écouler vers les eaux de surface avoisinantes et les eaux souterraines. Selon Kaushal *et al.* (2018), « l'échange cationique emmené par le sodium peut libérer 40 à 80% du calcium et du magnésium des sites d'échange du sol vers les eaux souterraines et cours d'eau », en plus d'affecter le carbone organique dissout, affectant ainsi la fertilité des sols. Néanmoins, la richesse du sol étant variable, les sols riches en calcium tendent à retenir plus fortement le sodium (Environment Canada, 2001), menant à un débalancement du ratio de Na^+ : Cl^- migrant vers les eaux souterraines.

Dus aux « conditions d'écoulement de base » (Kaushal *et al.*, 2005) de l'été, les ions chlorure peuvent de plus s'accumuler à des niveaux élevés dans la nappe phréatique, pouvant atteindre des concentrations de 2800 mg/L^{-1} (Schuler *et al.,* 2019) et ainsi, ultimement rejoindre les eaux de surfaces s'approvisionnant de celles-ci. Bien qu'il ne se biodégrade pas et qu'il ne soit pas bioaccumulé (Kaushal *et al.*, 2005), une partie de la charge en chlorure peut cependant être

conservée à travers la « chloration de la matière organique naturelle » (Daley *et al.*, 2009) et la prise en charge microbienne. Cette prise en charge peut s'avérer très néfaste dans les habitats terrestres comme aquatiques, puisque l'exposition au Cl^- peut être un inhibiteur efficace de l'oxydation du $NH4^+$ ($NH_4^+ \rightarrow NO_3^-$), de la nitrification ($NH_4^+ \rightarrow NO_2^-$) (Groffman *et al.*, 1995 ; Hunt *et al*, 2012) et de la dénitrification ($NO_3^- \rightarrow N_2$) (Kaushal *et al.*, 2005), le tout étant essentiel au cycle de l'azote et au maintien de l'apport en nutriments au niveau de l'épilimnion. L'azote ainsi rendu disponible peut être ultérieurement assimilé par d'autres organismes pour la production d'acides aminés, de protéines ou d'acides nucléiques (Bari et Yeasmin, 2022).

Conjugués, le chlorure et le sodium peuvent avoir un effet indirect sur la disponibilité d'autres nutriments en altérant la densité de l'eau (Judd *et al.*, 2005 ; Wyman et Koretsky, 2018), interférant dans les échanges possibles entre l'hypolimnion, le métalimnion et l'épilimnion (Planas *et al.*, 2014), normalement réalisé lors du brassage. En effet, les lacs sont assujettis à l'influence de la radiation solaire, de la température de l'air et de l'énergie des vents (Tockner et Likens, 2009), menant à un changement de température des eaux de surface et engendrant un changement de densité qui laisse place à sa stratification. Au printemps et à l'automne, toutefois, l'homogénéisation de la température des plans d'eau lentiques mène à l'érosion de leur stratification et permet dès lors les échanges entre l'épilimnion et l'hypolimnion (Boehrer et Schultze, 2008). Précédemment ségrégué sous le métalimnion et sa thermocline, l'hypolimnion pourra dès lors se réapprovisionner en oxygène, alors que l'épilimnion pourra bénéficier d'un apport important en nutriment fourni depuis les sédiments (Kansman, 2015). Toutefois, l'introduction de sel en eaux douces a pour effet d'en augmenter sa densité, particulièrement en eaux froides (Boehrer et Schultze, 2008), et ainsi augmenter la stabilité de la colonne d'eau, laquelle détermine le niveau d'énergie externe nécessaire pour en engendrer le brassage (Kirillin et Shatwell, 2016). Globalement, l'accumulation de sel dans l'hypolimnion, et donc l'augmentation de sa stabilité, aurait pour effet de retarder les périodes de brassage, empêchant l'oxygène d'atteindre les sédiments (Novotny et Stefans, 2012) et prolongeant ainsi la période d'anoxie. Toutefois, l'atteinte d'un seuil de salinité aurait le potentiel de transformer un milieu dimictique en milieu méromictique ou périodiquement monomictique (Ladwig *et al*., 2021; Wyman et Koresky, 2018). Cet effet de la salinisation des milieux aquicoles a d'ailleurs été observé au cours de diverses études, notamment par Novotny *et al.* (2008), Judd *et al.* (2005), Bridgeman *et al.* (2000), Kaushal

et al. (2008) ainsi que Judd (1970), et pourrait engendrer des conséquences significatives au niveau des cycles biogéochimiques, des caractéristiques physico-chimiques, et de la structure des écosystèmes affectés, en plus de l'effet direct réalisé sur les organismes.

Aussi, bien que les ions chlorures et sodium tendent à rester libres une fois en solution, de fortes concentrations de sels peuvent mener à la complexation du chlorure avec d'autres éléments, tel que des métaux lourds comme de cadmium (Environment Canada, 1994), et ainsi favoriser leur dissolution et leur biodisponibilité, pouvant accroître la toxicité de certains composés. De plus, tandis que la distribution des ions K+ et Cl^- tend à être spatialement et temporellement homogène (Mayer *et al.,* 1999), entre 1 et 2 % du sel présent dans l'eau peut s'accumuler dans les sédiments (Etzel et Maurer, 1950) au niveau de l'eau interstitielle, pouvant s'étendre jusqu'à 40 cm sous la surface (Environment Canada, 2001), et pouvant affecter les organismes y vivant.

Dans son ensemble, les limites d'exposition au Cl^- au Canada sont limités à 120 mg/L^{-1} pour une exposition chronique, et 640 mg/L^{-1} pour une exposition aigüe (Schuler *et al.,* 2019), mais le suivi et la gestion des écoulements salés constituent des contraintes au respect de ces limites. Hors de ces limites, une exposition chronique à 240 mg/L^{-1} de Cl^- aurait un effet sur 10% des espèces aquatiques (Environment Canada, 2001), pouvant atteindre des proportions plus grandes lorsque les milieux affectés sont des habitats vierges.

1.2 Sels de voiries et syndrome de salinisation des eaux douces

Chaque année, des milliers de tonnes de sel sont déversés sur les routes du Québec et du Canada, et sont drainés vers les cours d'eau lors des fontes printanières (Environment Canada, 2001). Les entrepôts de sels des municipalités et des compagnies privées, lorsque gérés de façon non conforme, peuvent également contribuer à la charge de sel dirigé vers les environnements aquatiques avoisinants. En 1997-1998, ce serait près de 4 418 462 tonnes de NaCl qui auraient été épandues sur les routes du Canada (Environment Canada, 2001). Alors que les neiges sont redirigées vers des sites d'élimination, une étude réalisée par Pinard *et al.* (1989) dévoile que 2 % du NaCl serait toujours présent dans l'eau de fonte, signifiant donc que la majeure partie du sel serait déjà introduit dans l'environnement avoisinant.

Pratique courante aux États-Unis depuis près de 80 ans (Corsi *et al*., 2010), l'épandage de sel de déglaçage et son introduction dans les eaux avoisinantes se sont montré être directement lié à la présence de couverture terrestre imperméable (Dugan *et al.*, 2017 ; Galella *et al.,* 2019). En effet, une étude réalisée par Dugan et al. (2017) sur la relation entre la salinisation des étendues d'eau et la présence avoisinante d'infrastructures humaines montre qu'une hausse des niveaux de chlorure est observée dans la plupart des lacs et rivières urbains et ruraux possédant plus de 1 % de couverture terrestre imperméable en périphérie. Cette statistique est d'autant plus alarmante quand il est considéré que cette catégorie d'étendue d'eau représente près de 27 % des lacs aux États-Unis, et est en proie au développement urbain. S'il y a 50 ans l'utilisation de sel de déglaçage s'élevait à 0,15 million de tonnes par année aux États-Unis, elle est présentement estimée à 18 millions de tonnes par année, et 5 millions de tonnes par année au Canada de 1995 à 2001. Bien que des mesures soient maintenant prises afin d'assurer une meilleure gestion de l'épandage depuis la mise en place du code de pratique de la gestion environnementale des sels de voirie (Environnement Canada, 2004) au Canada, le développement humain sur ce territoire, notamment les routes, risque d'engendrer une augmentation des niveaux de sels épandus et ainsi donc, des niveaux de sels lessivés lors des fontes, si aucune alternative écologiquement et économiquement plus favorable n'est trouvée.

Tandis que le Canada et les États-Unis sont présentement en prise avec des niveaux de Cl^- considérés comme assez élevés pour menacer les organismes aquatiques (Cañedo-Argüelle *et al*., 2016), les législations mises en place sont présentes afin d'assurer la potabilité de l'eau et la santé des gens souffrant d'hypertension (WHO, 1996) plutôt que la biodiversité. La potabilité des eaux (Cañedo-Argüelle *et al.*, 2016) et la sécurité routière (ATC, 2003) sont prioritaires, mais considérer l'effet global du syndrome de salinisation des eaux douces constituerait la pierre angulaire non seulement de la sauvegarde environnementale, mais également économique à long terme. Lorsqu'un écosystème entier est affecté par la hausse de salinité, les retombées peuvent être désastreuses. Un illustre exemple d'un tel effet s'est produit au cœur de la mer d'Aral, où une mauvaise gestion des ressources aquatiques a mené à une hausse de salinité de 10 g/L^{-1} à plus de 100 g/L^{-1}, depuis 1960 (Micklin, 2007). La perte de diversité observée a mené à la perte de près de 60 000 emplois (Micklin et Aladin, 2008), en plus d'une transition des communautés microbiennes halophiles vers des communautés extrêmophiles (Shurigin *et al*., 2019). Des mesures ont toutefois

été prises afin de promouvoir un retour de la faune et la flore et ont permis une réhabilitation partielle de la biodiversité (Aladin *et al*., 2009), démontrant alors la possibilité de contrevenir aux effets néfastes emmenés par une hausse des niveaux de salinité.

Tandis que des espèces vertébrées de large taille peuvent être affectées (e.g., le recrutement et la dynamique des populations des salmonidés ; Hintz et Relyea, 2017), elles sont cependant reconnues comme tolérantes à l'exposition au NaCl, comparé aux petits invertébrés, qui eux, sont plus sensibles (Schuler *et al.*, 2019). D'autre part, l'effet du NaCl sur les communautés procaryotes, bien qu'encore élusif, a été étudié.

1.3 Les procaryotes et la salinité

Divisés entre le domaine des *Bacteria* et le domaine *Archaea*, les procaryotes constitueraient 2,2 pétagrammes de carbone dans les habitats aquatiques sur terre (Karp *et al.*, 2018), répartis en près de 10^{29} organismes (Lavergne, 2014), et représentant 2.2 à 4,3 millions d'espèces (Louca *et al.*, 2019 ; Hugenholz *et al.*, 2021). La prédation de ces microorganismes unicellulaire, constituant un facteur limitant à leur croissance et à leur multiplication, est principalement réalisée par le zooplancton ainsi que par des protistes hétérotrophes, pour qui la qualité de l'apport nutritif microbien constitue un élément essentiel à ne pas négliger (Tomas, 1980 ; Ikeda, 1977). Les procaryotes contribuent toutefois à bien des égards au recyclage de la matière, à travers une multitude de voies métaboliques promouvant certains processus, dont les plus connus sont la fixation de l'azote et la reminéralisation de la matière organique. Ces organismes ne sont toutefois pas dépourvus d'un besoin en apport en nutriment, notamment le carbone, l'azote, le phosphore, et des minéraux comme le fer et le calcium. Cependant, même lorsque leurs besoins sont rencontrés, ils ne sont pas à l'abri des effets néfastes ou délétères d'une hausse de la salinité dans l'environnement qui les accueille, et de la hausse de la pression osmotique ainsi engendrée.

Une étude relatant l'effet de la salinité sur le microbiote d'un petit ruisseau, et portant sur l'effet de la salinité sur les procaryotes a été réalisée par Dickman et Gochnauer (1978), et a obtenu pour résultats une croissance des communautés microbiennes normales. Ces résultats, aussi surprenants soient-ils, ont pu être attribués à une diminution du nombre d'organismes brouteurs, tels que les ciliés et les flagellés, réduisant donc la prédation sur les organismes microbiens, plutôt qu'à un

effet direct du NaCl. Une influence similaire des brouteurs et autres strates supérieurs du réseau trophique a également été observée dans les milieux où le brassage est limité et l'apport en nutriments est principalement médié par les tempêtes (Cottingham et Schindler, 2000).

Une seconde étude, réalisée par Herlemann *et al.* (2011) sur la transition des communautés microbiennes dans la mer Baltique, à travers un gradient de salinité s'étendant sur 2000 km, présente une transition dans la dominance des communautés microbiennes, avec les actinobactéries et les Betaprotéobactéries comme embranchement dominant dans la zone d'eau douce à saumâtre (0 ~ 5 ‰), accompagné d'une transition de dominance graduelle vers les Alphaprotéobactéries et Gammaprotéobactéries à travers le gradient de salinité. Ces résultats concordent avec les résultats d'autres études réalisées (Cottrell et Kirchman, 2004 ; Kan *et al.*, 2008 ; Bouvier et del Giorgio, 2002), ainsi qu'avec les besoins en nutriments des organismes, les Alphaprotéobactéries étant généralement des organismes oligotrophes, pouvant survivre dans des environnements moins riches en nutriments, contrairement aux Betaprotéobactéries qui sont eutrophes et nécessitent un apport plus grand (Filion, 2012). L'effet engendré sur les Betaprotéobactéries est d'ailleurs mis de l'avant par Bouvier et del Giorgio (2002) et par Cottrell et Kirchman (2004), imputant la diminution des Betaprotéobactéries à un déclin d'efficacité de croissance bactérienne, bien que l'effet ne soit pas graduel dans l'étude de Bouvier et del Giorgio, puisque les sources d'eau douce et marine sont entrecoupées par une zone de forte turbidité. Un autre élément très intéressant sortant de l'étude de Herlemann *et al.* (2011) est la présence de *Verrucomicrobia* à des salinités variant entre 5 et 10 ‰, alors que ce phylum se trouve également dans les milieux d'eaux douces (He *et al.*, 2017), démontrant une certaine plasticité d'acclimatation à la salinité. Une autre étude, réalisée par Coci *et al.* (2005) sur l'effet de la salinité sur les bactéries benthiques oxydant l'ammoniac des sédiments d'estrans met de l'avant une transition des communautés bactériennes de surface par des membres d'une différente espèce du même genre (*Nitrosomonas oligotropha* → *Nitrosomonas marina*).

Tandis que les concentrations en sel des environnements d'eaux douces sont souvent très basses, allant de 1 à 10 mg/L^{-1} Cl^- (0.001 à 0.01 ppt), elles peuvent atteindre des niveaux aussi élevés que 5000 mg/L^{-1} (5 ppt) (Shambaugh, 2008) à certains endroits suite à l'infiltration des eaux des fontes printanières, souvent à proximité des développements humains. Bien que des organismes amphihalines sont en mesure de s'acclimater aux changements de salinité rencontrés dans des

milieux estuariens, passants d'un environnement avec moins de 0,05 % de sel (0.5 ppt) (Cavin, 2017), a un environnement à près de 3,5 % (35 ppt), ces organismes ont toutefois des mécanismes d'adaptation qui leur sont bien distinct, et restent fortement affectés lorsqu'est considéré la succession des espèces dominantes à travers le gradient de salinité, et à travers les zones de fortes turbidités, dont la zone de transition où se rencontrent les masses d'eau douce et d'eau salée (Herlemann *et al.*, 2011 ; Cottrell et Kirchman, 2004 ; Bouvier et del Giorgio, 2002). De tels mécanismes d'acclimatation ou d'adaptation existent toutefois chez des organismes dulcicoles stricts, lorsqu'exposés à des concentrations non létales de NaCl.

1.4 Adaptations et acclimatations procaryotes.

Bien que les adaptations et acclimatations possibles face à la salinité chez les procaryotes ne seront pas approfondies lors des chapitres subséquents, la littérature se rapportant à ceux-ci sera revue brièvement. Lorsque la pression osmotique du milieu est supérieure à la pression osmotique intracellulaire, la déshydratation est engendrée par excrétion d'eau cytosolique à travers les aquaporines bordant la membrane plasmique. La pression osmotique peut, toutefois, être contrebalancée par la présence d'un cytoplasme iso-osmotique engendré, par exemple, par une augmentation des concentrations cytoplasmiques en ions potassium (K+) ou en chlorure de potassium (KCl) (Oren, 1999 ; Varnam et Evans, 2000). Ces concentrations en ions doivent toutefois être accompagnées d'enzymes adaptés, notamment par la présence de résidus acides à la surface des enzymes. Jusqu'à ce jour, la forte accumulation de KCl n'aurait été observée que chez des *Archaea* de l'ordre Halobacteriales, ainsi que par des bactéries du genre *Salinibacter*. Les espèces bactériennes comportent toutefois différentes concentrations normales de K+ et une capacité de captation qui leur est propre, étant généralement plus élevée chez les bactéries à Gram négatifs (Poolman et Glaasker, 1998). De façon similaire, la formation de solutés compatibles, ou osmolytes, définit comme des « petits solutés utilisés par les cellules de nombreux organismes et tissus stressés par l'eau pour maintenir le volume cellulaire » (Yancey, 2005), permettant également de contrer la pression osmotique et thermique sans perturber l'activité cellulaire. Bien que ces voies adaptatives soient considérées comme ubiquitaire chez les eubactéries, elles se retrouvent également chez les archées, favorisant toutefois l'accumulation d'osmolytes peu communs (Martin *et al.*, 1999) chargés négativement (Roeßler et Müller, 2001). Ces voies

métaboliques ne sont toutefois activées que suite à l'exposition à certaines concentrations de sel (Yeo, 1998).

Une troisième adaptation possible est le resserrement de la membrane cellulaire, laquelle est réalisée par contraction électrostatique plutôt que par réponse cellulaire aux changements osmotiques (Marquis, 1968). Ce resserrement permet aux cellules exposées à la pression osmotique de réduire leur perméabilité, et permet de réduire les concentrations en eau présentes dans la membrane cellulaire (Vreeland *et al.*, 1984).

Finalement, un mécanisme d'acclimatation extracellulaire est la production d'exopolysaccharides afin de former un biofilm protecteur (Decho, 2000). Pouvant comporter également des protéines, des glycolipides, des glycoprotéines et de l'ADN (Prescott *et al.*, 2018), elles offrent aux organismes liés aux sédiments de fond ou en suspension une protection physique contre la pression osmotique engendrée par la présence de sel dans le milieu environnant (Decho, 2000). Ce mécanisme comporte toutefois l'implication de la sessilité des communautés produisant la matrice. En contrepartie, l'hétérogénéité des espèces microbiennes pouvant être présentes dans un biofilm laisse place à la possibilité d'échange génique par l'entremise du transfert horizontal, pouvant représenter un atout pour la survie lors du détachement des organismes suite au retour à des conditions adéquates du milieu. De retour au mode de vie planctonique, les organismes microbiens pourront se rattacher et former de nouveau une matrice d'exopolysaccharides si nécessaire.

Il va sans dire que les communautés habitant les sédiments différents de celles trouvées dans l'eau, et du même fait possèdent des rôles écosystémiques distincts (Ren *et al.*, 2019). Tandis que les organismes planctoniques peuvent bénéficier des conditions rencontrées dans les différentes strates d'eau (oxygène, lumière), les organismes benthiques composent avec des températures inférieures, l'absence de lumière ainsi que l'anoxie, sans compter une différence des paramètres physico-chimiques (Bandh, 2019). Conséquemment, l'étude de l'impact de l'introduction de sel dans les milieux d'eau douce se doit de considérer l'impact possible sur ces deux parts du milieu (épilimnion, hypolimnion), et s'avère d'autant plus importante vu les conséquences possibles sur la dynamique des nutriments dont peuvent dépendre la faune et la flore avoisinante, en particulier en milieux non altérés. Ainsi donc, ce projet de maîtrise considérera aussi bien l'effet du NaCl sur

les communautés microbiennes présentes dans l'épilimnion que celles présentes de l'hypolimnion et des sédiments, par l'entremise de mésocosmes et de microcosmes, et sera exploré au cours des deux prochains chapitres.

1.5 Hypothèses de travail

1.5.1 Mise en contexte du projet et objectifs

Afin de mieux comprendre l'effet réalisé par le NaCl sur les communautés procaryotes lacustres, en particulier sur leur abondance et leur diversité, deux projets ont été mis en place et seront présentés en Chapitres 2 et 3, sous forme d'un article accepté et publié dans Applied Microbiology (Chapitre 2) et d'un article en préparation. Tous deux ont été réalisés à l'aide d'échantillons prélevés dans le lac Croche (Laurentides, Québec, Canada - 45°59'17.34"N / 74°0'20.75"W) et sont représentatifs d'un milieu lacustre laurentien peu ou pas affecté par le développement humain. Un premier axe (Chapitre 2), constitue une expérience en mésocosmes comportant différents niveaux de salinité variant entre 0.01 et 3.22 ppt NaCl, et permettra d'observer l'effet de la salinisation des eaux douces sur la diversité et l'abondance des communautés bactériennes et archées résidant dans l'épilimnion. Le second axe de recherche (Chapitre 3) est basé sur une expérience en microcosmes, comportant également un ajout de sel variant entre 0.01 et 3.22 ppt NaCl, afin d'observer l'effet engendré par la salinité sur l'abondance et la diversité des communautés procaryotes de l'hypolimnion et des sédiments. Les questions et hypothèses rattachées aux deux projets mis en place sont présentées ci-bas.

1.5.2 Questions et hypothèses

Q1 : Quel est l'effet qu'une hausse de salinité engendre sur l'abondance absolue et diversité procaryote au niveau de l'épilimnion, de l'hypolimnion et des sédiments?

H1. La présence additionnelle de sel en eau douce mènerait à une baisse la diversité alpha (H de Shannon) dans l'épilimnion (mésocosmes, chap. 2), l'hypolimnion et les sédiments (microcosmes, chap. 3), proportionnelle à la hausse de salinité après trois semaines d'exposition (T3). Une hausse des valeurs de diversité après six semaines d'exposition (T6) est attendue par rapport aux valeurs observées au T3 dû à une acclimatation des communautés microbiennes face à leur nouveau milieu.

H2. La hausse de salinité des eaux douces mènerait à un changement dans l'abondance absolue, proportionnel à la salinité, dans l'épilimnion (mésocosmes, chap. 2) tout comme dans l'hypolimnion et les sédiments (microcosmes, chap. 3) après trois semaines d'exposition (T3), suivi d'une hausse après six semaines (T6) suite au développement des cellules microbiennes.

Q2 : Un seuil de salinité engendrant une transition significative des communautés microbiennes est-il présent? Un domaine fait-il preuve d'une plus grande sensibilité à la salinité dans l'une des strates lacustres?

H3. Un seuil de salinité engendrant une transition significative des communautés microbiennes de l'épilimnion (mésocosmes, chap. 2) et l'hypolimnion (microcosmes, chap. 3) serait présent et se situerait entre les valeurs minimales (0.01 ppt) et maximales (3.22 ppt) de salinité induites dans le cadre de notre étude.

H4. Les communautés procaryotes et eucaryotes ne démontreraient pas de transition significative des communautés sédimentaires (microcosmes, chap. 3) suite à l'introduction de 0.01 ppt à 3.22 ppt NaCl, malgré une incubation de six semaines.

H5. Une transition des communautés eucaryotes dans l'épilimnion (chap. 2) et l'hypolimnion (chap. 3) serait réalisée à des salinités inférieures à celle réalisée par les procaryotes, dès la troisième semaine d'incubation. Une transition des communautés bactériennes serait réalisée à des salinités inférieures à celle réalisé par les archées, aussi bien dans l'épilimnion que dans l'hypolimnion, dès la troisième semaine d'incubation.

CHAPITRE 2

RESPONSE OF PROKARYOTIC COMMUNITIES TO FRESHWATER SALINIZATION – A MESOCOSM EXPERIMENT

Publié dans Applied Microbiology, Mai 2022 (https://doi.org/10.3390/applmicrobiol2020025)

Jean-Christophe Gagnon [1,2], Louis Astorg [1,2], Alison M. Derry [1,2] and Cassandre Sara Lazar [1,2,3].

1. Department of Biological Sciences, University of Québec at Montréal, Montréal, Québec, Canada.
2. Interuniversity Research Group in Limnology/Groupe de Recherche Interuniversitaire en Limnologie (GRIL), Montréal, Québec, Canada.
3. Corresponding author.

2.1 Introduction

Each year, millions of tons of road salt, mainly composed of sodium chloride (NaCl), are applied on roads in northern regions, some of which can enter waterways during spring melts. Despite the regulations in place (Government of Canada, 2018) to limit the acute (640 mg/L^{-1} Cl^- ; Schuler *et al.*, 2019) or chronic (120 mg/L^{-1} Cl^-) toxicity of chloride on sensitive species (daphnids and amphipods ; CCME, 2011), the increase in roads (Statistics Canada, 2020) and the resulting increased salt application for northern regions increase the prevalence of freshwater salinization (Galella *et al.*, 2019, Kelly *et al.*, 2019).

Microbial communities are crucial components of food webs in aquatic ecosystems, comprising eukaryotes (fungi, algae, protozoans, ciliates etc.) and prokaryotes (Archaea and Bacteria). In conjunction with our study, research by Astorg *et al.* (2022) uncovered the effect caused by Cl^- at concentrations of 0.27 to 1400 mg Cl L^{-1} on eukaryotic communities. Overall, although there was no change in total phytoplankton biomass, a transition from Cryptophyta and Chlorophyta to Ochrophyta dominance with increasing salinity was present. Combined with the disappearance of rotifers and zooplankton, these results are consistent with several studies stating the sensitivity of zooplankton to salinity (Lionard *et al.*, 2005 ; Tavsanoglu *et al.*, 2015 ; Franceschini, 2019 ;

Mofffett *et al.*, 2020), both following sudden and gradual exposure (Nielsen *et al.*, 2008), although the development of tolerance is possible (Hintz *et al.*, 2019 ; Coldsnow *et al.*, 2017) and each species has its salinity optimum (Ishika *et al.*, 2018).

The effect of the addition of sodium chloride on prokaryotic community structures has been widely studied in environments with a natural salinity gradient such as estuaries (Cottrell & Kirchman, 2004 ; Bouvier & del Giorgio, 2002 ; Herlemann *et al.*, 2011). In these studies, a general transitional trend is observed, with Beta-proteobacteria dominating the freshwater parts of estuaries, while Alpha-proteobacteria dominate in salty environments. On the other hand, other groups dominate, notably the Gamma-proteobacteria in saline environments, and the Delta-proteobacteria and Epsilon-proteobacteria in fresh waters. However, the phylum Bacteroidetes has been shown to be "found in all marine and freshwater systems frequently as one of the dominant bacterial groups" (Henriques *et al.*, 2006). Although other factors, such as viral lysis, predatorial grazing, nutrients concentrations or hydrological conditions have an influence as well, it is clear that the gradual change of salinity along these natural salt gradient environments constitutes an essential factor that drives part of the observed shift in estuarine prokaryotic communities. However, despite existing studies (Bartolomé *et al.*, 2009 ; Kartal *et al.*, 2006) less is known about freshwater bacterial and archaeal communities exposed to anthropogenic salt sources. The urgency to understand the extent of the possible consequences is growing, as freshwater environments face the freshwater salinization syndrome (Kaushal *et al.*, 2018). Combining an increase in water salinity with its alkalinization, this problem has several sources, including agriculture and mining. In recent years, however, the use of de-icing salt, mainly composed of NaCl, has been shown to be a major contributor to this phenomenon, particularly at latitudes above 39°N (Kaushal *et al.*, 2005) and near roads (Dugan *et al.*, 2017). With the increase in roads (Statistics Canada, 2020), we must therefore demystify the possible consequences that prokaryotic communities could face, should NaCl leach into natural freshwater environments, the first step in the development of freshwater salinization syndrome.

Our study is one of the first to assess community changes in diversity and absolute abundance of freshwater prokaryotes in a pristine lower Laurentians temperate lake in response to increasing salinity. Our objectives were to: (1) Determine the effect of salinity on prokaryotic diversity and

absolute abundance, in addition to identifying the taxa affected by it; (2) establish whether a salinity threshold causes a significant differentiation of prokaryotic communities, as well as its relationship to the standards for chloride exposition; and (3) see the possible sources and overall trend of variation of prokaryotic communities exposed to salinity. Thus, using mesocosms comprising different levels of salinity established in a pristine lower Laurentians temperate lake, we used 16S rRNA gene sequencing and digital polymerase chain reaction (dPCR) to assess archaeal and bacterial gene abundance and community diversity shifts, as well as community structure across the salinity gradient, after three and six weeks of exposure. As eukaryotes play an important role in prokaryotic development, they will be considered as well throughout this study, based on data from Astorg *et al.* (2022).

2.2 Methods

2.2.1 Experimental setup

During spring 2018, mesocosm bags were placed in a freshwater Laurentian Lake (Lac Croche, Laurentians Biological Station, Quebec, Canada – 45°59'17.34" N / 74°0'20.75" W, Fig. 2.7.S1a), as detailed in Astorg *et al.* (2022). Installed in June 2018, the mesocosms were made of polyethylene, composing a total volume of 2000L and a depth of 2.5m, and were filled with water from Lac Croche that had been filtered using Wisconsin nets, in order to homogenize the addition of zooplankton. A waiting time of 48 hours was achieved before adding NaCl. The addition of salt was carried out across the mesocosms, from 0.01 to 2.74 ppt NaCl (Fig. 2.7.S1b), or 10 to 2740 mg/L^{-1} NaCl, using sodium chloride (99.9% molecular grade NaCl), inducing chloride levels ranging from 0.265 to 1110.86 mg/L^{-1} Cl^-. In addition, during the period from 2018/06/23 to 2018/08/03 during which the study took place, an addition of 0.0193g of KH_2PO_4 was carried out twice (2018/07/06, 2018/07/20) in order to compensate for the incurred loss of nutrients following possible sedimentation or consumption by organisms.

2.2.2 Sampling and physicochemical measurements

A 1L sample from the salt-free mesocosm was used as the control sample at the start of the experiment (T0). Each mesocosm was stirred, and 1L was collected from each mesocosm with

autoclaved 1.14L glass bottles (VWR® CAT NO. 10754-820) triple rinsed beforehand. This was done after salt addition (T0; 2018/06/23), after three (T3; 2018/07/13), and six weeks (T6; 2018/08/03) incubations. The threshold of six weeks of incubation was chosen to limit the "bag" effect in the mesocosms in which an improper water mixing or the disappearance of certain species (e.g., saprotrophic decomposers, nitrate-reducing bacteria) could not ensure proper nutrient recycling and exchange, and to keep an environment more representative of the pelagic communities.

To measure phosphorus levels, 50 ml of water from the mesocosms were collected using a triple rinsed syringe, to which was added a 0.45 µm syringe filter. The collected water was contained in sterilized plastic cap vials. The phosphorus measurement was carried out according to Wetzel and Likens (2000) protocol. Readings were done by spectrophotometry at a wavelength of 890 nm and compared to a standard curve. Conductivity, salinity, pH, temperature and dissolved oxygen were measured with a YSI multi-parameter probe (model 10102030; Yellow Springs Inc., USA). Chloride (Cl^-) concentrations were first assessed after NaCl addition from samples collected following a triple bottle rinsing and kept at 4°C. Analysis was carried out using Dionex DX-600 Ion Chromatography (Pfaff, 1993). Further Cl^- concentration were extrapolated from the conductivity values measured with the YSI probe following a regression carried out linking the conductivity and Cl^- (see Astorg *et al.*, 2022).

2.2.3 Filtration, DNA extraction and dPCR

The water samples were filtered with 0.2 µm polyethilsulfone filters (Sartorius, Germany). We used the Dneasy PowerWater® kit (Qiagen, 2017) to extract DNA from the filters. The DNA was stored at -20°C until use. Absolute abundance based on the copy number of the 16S and 18S rRNA genes contained in each sample was determined with digital PCR (dPCR) (Applied biosystems by Life technologies). dPCR was carried out using a QuantStudio ™ 3D device (Thermofisher Scientific, N.D) using SYBR® Green dye, adapting the methodology provided by ThermoFisher (Thermofisher Scientific, 2014) for a volume of 1 µl DNA sample per chip. We measured absolute abundance of Archaea, Bacteria, and Eukaryotes (using DNA recovered from the Astorg *et al.*, 2022). The DNA samples from the different mesocosms were diluted to different concentrations

(1/25, 1/50) in bacteria and eukaryotes, in order to avoid overloading the chips and thus optimize their reading. The samples used in the context of the archaeal dPCR were not diluted. dPCR was performed using the bacterial primer pair B341F (5 '-CCTACGGGIGGCIGCA-3') and B785R (5'-GACTACHVGGGTATCTAATCC-3 ') (Sun *et al.*, 2020), and archaeal pair A340F (5'-CCCTAYGGGGYGCASCAG -3 ') and A915R (5'-GTGCTCCCCCGCCAATTCCT-3') (Lazar *et al.*, 2017).Details about chip loading mixture, primers, and cycles steps are provided in Tables 2.7.S1 and 2.7.S2. (Supplementary Material).

2.2.4 Sequencing and sequence processing

The 16S rRNA gene sequencing was carried out using the same primers as for dPCR, at the Center of Excellence in Research on Orphan Diseases platform (Department of Biological Sciences, UQAM) using Illumin Miseq. The raw sequence data was deposited in NCBI Sequence Read Archive, accession numbers SAMN17917512 to SAMN17917568. All analyses using the 18S rRNA gene diversity are based on data available in Astorg *et al.* (2022). The sequences obtained were analyzed using the mothur software (v.1.44.3 Schloss *et al.*, 2009), and were classified using the SILVA database v.138. Archaeal classification was further implemented with reference sequences from Liu *et al.* (2018) and Zhou *et al.* (2018). The sequences were grouped into operational taxonomic units (OTU) by grouping sequences with more than 97% similarity. When needed, OTU tables were rarefied to 19,582 reads for the bacterial 16S rRNA gene datasets. Archaeal 16S rRNA gene reads were too low for rarefaction and subsequent statistical analyses.

2.2.5 Statistical analyses

Statistical analyses were run using R software (Team, 2020). The α diversity indices (Shannon H) were obtained with the raw OTU tables, using the *Phyloseq* package (Bioconductor v3.12 ; McMurdie & Holmes, 2013) using the *plot_richness* function, and the values were used as a dependent variable in linear regressions, with Cl^- values as the independent variable, to see how much variance can be explained by salinity on diversity variation. To test for differences between 3- and 6-weeks' exposure to the salinity gradient, in absolute abundance numbers and α diversity indices, we carried out Mann-Whitney-Wilcoxon tests using the *wilcox.test* function in R. Spearman correlations between class/order relative abundances on the 500 most abundant taxa and

Cl^- concentrations were performed using the *Phylosmith* function (Smith, 2019), using rarefied and Hellinger transformed OTU tables, to see the relationship between major taxa and salinity.

We used distance-based redundancy analysis (db-RDA) to determine which variables had a significant impact on bacterial community composition (ß diversity). The bacterial OTU table was Hellinger transformed and used to calculate a Bray-Curtis dissimilarity distance matrix. The explanatory variables included the environmental parameters (total phosphorus, salinity, pH, temperature, dissolved oxygen, and chloride), as well as absolute abundance numbers of Eukaryotes, Archaea and Bacteria, and eukaryotic community composition. Indeed, not only abiotic factors influence bacterial community composition, but also biotic factors such as the absolute abundance of other microbes present, or the Eukaryotes present which can act as predators or positively interact with the bacterial community. For this analysis, the eukaryotic community composition was represented using the scores of the first 2 axes of a PCoA ordination using 18S rRNA gene datasets available in Astorg *et al.* (2022). Non-normal variables were box-cox transformed to approach a normal distribution. The db-RDA was applied to the distance matrix and the set of explanatory variables using the *capscale* function of the vegan package in R, and significance of explanatory variables was assessed with the *anova* function in R software with 200 permutations. The unique and shared contributions of each significant explanatory variable to bacterial community composition was determined using variance partitioning with the *varpart* function of the vegan package in R.

We used the linkage tree analysis (LINKTREE) of the PRIMER v.6 software package (Clarke & Gorley, 2006), to correlate thresholds of explanatory variables with bacterial community composition (ß diversity) partitioned into groups (or clusters), based on a Bray-Curtis dissimilarity distance matrix. We used the explanatory variables that were shown to be significant after the db-RDA, and the Hellinger-transformed OTU table. Differences between 2 groups formed at each division are quantified with ANOSIM R statistics (Clarke & Green, 1988). R provides a measure of the degree of separation of 2 sample groups and are variable at each step of the partition sequence, and because R is a linear function of the average rank dissimilarity between sample groups, the original rank dissimilarities during the first ranking step of the entire dataset are plotted on the y-axis using a % scale (B%) (Clarke *et al.*, 2008). The normalized bacterial OTU table was

used to produce a Principal Coordinate Analysis (PCoA, Phyloseq package) to view structural differences between samples, using Bray-Curtis as a dissimilarity index, showing the clusters created within the LINKTREE analysis for better visualisation.

To test whether bacterial community composition varied significantly depending on exposure time (3 or 6 weeks) and the sample clusters that were determined with the LINKTREE analysis, we ran permutational multivariate analyses (PERMANOVA) on the rarefied OTU tables in R, using the *adonis* function of the *vegan* package (Oksanen, 2007).

We determined which community was a source to the bacterial communities exposed to the salinity gradient after 6 weeks (T6), using fast expectation-maximization for microbial source tracking (FEAST ; Steinberger, 2020) in R, based on the raw OTU tables without transformation. For each bag, the sample from T6 was treated as a sink, and the corresponding sample at T3 as well as the T0 sample (initial lake water used to prepare the mesocosms) were considered as a source. Finally, we identified which OTUs differed significantly between clusters identified in the LINKTREE analysis using a similarity percentage analysis (SIMPER) with a Bray-Curtis matrix, combined with a Kruskal-Wallis test ($\alpha = 0.05$). The SIMPER analysis and the Kruskal-Wallis tests were produced using the *Simperpretty* and *Rkrusk* functions (Shenhav *et al.*, 2019) of the *vegan* package.

2.3 Results

All the temperature, conductivity, salinity, pH and DO values established using the YSI probe in the mesocosms at T0, as well as the Cl^- values measured for that sampling time are presented in Table S3. The temperature values, pH, Cl^-, TP, DO, absolute bacterial, archaeal and eukaryotic abundances, as well as bacterial, archaeal and eukaryotic diversity indice for T0 are available in Table S3, while values for T3 and T6 are made available in Table 2.7.S4. The values for the two main axes of the eukaryotic PCoA, representing eukaryotic beta diversity and further used within the frame of the db-RDA and LINKTREE, are available in Table 2.7.S5.

2.3.1 Archaeal absolute abundance and 16S rRNA gene diversity

The recovered number of archaeal sequences was extremely low for half the samples (below 100 reads); therefore, we could not carry out any statistical analyses on the archaeal 16S rRNA gene datasets. Absolute abundance numbers were low (229 to 4824 gene copies/L^{-1}) and were not significantly different between weeks 3 and 6 (Mann-Whitney-Wilcoxon, p=0.16). Regressions carried out on archaeal absolute abundance and Cl^- (Figure. 2.7.S2a) were not significant (p=0.5229 for T3 and p=0.662 for T6), while the regression carried out between archaeal absolute abundance and eukaryotic diversity (Figure. 2.7.S3a) resulted in an R^2 of 0.0024 (p=0.9005) for T3 and 0.0293 (p = 0.6596) for T6. Regression carried out on archaeal diversity and Cl^- are available in Figure 2.7.S2b, resulting in an R^2 of 0.4273 (p=0.05621) after 3 weeks (T3) and 0.3495 (p=0.09363) after 6 weeks (T6), while the regression carried out between archaeal diversity and eukaryotic diversity (Figure. 2.7.S3b) resulted in an R^2 of 0.4203 (p=0.05897) for T3 and 0.3448 (p=0.09644) for T6. All regressions statistics are supplied in Tableau Annexe A1.

The T0 sample (lake water used to fill the mesocosms) was the only sample containing a high number of reads (25,085), and was dominated by Woesearchaeota subgroups 5a and 5b, and 8, unclassified Woesearchaeota, Methanoregula and Micrarchaeales (Fig. 2.7.S4a). The low absolute abundances and gene reads recovered in the subsequent mesocosms experiences highlight a high sensitivity of the Archaea to the addition of salt and/or incubation. For the mesocosms exposed to the salt gradient after 3 weeks, we show results for samples S0 (132 reads) and S05 (351). The sample which was not amended with salt (S0) showed a shift to a dominance by Woesearchaeaota subgroup 24, and sample S05 was dominated by the Rice Cluster I and the Woesearchaeaota subgroup 24. For the mesocosms exposed to the salt gradient after 6 weeks, we show results for samples S03 (214), S05 (171), S11 (348), S13 (643), S15 (233) and S20 (305), highlighting a higher number of reads recovered after 6 weeks exposure, and in mesocosms with a higher amount of salt than week 3. Samples S03 to S13 were dominated by candidatus Nitrosotalea, whereas sample S15 was dominated by Woesearchaeota subgroup 8, and sample S20 was dominated by Bathyarchaeota subgroup 6, Woesearchaeota subgroup 5a and 5b, and Methanoregula.

2.3.2 Bacterial absolute abundance, alpha diversity indices, and 16S rRNA gene diversity

Bacterial absolute abundance values varied from 4.38×10^7 to 7.03×10^8 gene copies/L, 4 orders of magnitude higher than that for the archaea (Table S4). Furthermore, the absolute abundances were not significantly different between weeks 3 and 6 (Mann–Whitney–Wilcoxon, p=0.094). Regressions for bacterial absolute abundances and Cl^- (Figure. 1a) resulted in an R^2 of 0.5469 (p=0.02276) at T3 and 0.0043 (p = 0.8669) at T6, showing that Cl^- explained 54.7% of the variance in absolute abundance after 3 weeks, and 0.4% of the variance after 6 weeks. Regressions for bacterial absolute abundances and eukaryotic diversity (Figure. S5a) had an R^2 of 0.2063 (p=0.2194) at T3 and 0.0019 (p = 0.9112) at T6.

Alpha diversity indices (Table 2.7.S4) were not significantly different between weeks 3 and 6 (p=0.86), showing that longer exposition time to an exogenous input of salinity did not significantly change diversity or abundance of Bacteria after 3 weeks of exposure. The regression between bacterial diversity and Cl^- (Figure. 2.6.1b) showed an R^2 of 0.1661 (p=0.2763) and 0.1664 (p=0.2757) at T3 and T6, respectively. While bacterial diversity and eukaryotic diversity (Figure. 2.7.S5b) had an R^2 of 0.1458(p=0.3106) after 3 weeks and 0.319 (p=0.1131) after 6 weeks. All regressions statistics are supplied in Tableau Annexe A1.

In T0 sample, the community composition (Fig. 2.7.S6) was dominated by Actinobacteria and Gammaproteobacteria, as well as a noticeable percentage of the relative abundances of Alphaproteobacteria and Bacteroidia. Across the salinity gradient, both at T3 and T6, Actinobacteria were part of the dominant taxa in samples S0, S03, S05 and S08, but were scarcer at higher salinity, while Alphaproteobacteria were shown to gradually increase through the gradient, becoming the dominant taxa in samples S11, S13, S15 and S20, both for T3 and T6 samples. Other taxa, such as Bacteroidia and Gammaproteobacteria showed inconsistent variation through the samples. Bacteroidia became more dominant in samples S15, S18 and S20 of T6, but were also very present in samples S0 and S05 of the same sampling time. For T3, however, their relative abundance followed a similar pattern in all samples, which were similar to the values in T0. Gammaproteobacteria presented positive variations through the salinity gradient, but the most

abundant order, Burkholderiales, was seen to have a decreasing relative abundance along the gradient, thus representing a transition of the dominant order within this class.

2.3.3 Correlation between bacterial taxa relative abundances and chloride levels

The Spearman correlation performed between the values of Cl^- and the 500 most abundant bacterial taxa, at the class (Fig. 2.7.S7a) and order (Fig. 2.7.S7b) levels, presents a very strong significant and positive relationship ($p \leq 0.001$) for Alphaproteobacteria, but a very strong significant negative relationship ($p \leq 0.001$) for Gammaproteobacteria, Oligoflexia and unclassified Proteobacteria. Planctomycetes and Actinobacteria showed a significative strong negative relationship ($p \leq 0.01$), while Verrucomicrobiae, Thermoleophilia, SL56 Marine group and Bacteria (Unclassified) showed a significant ($p \leq 0.05$) negative relationship to Cl^- values. The tests were significant for samples after 3 weeks, but not for samples after 6 weeks.

2.3.4 Correlation between bacterial beta diversity and abiotic factors

The db-RDA (Fig. 2.6.2a) indicated that salinity and eukaryotic community composition were strongly and significantly correlated to the bacterial community composition (p=0.001, Table S6), and that TP (p=0.012), temperature (p=0.017) and absolute abundance of eukaryotes (p=0.044) were also significantly correlated to bacterial community composition. We used variance partitioning to evaluate the unique and shared contributions of salinity, eukaryotic community composition and absolute abundance of eukaryotes to bacterial community composition (Fig. 2.6.2b). Taken together, these factors explained 29.4% of the overall variation, with eukaryotic community composition describing it the best (12%), salinity explained 5.6% and absolute abundance of eukaryotes explained 2.1%. Salinity and eukaryotic community composition had shared components explaining 9.8% of the mesocosm bacterial population variation.

Clustering of samples with the LINKTREE analysis (Fig. 2.6.3) highlighted a total of 7 nodes, which were the regrouped in four clusters (K1, K2, K3 and K4) for further analysis. Node G divides the highest salinity samples at week 3 (T3S15, T3S18, T3S20) and week 6 (T6S15, T6S18, T6S20), and was explained by lower temperatures at week 3 compared to week 6, higher total phosphorus concentrations at week 3, higher eukaryotic absolute abundances at week 3, and differences in

eukary-otic community composition. This division was then taken to create cluster K4 and K3. Node A divides the samples between S0 to S13 and S15 to S20 and was explained by differences in eukaryotic community composition and higher salinity for samples S15 to S20. Node B divides the samples between mid-salinity (T3S11, T3S13 and T6S13) and low salinity (T0, T3S0, T3S05, T3S08, T6S0, T6S03, T6S05, T6S08 and T6S11) and was explained by salinity. Samples T3S11, T3S13 and T6S13 were grouped together to cre-ate cluster K2. Nodes C, D, E and F further divide samples within the K1 cluster (T0, T3S0, T3S03, T3S05, T3S08, T6S0, T6S03, T6S05, T6S08 and T6S11), which is the group exposed to the lowest salinity. Node C divides samples from week 3 and week 6 and was explained by lower temperatures at week 3 compared to week 6. Node D isolates samples T3S08 from samples T0, T3S0 and T3S05 and was explained by salinity, temperature, and eukaryotic community composition differences. Node E further isolates sample T0 from samples T3S0, T3S03 and T3S05 and was explained by a lower temperature at T0 and eukaryotic community composition differences. Finally, node F divides samples T6S0, T6S03, T6S05 and T6S08, T6S11 and was explained by salinity differences. Nodes D, E and F show that bacterial community composition in meso-cosms exposed to low salinity were closer to the initial freshwater lake community at week 3 than week 6 and is explained mostly by differences in temperature and eukaryotic community composition. A visualisation of the dissimilarity (Bray-Curtis) between bacterial communities by samples and the clustering realised following the Linktree analysis is provided within the framework of a PCoA (Fig. 2.7.S8), with the first axis explaining 33.18% of the variation, while the second axis accounted explained 15.36% of the variation.

Salinity groups (based on the 4 groups defined in the LINKTREE analysis) explained half of the variation in the bacterial mesocosms (PERMANOVA; $R2=0.49$, $p=0.001$), whereas exposure time explained an additional 11% of the variation ($R2=0.11$, $p=0.002$) (Table 2.7.S7), indicating that most of the variation occurring in the mesocosms was due to the addition of salt, and that bacterial populations in each salinity group had distinct community structures.

2.3.5 Microbial source tracking

In order to establish the contribution made by the bacterial communities present in the initial water sample (T0) and after three weeks (T3) on those present after six weeks (T6), a Fast expectation-maximization microbial source tracking analysis (FEAST) was performed (Fig. 2.6.4). In mesocosms S0 to S13 of T6, a contribution varying between 2.63% and 48.13% was made by the bacterial communities coming from T0, and between 6.98% and 48.55% coming from the communities after three weeks, thus leaving between 33.72% and 68.74 % of community contribution associated with an unknown source. For samples S15 to S20, little or no (<1%) contribution from T0 communities was observed, and only 2.78% to 13.88% would be related to T3 communities, thus leaving between 86.12% and 97.06%% from an unknown source.

2.3.6 Significantly different OTUs between bacterial sample groups

The results of the SIMPER and Kruskal-Wallis analysis carried out on the clusters identified in the LINKTREE analysis (Table S8). These cluster are G1(T0, T3S0, T3S03, T3S05, T3S08, T6S0, T6S03, T6S05, T6S08, T6S11), K2 (T3S11, T3S13, T6S13) K3 (3S15, T3S18, T3S20) and G4 (T6S15, T6S18, T6S20). The difference in transitional contributors between the four clusters constitutes an indicator of the difference in the mesocosm community composition, as well as their relative abundance. Between cluster K1 and K2, 3 OTUs associated to Actinobacteria (Frankiales, Micrococcales, Corynebacteriales) were shown to differ significantly, but only 2 of them remained (Frankiales, Micrococcales) after correction for false discovery rate (fdr). Between cluster K1 and K3, 5 OTUs associated to Actinobacteria were identified (2 Frankiales, 2 Micrococcales). Two others belonged to the Burkholderiales, and 1 to Bacteroidia (Flavobacteriales), and 2 belonged to Alphaproteobacteria (Azospirillales, Ferrovibrionales). Another OTU, associated to Gammaproteobacteria (Pseudomonadales) showed a significant differentiation that did not stand after fdr correction. Finally, between K1 ans K4, 5 OTUs associated to Actinobacteria (Micrococcales, Corynebacteriales, three Frankiales), 2 to Alphaproteobacteria (Rhizobiales, Ferrovibrionales), 1 to Burkholderiales and 1 to Bacteroidia (Cytophagales) were identified as significantly differing between clusters.

2.4 Discussion

Our study sought to determine the effect of sodium chloride on freshwater prokaryotic communities. Although microbial community transitions in estuaries are well studied, few of them focus on pristine freshwater environments affected by salinization, particularly at concentrations approaching both Canadian and American chronic and acute chloride exposure regulations. We analyzed the effect generated by the sodium chloride gradient on the absolute abundance, diversity and structure of archaeal and bacterial communities. To do this, the concentrations of Cl^- were considered, rather than NaCl, in order to standardize with the literature and to better consider the mobility of Cl^- (MTQ, 2019). We also chose to include the effect of absolute abundance, α- and ß-diversities of eukaryotic communities on the prokaryotic communities, as they can be potential predators of prokaryotes and have an impact on their activities (Pernthaler, 2005 ; Jousset, 2012).

2.4.1 Direct and indirect effect of salinity on prokaryotic communities

For the Archaea, the values of Cl^- explained a very low rate of change in absolute abundance, both after three and six weeks. No significant difference was observed between week 3 and week 6. However, the high absolute abundance observed at the initial time (T0) compared to the salt-supplemented mesocosms suggests a strong sensitivity to salinization and/or to incubation, as well as the preference of some archaeal taxa for halophily, thermophilia, or a methanogenic lifestyle (Zou *et al.*, 2020).

Although the absence of archaeal taxa in some samples suggests an overestimation of diversity values, thus making it impossible to rule on the effect of Cl^- on archaeal diversity, the analysis of relative abundance nevertheless makes it possible to observe overall trends across the gradient. Among these, it is possible to see the persistence of Nanoarchaeota, present both at T0 and in multiple samples having undergone salt supplementation, even in samples with higher salinity. These organisms, known for their small size and their favoritism for interspecies association (John & Reysenbach, 2019), or even a parasitic/ectoparasitic way of life (Jarrell & Albers, 2019), have been found in several places in the world, and a study by Leoni *et al.* (2020) demonstrated their presence at salinities up to 145 ppt. It is therefore not surprising to find these organisms at various salinities, even higher ones. Another group present across the gradient, that of the Woesarchaeota,

is dominant at very low salinity but also seems to become more important at higher salinity, while the Bathyarchaeota group was found to be practically exclusive at the highest salinity samples. As such, the Bathyarchaeota therefore once again contribute to "maintaining the stability and adaptability of the archaeal community" (Zou *et al.*, 2020), but their global distribution has been linked to TOC rather than salinity, according to a study by Yu *et al.* (2017). On the other hand, the Crenarchaeota, represented by the Nitrosotalea, stood out particularly at lower salinity in T6, where their relative abundance revealed them to be a major taxon. Nevertheless, the presence of these autotrophic ammonia oxidizers is surprising since they would not normally be able to grow in a neutral pH environment (Prosser & Nicol, 2015), whereas the samples taking their presence into account presented a varying pH. between 6.82 and 7.75.

Our results did not allow us to conclude to an effect of salinity on bacterial diversity, with very little variability in the diversity indices observed after both exposure times. Such effect could be mediated by a variety of factors, including the transition of communities to adapted/acclimatized species. But as values are proximal and that no significant differentiation is present between sampling times, it could be hypothesized that major succession could have taken place soon after the introduction of NaCl in freshwater (weeks 0-3). Other variables, such as fluctuation in predation pressure and association with eukaryotic species, could have an influence, as well as viruses, known to be a main driver of variation in prokaryotic diversity (Pernthaler, 2005 ; Tang *et al.*, 2020).

As for bacterial abundance, our results established that the Cl^- levels significantly explained 55% of the variation in bacterial abundance, after three weeks. After six weeks, however, this relationship only explains 0.4% of the variation. With no significant difference in bacterial abundance between T3 and T6, the observable growth seen through the salinity gradient at both sampling times is indicative of an effect produced by the introduction of NaCl on bacteria in fresh water. Other dynamics can be hypothesized, including the development of taxa adapted to individual mesocosm conditions over a longer period of time, or the development of a top-down system, both of which would promote the general bacterial abundance growth observed after a 6-week period across the salinity gradient.

Increased chloride levels could promote the development of bacterial species that benefit from higher salinity and conductivity. The Alphaproteobacteria were significantly positively correlated to the values of Cl^-, and the observed relative abundance increase of this class across the salinity gradient clearly demonstrates that it benefits from these fluctuations. This effect could, however, be indirect. Bacterial communities may have benefited from the decrease in eukaryotic diversity, which is closely related to the increase in Cl^- (Dickman & Gochnauer, 1978 ; Cañedo-Argüelles *et al.*, 2013 ; Cañedo-Argüelles *et al.*, 2016 ; Environment Canada, 2001). This element would prove to be key in Alphaproteobacteria, represented mainly by Rhizobiales and Ferrovibrionales, because these can be heavily consumed by flagellates (Pernthaler *et al.*, 1997) and compensate for this phagotrophy by a high cell division. Also, these Gram-negative bacteria could particularly benefit from a loss of eukaryotic diversity, because some grazing organisms can favor the predation of certain species in particular, according to their size (Gonzalez *et al.*, 1990), their morphotype (Pernthaler, 2005), but also their composition, by actively avoiding the consumption of Gram-positive species to the detriment of the Gram-negative. If the observable loss of diversity suggests predation decline, the joint research carried out by Astorg *et al.* (2022) on the effect generated on eukaryotes shows a clear disappearance of any potential predators across the salinity gradient, in favor of algae belonging to the Ochrophyta group. Most rotifers and other zooplanktons taxa are absent from mesocosms at chloride levels higher than 40 mg/L^{-1}, showing that the benefits brought about by the absence of some predators are, however, only one element of a multifactorial environment favoring the microbial development, of which the presence of salt is certainly part of when the relative abundances of dominant bacterial taxa are considered.

Conversely, in Actinobacteria, variations were shown to be negatively and significantly correlated with Cl^- values. Lower predation pressure (Gram-positive), amplified by their small size (Jezbera *et al.*, 2005), would therefore imply that this class was mainly affected by the increasing concentrations of salt, rather than predation pressure. A final major group strongly and negatively correlated with Cl^- values and whose relative abundance reflects their importance is that of Gammaproteobacteria, mainly represented by the Burkholderiales (Betaproteobacteria). Under normal circumstances, the predation of Betaproteobacteria can be thwarted by the production of inedible filaments (Pernthaler, 1997), a strategy necessary to counteract their low rate of division. By combining the existence of a predation escape method and their low division rate with the

increase in Cl^- levels and the decrease in predation, it appears clear that the observable variation of Betaproteobacteria is, at least in part, generated by NaCl addition and not predation.

Furthermore, as eukaryotic species are affected by the salinity and begin to perish, their decay is mediated by multiple processes, including microbial activity (Jackrel *et al.*, 2019). The involvement of bacterial groups in decomposition processes, can contribute to their development, growth and community transition, as well as their overall absolute abundance (Alonso *et al.*, 2007 ; Kirchman, 2002). Indicators of such processes are put forward, in the first place, within the framework of the db-RDA, where it is possible to see the involvement of variables such as TP, eukaryotic abundance, salinity and eukaryotic beta diversity in the variation of bacterial communities, especially at higher salinities (708.09 to 1353.73 mg/L^{-1} Cl^-). Taken together the salinity, eukaryotic beta diversity and eukaryotic absolute abundance explain nearly 30% of the bacterial variance encountered in the mesocosms, and the eukaryotic beta diversity proved to explain on its own the highest proportion of variation (12%).

These same variables are shown to be, in the context of the LINKTREE analysis, strongly involved in the variations encountered across the gradient, but also between sampling times. Some factors, such as temperature, are involved in the variations encountered, but do not vary across the salinity gradient and therefore only represent evidence of the existence of a natural transition of microbial communities during seasonal fluctuations (Zhu *et al.*, 2019) and a demonstration of the incubation time. However, the marked effect of eukaryotic beta diversity in the subdivisions observed across the samples making up the representation of the salinity gradient and time shows that this variable constitutes a key element in the bacterial variation encountered. Although the effect of eukaryotic beta diversity was also present at low salinity, the inclusion of absolute eukaryotic abundance as an explanatory variable for differentiation at higher salinity ($\geq$708.09 mg/L^{-1} Cl^-) between T3 and T6 could be an indicator of the dynamics at play. Many bacterial species develop in association with phytoplankton, and some can contribute to the degradation of algal polysaccharides (Goecke *et al.*, 2013). With a eukaryotic abundance loss of up to 90% at higher salinity between the two sampling times, and the increased presence of Ochrophyta (Astorg *et al.*, 2022) occupying the higher salinity mesocosms, it can be hypothesized that active and decaying eukaryotic organisms,

together with salinity, are among the main influencing factors in the establishment of salt-tolerant bacterial communities.

2.4.2 Influence of salinity on bacterial community transition

We sought to determine a threshold salinity concentration from which a significant transition of communities is generated. We observed a differentiation generating four clusters in the LINKTREE analysis, which were also identified within the PCoA of bacterial communities. The first cluster (K1, T0, T3S0, T3S03, T3S05, T3S08, T6S0, T6S03, T6S05, T6S08 and T6S11) consists of mesocosms with bacterial communities proximal to initial bacterial communities (T0 ; B% ≤ 30.9), and whose Cl^- concentrations reach 354.84 mg/L^{-1} having incubated up to six weeks, concentrations that are greater than the Canadian (120 mg/L^{-1} Cl^-) and American (230 mg/L^{-1} Cl^-) chronic exposure standards. The proximity of samples up to 354.84 mg/L^{-1} compared to the control sample shows that compliance with this standard would ensure the absence of a significant transition of bacterial communities. The communities exposed to Cl^- concentrations varying from 420.02 to 572.71 mg/L^{-1}, mainly for a three-week incubation period, composed a second cluster (K2, T3S11, T3S13 and T6S13) showing a very highly significant differentiation from the first, low salinity one. Exposure to Cl^- concentrations ranging from 708.09 to 1353.73 mg/L^{-1} led to the formation of two clusters, one being composed of sample T3S15, T3S18 and T3S20 (K3 ; 825.45 to 1353.73 mg/L^{-1} Cl^-), while the second was composed of sample T6S15, T6S18 and T6S20 (K4 ; 708.09 to 1165.94 mg/L^{-1} Cl^-), differing from each other by the duration of exposure to salinity. Although these two higher salinity clusters do not differ significantly from each other, it could be hypothesized that a longer residence time of the ions in the medium would be able to bring such significance. Together, these clusters demonstrate the influence of salinity, with salinity groups explaining as much as 49% of the variation encountered, while exposure time explained 11%.

2.4.3 Microbial source tracking and overall procaryotic transitional community trends

As environmental variations are inherent to aquatic habitats, those disturbances can influence the transition of microbial communities (Shabarova *et al.*, 2021 ; Li *et al.*, 2020) and a microbial source tracking analysis showed that salinity would greatly influence the resulting composition of such transitions. At lower salinity (0.265 to 455.585 mg/L^{-1} Cl^-), a reasonable contribution (>30%) is

made by native communities (T0) and three-week salt-exposed communities (T3) in the community's composition after a six-week incubation. However, the communities exposed to 511.2 mg/L^{-1} Cl^- or more (T6S15, T6S18, T6S20) are devoid of native communities in their composition (>85% unknown source). Thus, past this threshold, salinized freshwater environments would be highly dependent on the presence of "seed banks" (Lennon & Jones, 2011 ; Wisnoski & Lennon, 2021) in maintaining bacterial diversity, and in the transition to halotolerant homologs that may play a role in potential eukaryotic association and decay, as previously mentioned.

An element that should be noted in our overall results is the inclusion of the S11 sample after six weeks incubation in the first cluster (K1), but also its placement within the LINKTREE and the important contribution made by native communities in its composition (FEAST), suggesting altogether that a partial recovery to "pre-disturbance" communities is not impossible at such salinities, an effect encountered as well by Hu *et al.* (2018) in an extreme salinization-desalinization experiment.

Studies carried out on estuaries (Cottrell & Kirchman, 2004 ; Bouvier & del Giorgio, 2002 ; Herlemann *et al.*, 2011) highlight the transition within these systems. Among these, the gradual transition of dominance of Alphaproteobacteria and Gammaproteobacteria, at the expense of Actinobacteria and Betaproteobacteria was be raised. Unexpectedly, a similar transition of these major groups could be observed in our lake samples and constitute the drivers for significant differentiation between the low and high salinity clusters, as demonstrated by the SIMPER/Kruskal-Wallis analysis. In the differentiation that occurs along the salinity gradient and between clusters, Actinobacterias relative abundance have shown to be a key player. As stated above, they were negatively correlated to Cl^- values, and were noticeably present within the framework of the aforementioned Simper/Kruskal-Wallis analysis. As samples collected are but a part of the total community within the mesocosm, there's no doubt that more species can be affected by NaCl introduction, in our study and in natural habitat, and that the observed effect across the salinity gradient, could potentially increase with time and with increasing salinity. While the bacterial transition in estuaries is majorly driven by hydrologic conditions (Bouvier & del Giorgio, 2002) and spring–neap tidal cycle (Khandeparker *et al.*, 2017), the implication of nutrient supply variations is nonetheless intrinsic to those notions. As freshwater lakes tend to have a longer

residence time, and that a link between microbial development, salinity, time and potentially eukaryotic decay was present in our study, the implication of nutrients fluctuations in community changes could represent a good research path to really understand the effect of freshwater salinization syndrome on microbial communities. Considering the increase in Alphaproteobacteria at higher salinity, with Rhizobiales as the main members, and that the latter may be associated with an increase in nutrients with the potential to induce acidification and hypoxia in oceanic environments (Lemos *et al.*, 2021), carrying out a longer-term study could also be appropriate to better consider the issues encountered in understanding the effect of salinity on microbial communities in lake environments.

2.5 Conclusions

Overall, no clear linearity between the introduction of NaCl and prokaryotic diversity was present in our study, after three and six weeks. However, a positive relationship appears to be present between NaCl and absolute bacterial abundance after three weeks. An increase in abundance was seen and amplified over time. Salinity clearly plays an important role in the observed bacterial abundance increase, as well as other potential factors, such as loss of eukaryotic diversity and the potentially associated decomposition. While our results show an effect of salinity on prokaryotic organisms, they also raise the existence of multifactorial dynamics. Some taxa may potentially be directly affected by salinity levels (ie: Actinobacteria, Burkholderiales), while others (ie: Alphaproteobacteria; Rhizobiales, Ferrovibrionales) could benefit from the loss of predation brought about by the loss of eukaryotic diversity. However, the increase in Ochrophyta, as demonstrated by the joint study by Astorg *et al.* (2022) also leaves room for potential associations between prokaryotes and phytoplanktons, active or decaying, and the variance explained by eukaryotic beta diversity on bacterial community variations suggests the same.

Furthermore, we were also able to observe that a significant transition in bacterial communities was present from a threshold of 420.02 mg/L^{-1} Cl^-, a level higher than the Canadian recommendations (120 mg/L^{-1} Cl^-) and American (230 mg/L^{-1} Cl^-) in terms of chronic exposure, and higher than the sensitivity threshold of other organisms (ie: zooplankton). Thus, compliance with the standards in place would be able to ensure the sustainability of freshwater prokaryotic

communities. While other transition thresholds were present, those operated at higher salinity suggest that they would not be possible without the presence of seed banks. Conversely, we did observe a partial recovery of "pre-disturbance" freshwater bacterial communities during a drop in salinity, which could only have been possible through "native" communities capable of resilience. Finally, a transition of dominance of Actinobacteria and Betaproteobacteria towards Alphaproteobacteria and Gammaproteobacteria could be observed during our study, and is in part similar to results obtained in the context of studies carried out in estuaries. Although these results hint at a possible long-term effect, consideration of nutrient variations in further studies may be essential to better understand the effect of freshwater salinization on microbial communities.

2.6 Figures

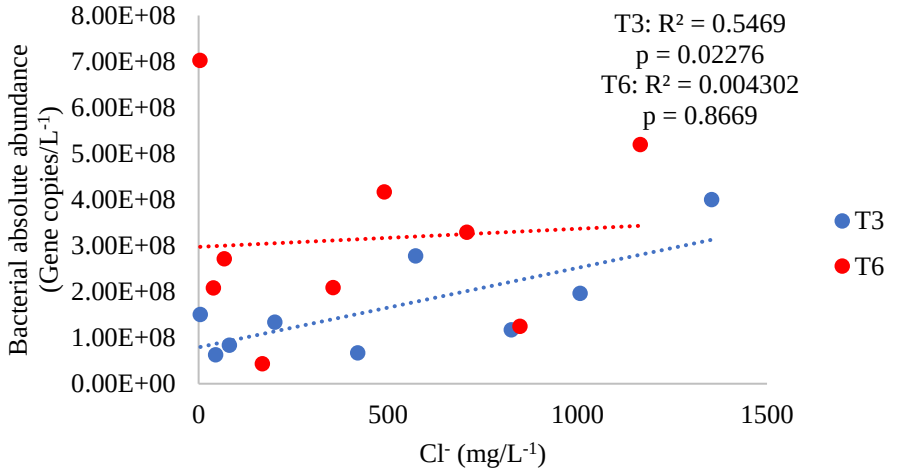

(a)

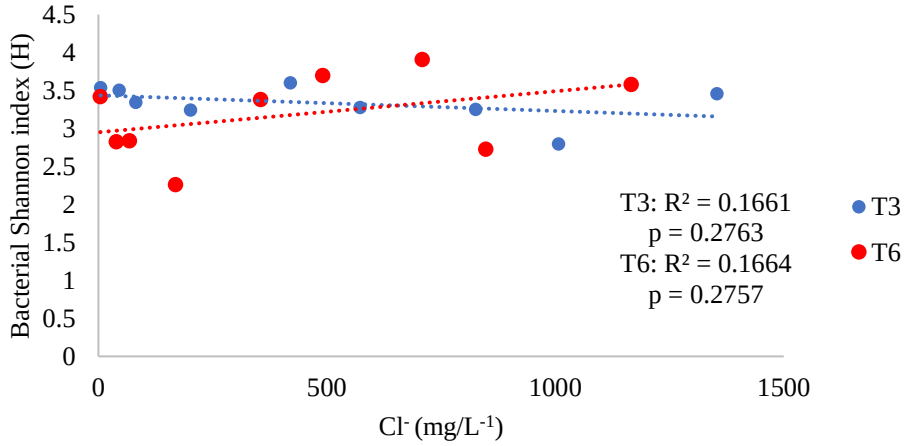

(b)

Figure 2.6.1. **(a)** Regression of bacterial absolute abundance and Cl^- in mesocosms at T3 and T6. **(b)** Regression of bacterial diversity (Shannon's H) and Cl^- in mesocosms after three (T3) and six weeks (T6) exposition.

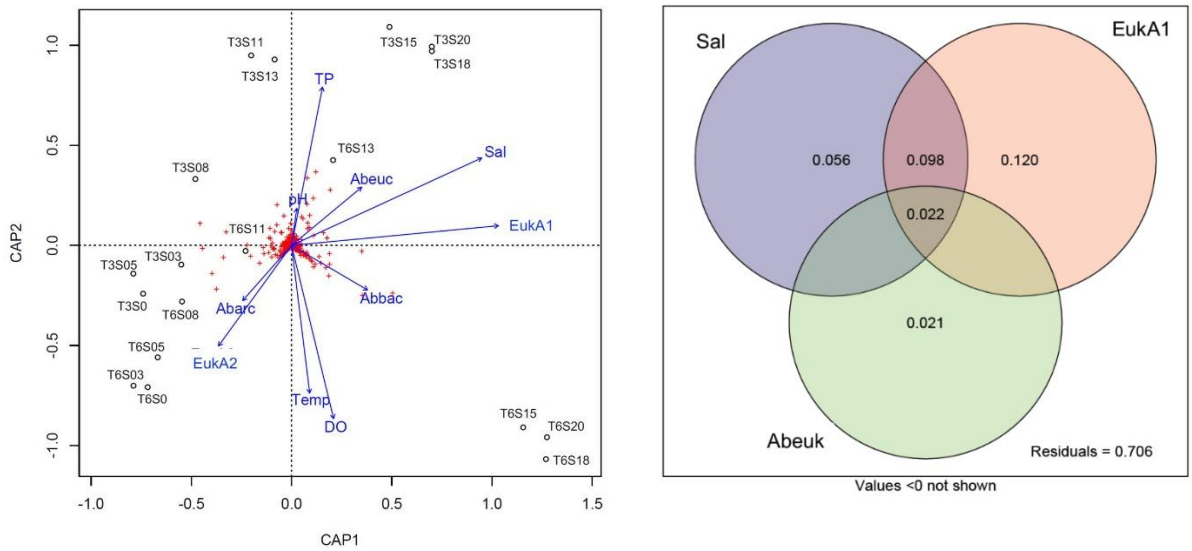

(**a**) (**b**)

Figure 2.6.2. **(a)** Correlation between bacterial mesocosm community composition and explanatory factors, using db-RDA. T3, 3 weeks exposure to the salinity gradient; T6, 6 weeks exposure; TP, total phosphorus; Sal, salinity; Temp, temperature; DO, dissolved oxygen; Abarc, absolute abundance of Archaea; Abbac, absolute abundance of Bacteria; Abeuk, absolute abundance of eukaryotes; EukA1, eukaryotic community composition represented by the first axis of a PCoA; EukA2, eukaryotic community composition represented by the second axis of a PCoA. **(b)** Variance partitioning analysis separating variation in bacterial mesocosm community composition between 3 explanatory variables: salinity (Sal), eukaryotic community composition represented by the first axis of a PCoA (EukA1), and absolute abundance of Eukaryotes (Abeuk). Values represent the portion of variation explained by the explanatory variables.

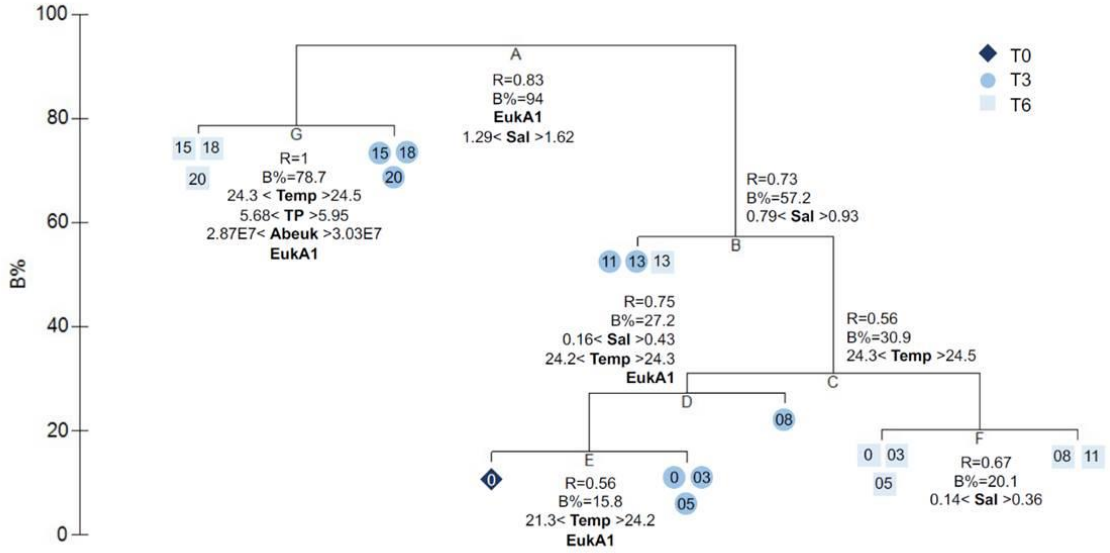

Figure 2.6.3. Linkage tree analysis showing clustering of bacterial mesocosm samples constrained by significant explanatory variables: TP, total phosphorus; Sal, salinity; Temp, temperature; Abeuk, absolute abundance of eukaryotes; EukA1, eukaryotic community composition represented by the first axis of a PCoA. For each cluster, R is the optimal ANOSIM R value (relative subgroup separation). The B% axis shows the absolute group separation which is scaled to maximum for first division.

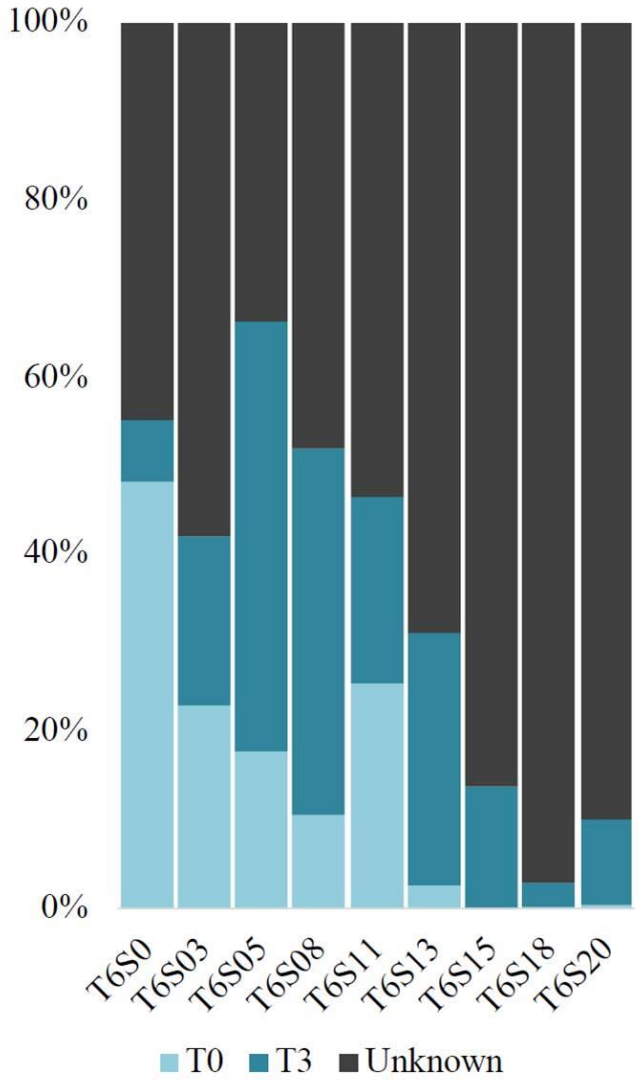

Figure 2.6.4. Bacterial source tracking of bacterial samples from week 6, carried out using FEAST. The source samples are the initial freshwater lake sample used to set up the mesocosms (T0), and the samples for each bag at week 3 (T3).

2.7 Supplementary material

2.7.1 Supplementary figures

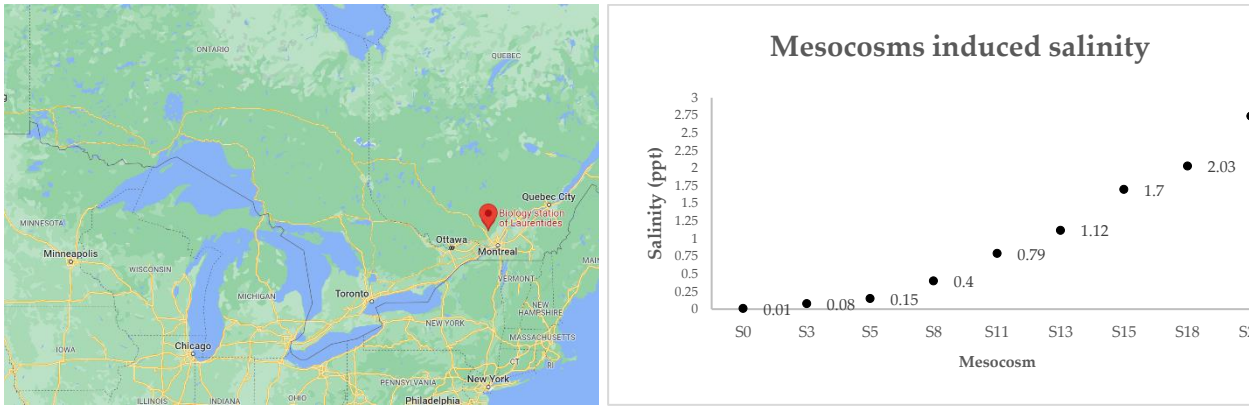

(a) **(b)**

Supplementary figure 2.7.S1. **(a)** Location of the Laurentians Biological Station, Quebec, Canada, site of the mesocosm installations. **(b)** Salinity levels in the mesocosms.

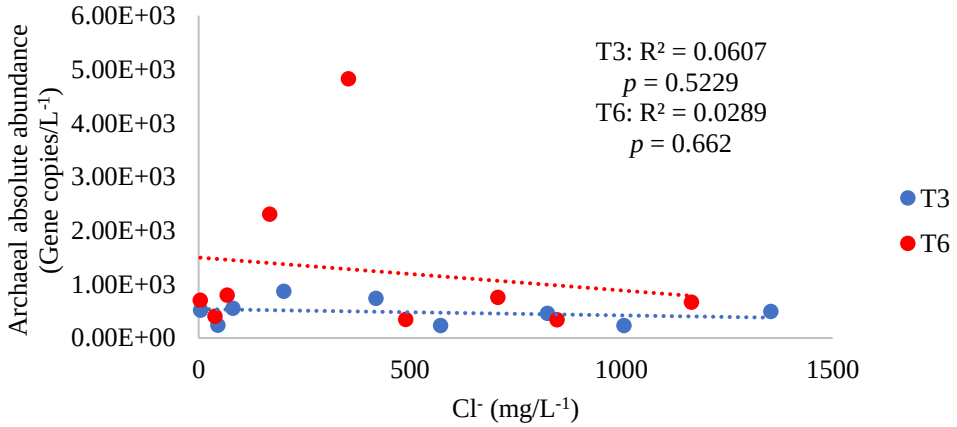

(a)

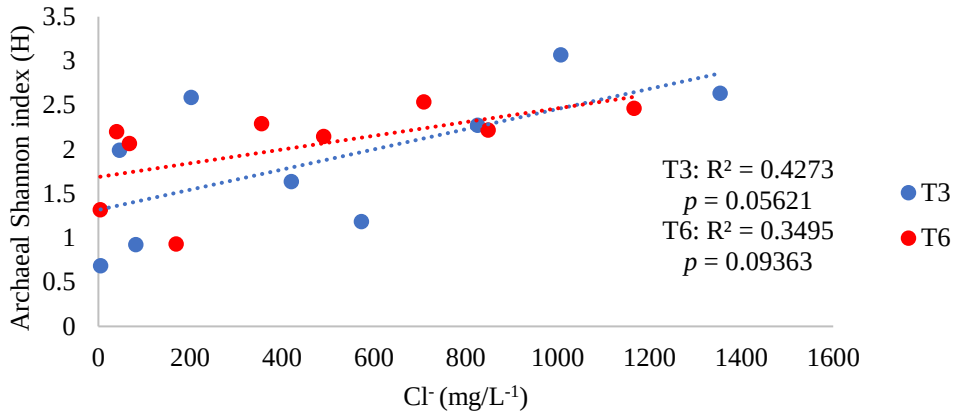

(b)

Supplementary figure 2.7.S2. **(a)** Regression of archaeal absolute abundance and Cl- in mesocosms at T3 and T6 **(b)** Regression of archaeal diversity indices (Shannon's H) and Cl- in mesocosms at T3 and T6.

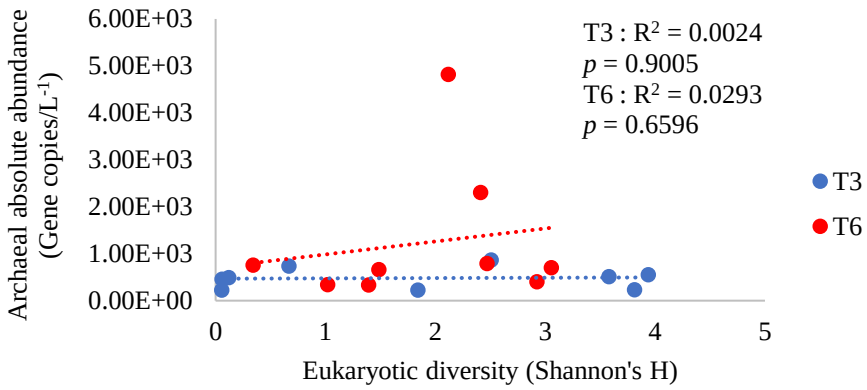

(a)

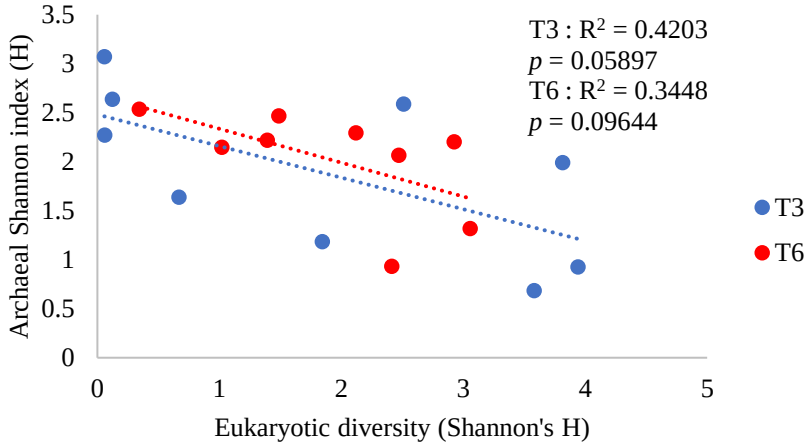

(b)

Supplementary figure 2.7.S3. **(a)** Regression of archaeal absolute abundance and eukaryotic diversity (Shannon's H) in mesocosms at T3 and T6. **(b)** Regression of archaeal diversity (Shannon's H) and eukaryotic diversity (Shannon's H) in mesocosms at T3 and T6.

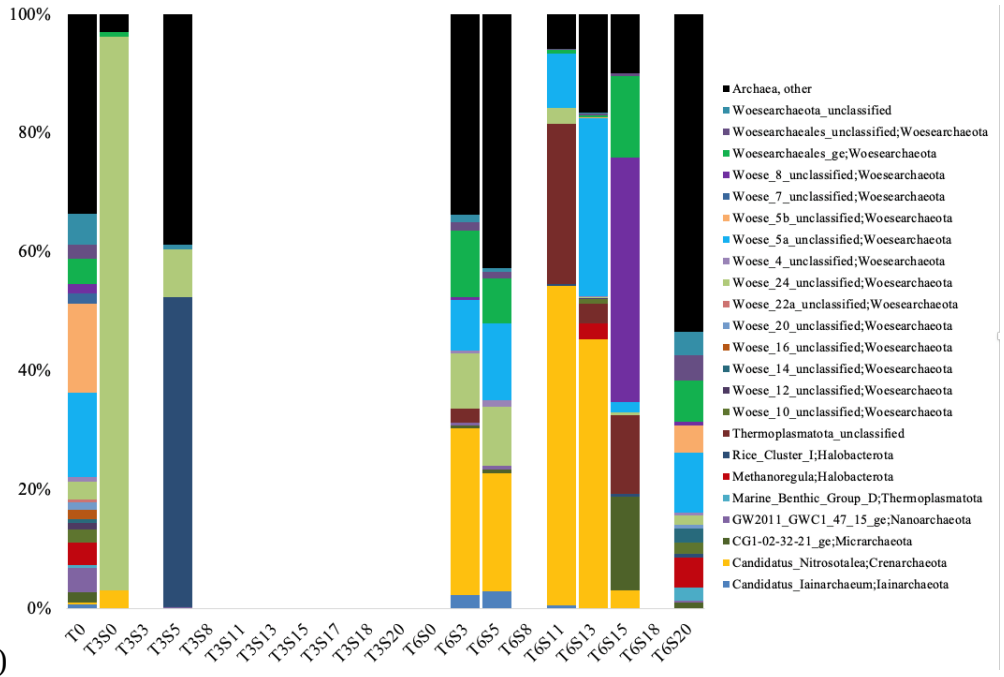

(a)

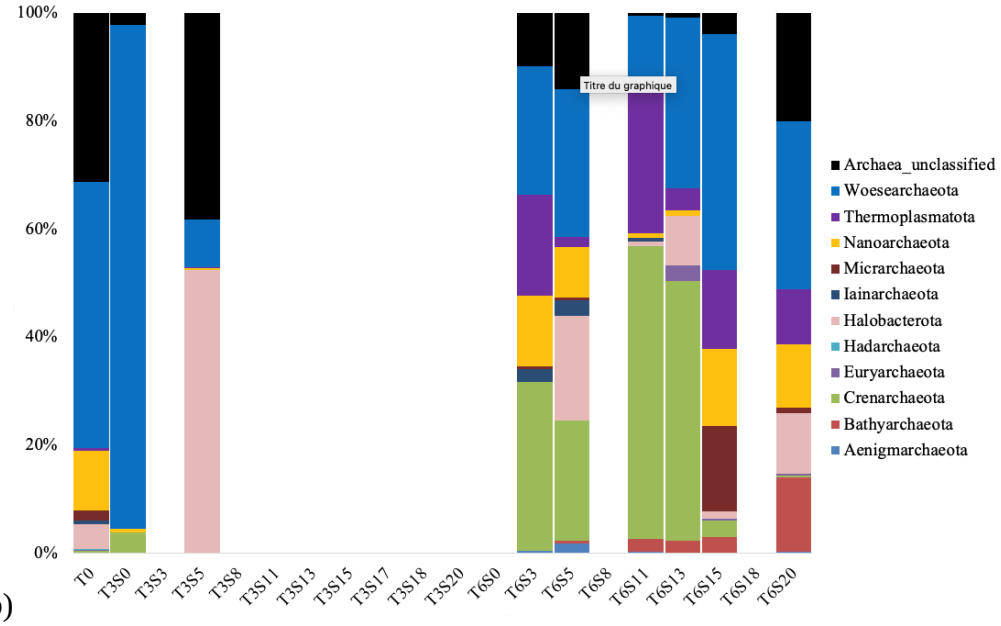

(b)

Supplementary figure 2.7.S4. Taxonomical classification of the archaeal 16S rRNA genes based on the SILVA database v.138. **(a)** Genus-level identification and ; **(b)** Phylum-level identification.

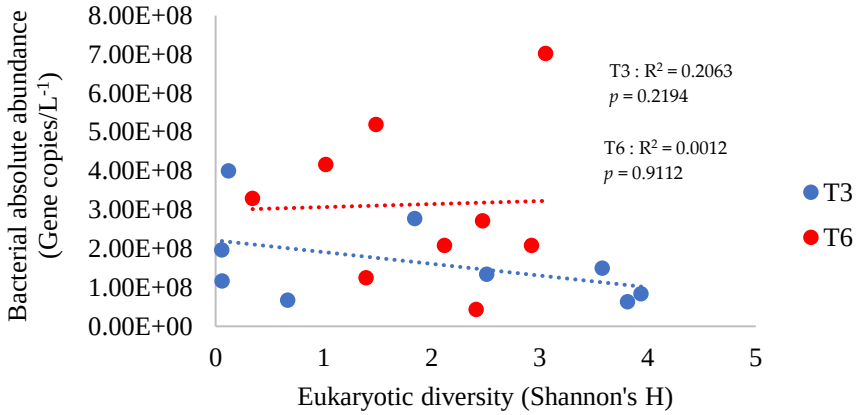

(a)

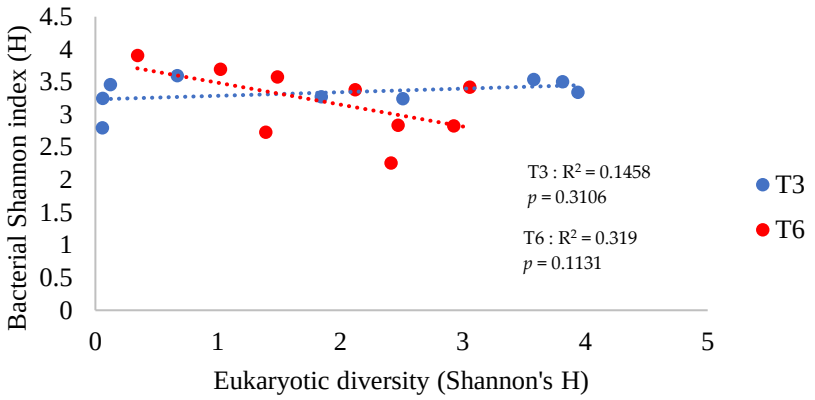

(b)

Supplementary figure 2.7.S5. **(a)** Regression of bacterial absolute abundance and eukaryotic diversity (Shannon's H) in mesocosms after three (T3) and six (T6) week incubation. **(b)** Regression of bacterial diversity (Shannon's H) and eukaryotic diversity (Shannon's H) in mesocosms after three (T3) and six weeks (T6) exposition.

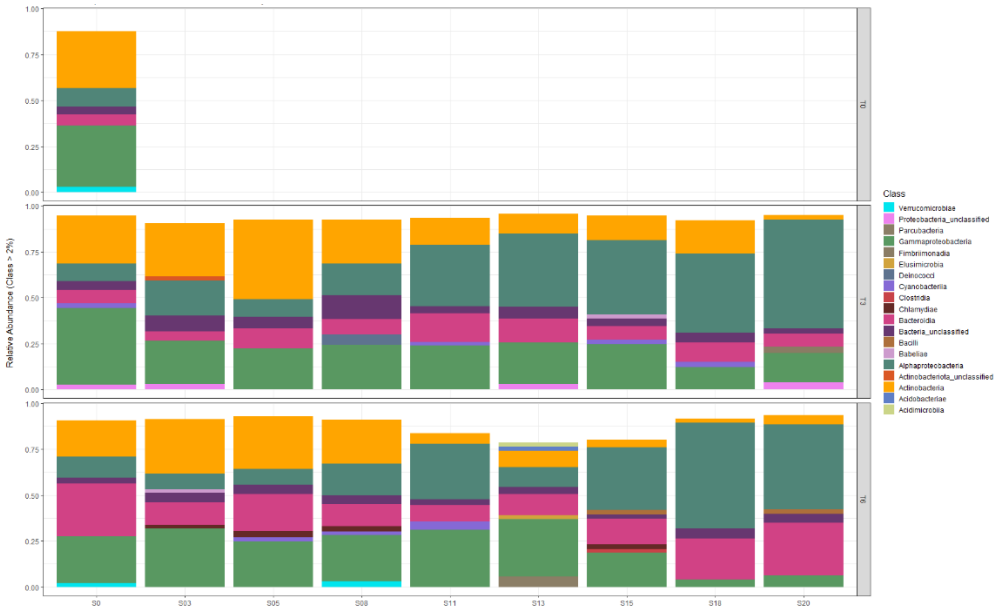

(a)

(b)

Supplementary figure 2.7.S6. Composition of bacterial communities representing a total of more than 2% at the level of **(a)** Classes and ; **(b)** Orders.

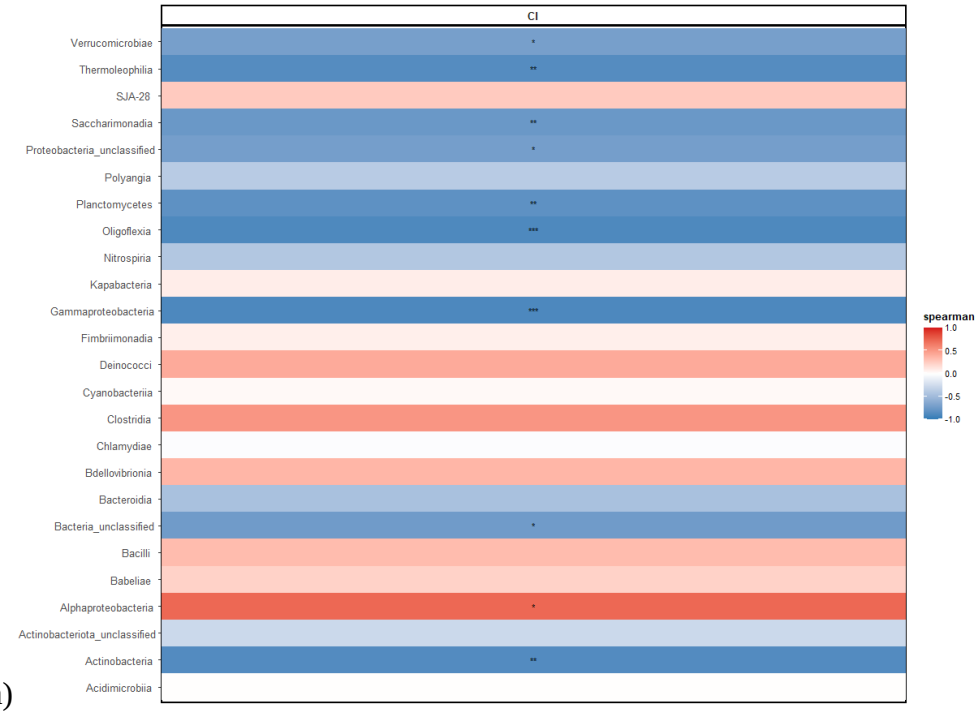

(a)

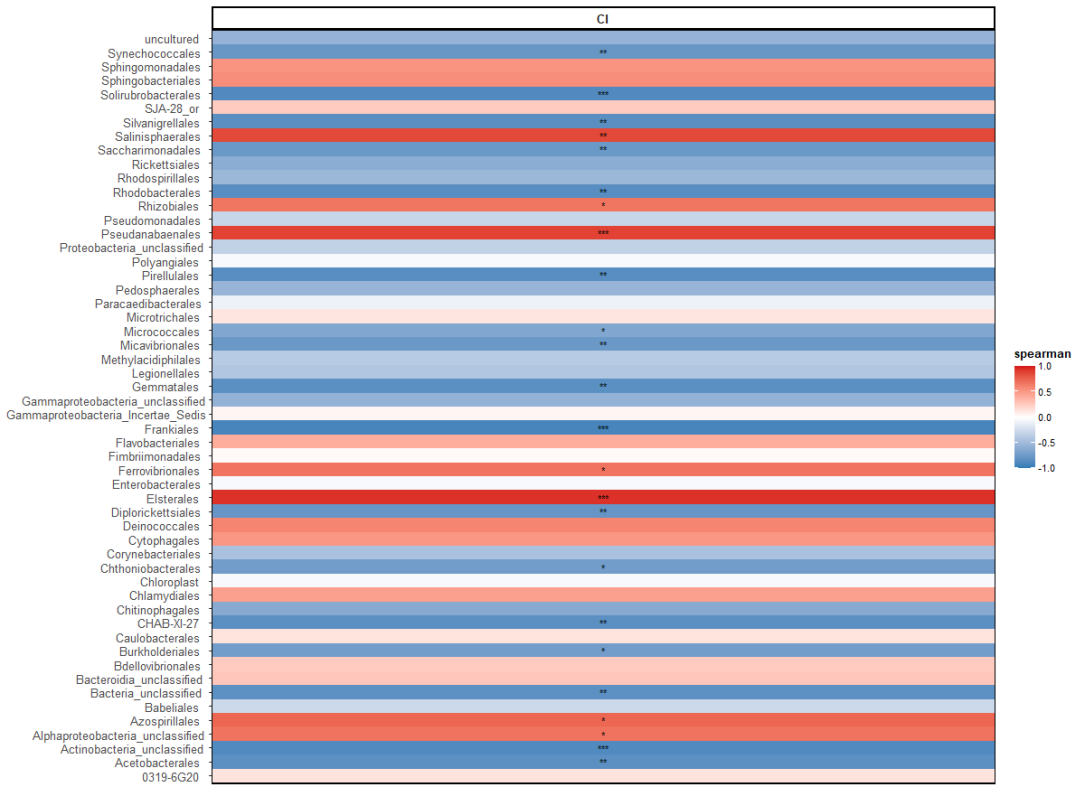

(b)

Supplementary figure 2.7.S7. Heatmap of correlations (Spearman) between Cl- values and the most abundant **(a)** classes and ; **(b)** order, representing the 500 most abundant taxa, in the mesocosms after three (T3) weeks incubation. None of the classes present showed significance after six (T6) weeks incubation, and were therefore not shown in the figure.

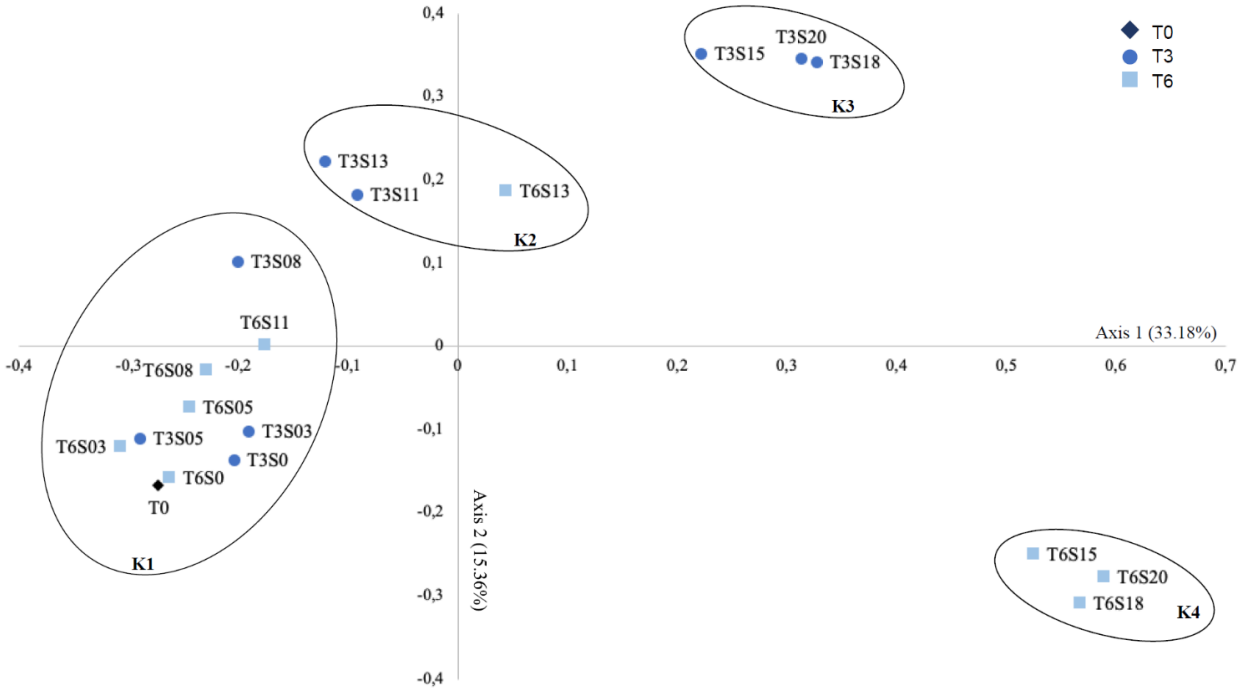

Supplementary figure 2.7.S8. Principal coordinate analysis based on a distance matrix between bacterial mesocosm communities. Variance explained by each axis is shown with the axis label. T3, 3 weeks exposure to the salinity gradient; T6, 6 weeks exposure.

2.7.2 Supplementary tables

Supplementary table 2.7.S1. Reaction mixture used for each chip in the context of dPCR.

Material	Volume per chip (µL)	Final concentration
QuantStudio™ 3D Digital PCR Master Mix	7.25	1X
20X SYBR Green 1 dye in TE buffer, pH 8	1.45	2X
Forward and reverse primer	0.3	200nM
cDNA sample	1	50ng total
Water	Bring to 14.5	-

Supplementary table 2.7.S2. Steps carried out during dPCR, depending on the primers used. The phases, temperatures, times and number of cycles are presented.

Eukaryotic primers E960F - NSR1438R				
	Phase	**Temperature**	**Number of cycles**	**Number of cycles**
Step 1	Initial denaturation	96°C	00:10:00	

				1X
Step 2	Denaturation Hybridization Elongation	58°C 98°C 60°C	00:02:00 00:00:30 00:02:00	39X
Step 3	Conservation	10°C	∞	1X

Bacterial primers B341F - B785R

	Phase	Temperature	Number of cycles	Number of cycles
Step 1	Initial denaturation	96°C	00:10:00	1X
Step 2	Denaturation Hybridization Elongation	56°C 98°C 60°C	00:02:00 00:00:30 00:02:00	39X
Step 3	Conservation	10°C	∞	1X

Archaeal primers A340F - A915R

	Phase	Temperature	Number of cycles	Number of cycles
Step 1	Initial denaturation	96°C	00:10:00	1X
Step 2	Denaturation Hybridization Elongation	58°C 64°C 60°C	00:02:00 00:00:30 00:02:00	39X
Step 3	Conservation	10°C	∞	1X

Supplementary table 2.7.S3. Water physico-chemical values measured using a YSI multi-parameter probe in the different mesocosms, at the beginning of the incubation, with measured Cl^- values, at T0.

Sample	Temp (ºC)	Cond (SPC)	Sal (ppt)	pH	DO (%)	Measured Cl^- (mg/L^{-1})
S0	21.3	17.4	0.01	6.26	99	0.265
S3	21.3	168.9	0.08	6.45	98.8	39.905
S5	21.3	305.5	0.15	6.68	99.3	106.675
S8	21.3	806	0.4	6.76	99.3	202.715

S11	21.4	1564	0.79	6.45	100.8	351.365
S13	21.3	2191	1.12	6.45	100.5	455.585
S15	21.4	2283	1.7	6.42	100.7	511.225
S18	21.4	3845	2.03	6.38	102.1	875.93
S20	21.4	5096	2.74	6.31	101.9	1110.86

Supplementary table 2.7.S4. Biotic and abiotic factor values used to carry out multivariate analyses, shown for every sample, composing the different mesocosms at the different incubation times. For T3 and T6 samples, Cl^- values were calculated following a linear regression using Cl^- (y) and conductivity (x) : (y= -1E-20*x^3 + 1E-16*x^2 + 0.2279*x).

Sample	Sampling time (week)	Temp. (°C)	pH	Cl- (mg/L^{-1})	Total phosphorus (µg.L-1)	Dissolved oxygen (%)	Bacterial abundance (Gene copies/L^{-1})	Eukaryotic abundance (Gene copies/L^{-1})	Archaeal abundance (Gene copies/L^{-1})	Eukaryotic diversity (H)	Archaeal diversity (H)	Bacterial diversity (H)
T0	0	21.3	6.26	0.27	3.574	99	111549000	12319200	1578	3.793332	4.883306	3.650698
T3S0	3	24.2	7.28	4.71753	2.945	96.3	150300000	17022000	514.8	3.579116	0.685688	3.537383
T3S03	3	24.2	7.26	45.3749	5.31	96.6	63334500	1539750	234	3.812996	1.99047	3.504182
T3S05	3	24.2	7.17	81.4743	7.23	96.2	83961000	2110800	552.6	3.938634	0.926154	3.341875
T3S08	3	24.3	6.98	201.692	4.033	97.3	133900500	2299875	870	2.508806	2.588274	3.242708
T3S11	3	24.5	6.7	420.02	7.36	96.8	67179000	29994900	738	0.668207	1.637801	3.598676
T3S13	3	24.3	6.77	572.713	8.38	94.4	277905000	19275000	229.8	1.842517	1.18385	3.274357
T3S15	3	24.3	7.64	825.454	12.99	97.7	116964000	30273000	456.6	0.058999	2.272586	3.249111
T3S18	3	24.2	7.32	1006.63	5.95	99.5	196560000	117834000	229.5	0.057467	3.07065	2.796754
T3S20	3	24.2	7.07	1353.73	7.93	94.2	400350000	95694000	494.4	0.120876	2.636184	3.457347
T6S0	6	24.6	6.87	4.07941	4.34	116.9	702945000	55291500	702.9	3.056106	1.31744	3.419336
T6S03	6	24.6	7.1	39.0393	4.085	115.3	208181250	18837000	401.85	2.924541	2.201943	2.825572
T6S05	6	24.6	7.06	67.5268	4.851	118.7	271800000	63058500	795.6	2.470229	2.066033	2.837106
T6S08	6	24.5	6.64	168.646	4.532	114.8	43832250	9610425	2304	2.413287	0.933618	2.260369
T6S11	6	24.6	7.75	354.84	4.723	119.8	208692000	33484950	4824	2.119586	2.293485	3.38135
T6S13	6	24.5	6.98	490.441	3.766	115.3	416790000	31560750	343.35	1.019819	2.148207	3.697428
T6S15	6	24.6	6.82	708.085	5.68	116.9	329305500	28736100	756	0.342372	2.536009	3.906411
T6s18	6	24.6	7.13	848.016	3.319	119	125055000	13992075	339.3	1.391766	2.218366	2.726809
T6S20	6	24.5	6.95	1165.94	4.085	117.6	519975000	9024750	665.1	1.486213	2.467024	3.577321

Supplementary table 2.7.S5. First 2 axes' values of a PCoA computed using the eukaryotic OTU table (the sequence data is available in Astorg *et al.* (2022).

group	axis1	axis2
T0	-0.198837	0.257246
T3S0	-0.207731	0.261959
T3S03	-0.222076	0.238455
T3S05	-0.280860	0.278656

T3S08	-0.297501	-0.419953
T3S11	-0.291871	-0.518987
T3S13	-0.034741	0.044833
T3S15	0.543059	-0.033957
T3S18	0.545052	-0.033708
T3S20	0.542808	-0.032694
T6S0	-0.208055	0.279988
T6S03	-0.255759	0.325092
T6S05	-0.209272	0.210855
T6S08	-0.225563	0.184650
T6S11	-0.297997	-0.445981
T6S13	-0.296064	-0.510137
T6S15	0.538738	-0.033616
T6S18	0.354396	-0.029152
T6S20	0.502275	-0.023549

Supplementary table 2.7.S6. Significant explanatory variables explaining bacterial mesocosm community composition variance, tested using db-RDA. Eukaryotic community composition was represented based on the scores of axes 1 and 2 (A1, A2) of a PCoA (see Table 2.S5).

	Df	**SumOfSqs**	**F**	**Pr(>F)**
Total Phosphorus	1	0.40077	2.1830	0.012
Temperature	1	0.41658	2.2691	0.017
Salinity	1	0.97199	5.2945	0.001
pH	1	0.20366	1.1094	0.317
Dissolved oxygen	1	0.26580	1.4478	0.126
Eukaryote community A1	1	0.55439	3.0198	0.001
Eukaryote community A2	1	0.21777	1.1862	0.244
Absolute abundance Eukaryote	1	0.32528	1.7718	0.044
Absolute abundance Bacteria	1	0.14999	0.8170	0.650
Absolute abundance Archaea	1	0.22345	1.2171	0.244

Chloride	1	0.20694	1.1272	0.299
Residual	6	1.10151		

Supplementary table 2.7.S7. Variation in bacterial mesocosm community composition explained by exposure time (3 and 6 weeks) and salinity groups (K1, K2, K3, and K4) defined in the LINKTREE analysis, tested using PERMANOVA.

	Df	**SumOfSqs**	**R2**	**F**	**Pr(>F)**
Exposure time	1	0.5952	0.11381	4.2359	0.002
Salinity group	3	2.5743	0.49223	6.1067	0.001
Exposure*Salinity	1	0.3742	0.07154	2.6627	0.003
Residual	12	1.6862	0.32242		
Total	17	5.2299	1.00000		

Supplementary table 2.7.S8. SIMPER and Kruskal-Wallis analysis table showing the OTUs that are significantly different according to the clustering established by the PCoA. The table shows the compared Clusters, the result of the SIMPER analysis, the OTU group, the initial Kruskal-Wallis *p*-value (Krusk.p.val) and corrected for false discovery rate (Fdr.krusk. p.val) and the taxonomy associated with UTO.

Clusters	**SIMPER**	**OTU**	**Krusk p.val**	**fdr_krusk p.val**	**Taxonomy**	**Left mean abund**	**Left stdev**	**Right mean abund**	**Right stdev**
K1 / K2	0.014965	Otu05	0.011230	0.028075	Bacteria(100);Actinobacteriota(100);Actinobacteria(100);Frankiales(100);Sporichthyaceae(100);Sporichthyaceae_unclassified(74);	0.025580	0.013154	0.002187	0.002308
K1 / K2	0.011071	Otu08	0.017960	0.038487	Bacteria(100);Actinobacteriota(100);Actinobacteria(100);Micrococcales(100);Microbacteriaceae(100);Microbacteriaceae_unclassified(84);	0.006505	0.002749	0.022223	0.012884
K1 / K2	0.010568	Otu04	0.027992	0.054367	Bacteria(100);Actinobacteriota(100);Actinobacteria(100);Corynebacteriales(100);Mycobacteriaceae(98);Mycobacterium(98);	0.027225	0.007603	0.010748	0.006358
K1 / K2	0.010234	Otu03	0.090969	0.097467	Bacteria(100);Actinobacteriota(100);Actinobacteria(100);Frankiales(100);Sporichthyaceae(100);hgcI_clade(88);	0.030314	0.023934	0.013330	0.005392
K1 / K3	0.017633	Otu12	0.005766	0.028075	Bacteria(100);Proteobacteria(100);Alphaproteobacteria(100);Azospirillales(98);Azospirillaceae(98);Azospirillum(96);	0.000386	0.000803	0.029241	0.026043
K1 / K3	0.016101	Otu02	0.011230	0.028075	Bacteria(100);Actinobacteriota(100);Actinobacteria(100);Frankiales(100);Sporichthyaceae(100);Sporichthyaceae_ge(75);	0.031136	0.016975	0.003542	0.001080
K1 / K3	0.015186	Otu03	0.011230	0.028075	Bacteria(100);Actinobacteriota(100);Actinobacteria(100);Frankiales(100);Sporichthyaceae(100);hgcI_clade(88);	0.030314	0.023934	0.003578	0.000382

K1 / K3	0.014947	Otu08	0.011230	0.028075	Bacteria(100);Actinobacteriota(100);Actinobacteria(100);Micrococcales(100);Microbacteriaceae(100);Microbacteriaceae_unclassified(84);	0.006505	0.002749	0.030731	0.014375
K1 / K3	0.014221	Otu10	0.026922	0.054367	Bacteria(100);Proteobacteria(100);Gammaproteobacteria(100);Pseudomonadales(100);Moraxellaceae(100);Acinetobacter(100);	0.005450	0.009761	0.027423	0.007042
K1 / K3	0.013751	Otu05	0.011230	0.028075	Bacteria(100);Actinobacteriota(100);Actinobacteria(100);Frankiales(100);Sporichthyaceae(100);Sporichthyaceae_unclassified(74);	0.025580	0.013154	0.002695	0.001554
K1 / K3	0.012012	Otu16	0.010897	0.028075	Bacteria(100);Proteobacteria(100);Gammaproteobacteria(100);Burkholderiales(100);Comamonadaceae(100);Ideonella(62);	0.001776	0.001284	0.021082	0.019667
K1 / K3	0.011699	Otu01	0.017960	0.038487	Bacteria(100);Proteobacteria(100);Gammaproteobacteria(100);Burkholderiales(100);Burkholderiaceae(100);Polynucleobacter(100)	0.037327	0.012281	0.017277	0.007419
K1 / K3	0.011290	Otu11	0.005766	0.028075	Bacteria(100);Proteobacteria(100);Alphaproteobacteria(100);Ferrovibrionales(85);Ferrovibrionales_unclassified(51);Ferrovibrionales_unclassified(51);	0.000357	0.000627	0.018477	0.014816
K1 / K3	0.011152	Otu17	0.017179	0.038487	Bacteria(100);Bacteroidota(100);Bacteroidia(100);Flavobacteriales(100);Flavobacteriaceae(100);Flavobacterium(100);	0.003852	0.008619	0.020506	0.013357
K1 / K3	0.011143	Otu07	0.011230	0.028075	Bacteria(100);Actinobacteriota(100);Actinobacteria(100);Micrococcales(100);Microbacteriaceae(100);Candidatus_Planktoluna(82);	0.019798	0.006877	0.001693	0.001004
K1 / K4	0.021400	Otu06	0.008903	0.028075	Bacteria(100);Proteobacteria(100);Alphaproteobacteria(100);Rhizobiales(100);Beijerinckiaceae(100);Bosea(97);	0.000485	0.000542	0.039979	0.023661
K1 / K4	0.017610	Otu01	0.011230	0.028075	Bacteria(100);Proteobacteria(100);Gammaproteobacteria(100);Burkholderiales(100);Burkholderiaceae(100);Polynucleobacter(100);	0.037327	0.012281	0.003421	0.003080
K1 / K4	0.017223	Otu09	0.007290	0.028075	Bacteria(100);Bacteroidota(100);Bacteroidia(100);Cytophagales(100);Spirosomaceae(100);Emticicia(100);	0.000415	0.000592	0.031707	0.004035
K1 / K4	0.014792	Otu03	0.011118	0.028075	Bacteria(100);Actinobacteriota(100);Actinobacteria(100);Frankiales(100);Sporichthyaceae(100);hgcI_clade(88);	0.030314	0.023934	0.000662	0.001146
K1 / K4	0.014346	Otu02	0.011230	0.028075	Bacteria(100);Actinobacteriota(100);Actinobacteria(100);Frankiales(100);Sporichthyaceae(100);Sporichthyaceae_ge(75);	0.031136	0.016975	0.002880	0.001848
K1 / K4	0.012804	Otu04	0.011230	0.028075	Bacteria(100);Actinobacteriota(100);Actinobacteria(100);Corynebacteriales(100);Mycobacteriaceae(98);Mycobacterium(98);	0.027225	0.007603	0.003363	0.000607
K1 / K4	0.012714	Otu05	0.011230	0.028075	Bacteria(100);Actinobacteriota(100);Actinobacteria(100);Frankiales(100);Sporichthyaceae(100);Sporichthyaceae_unclassified(74);	0.025580	0.013154	0.001286	0.001670
K1 / K4	0.012432	Otu11	0.005766	0.028075	Bacteria(100);Proteobacteria(100);Alphaproteobacteria(100);Ferrovibrionales(85);Ferrovibrionales_unclassified(51);Ferrovibrionales_unclassified(51);	0.000357	0.000627	0.023082	0.005709
K1 / K4	0.010501	Otu07	0.011118	0.028075	Bacteria(100);Actinobacteriota(100);Actinobacteria(100);Micrococcales(100);Microbacteriaceae(100);Candidatus_Planktoluna(82);	0.019798	0.006877	0.000255	0.000442
K2 / K3	0.017999	Otu02	0.049535	0.054367	Bacteria(100);Actinobacteriota(100);Actinobacteria(100);Frankiales(100);Sporichthyaceae(100);Sporichthyaceae_ge(75);	0.029020	0.015371	0.003542	0.001080
K2 / K3	0.017215	Otu12	0.049535	0.054367	Bacteria(100);Proteobacteria(100);Alphaproteobacteria(100);Azospirillales(98);Azospirillaceae(98);Azospirillum(96);	0.003000	0.002090	0.029241	0.026043
K2 / K3	0.013107	Otu01	0.126630	0.129508	Bacteria(100);Proteobacteria(100);Gammaproteobacteria(100);Burkholderiales(100);Burkholderiaceae(100);Polynucleobacter(100);	0.034943	0.013243	0.017277	0.007419
K2 / K3	0.012202	Otu10	0.126630	0.129508	Bacteria(100);Proteobacteria(100);Gammaproteobacteria(100);Pseudomonadales(100);Moraxellaceae(100);Acinetobacter(100);	0.009966	0.011963	0.027423	0.007042
K2 / K3	0.012201	Otu11	0.046302	0.054367	Bacteria(100);Proteobacteria(100);Alphaproteobacteria(100);Ferrovibrionales(85);Ferrovibrionales_unclassified(51);Ferrovibrionales_unclassified(51);	0.000318	0.000550	0.018477	0.014816

K2 / K3	0.011948	Otu17	0.049535	0.054367	Bacteria(100);Bacteroidota(100);Bacteroidia(100);Flavobacteriales(100);Flavobacteriaceae(100);Flavobacterium(100);	0.002355	0.001029	0.020506	0.013357
K2 / K3	0.010332	Otu16	0.275234	0.275234	Bacteria(100);Proteobacteria(100);Gammaproteobacteria(100);Burkholderiales(100);Comamonadaceae(100);Ideonella(62);	0.006549	0.004671	0.021082	0.019667
K2 / K4	0.020949	Otu06	0.049535	0.054367	Bacteria(100);Proteobacteria(100);Alphaproteobacteria(100);Rhizobiales(100);Beijerinckiaceae(100);Bosea(97);	0.001684	0.001351	0.039979	0.023661
K2 / K4	0.017946	Otu01	0.049535	0.054367	Bacteria(100);Proteobacteria(100);Gammaproteobacteria(100);Burkholderiales(100);Burkholderiaceae(100);Polynucleobacter(100)	0.034943	0.013243	0.003421	0.003080
K2 / K4	0.016387	Otu09	0.046302	0.054367	Bacteria(100);Bacteroidota(100);Bacteroidia(100);Cytophagales(100);Spirosomaceae(100);Emticicia(100);	0.002213	0.003833	0.031707	0.004035
K2 / K4	0.015028	Otu02	0.049535	0.054367	Bacteria(100);Actinobacteriota(100);Actinobacteria(100);Frankiales(100);Sporichthyaceae(100);Sporichthyaceae_ge(75);	0.029020	0.015371	0.002880	0.001848
K2 / K4	0.012593	Otu11	0.046302	0.054367	Bacteria(100);Proteobacteria(100);Alphaproteobacteria(100);Ferrovibrionales(85);Ferrovibrionales_unclassified(51);Ferrovibrionales_unclassified(51);	0.000318	0.000550	0.023082	0.005709
K2 / K4	0.010729	Otu08	0.049535	0.054367	Bacteria(100);Actinobacteriota(100);Actinobacteria(100);Micrococcales(100);Microbacteriaceae(100);Microbacteriaceae_unclassified(84);	0.022223	0.012884	0.003508	0.001603
K3 / K4	0.018689	Otu09	0.049535	0.054367	Bacteria(100);Bacteroidota(100);Bacteroidia(100);Cytophagales(100);Spirosomaceae(100);Emticicia(100);	0.001797	0.001961	0.031707	0.004035
K3 / K4	0.017284	Otu12	0.049535	0.054367	Bacteria(100);Proteobacteria(100);Alphaproteobacteria(100);Azospirillales(98);Azospirillaceae(98);Azospirillum(96);	0.029241	0.026043	0.000637	0.000584
K3 / K4	0.016970	Otu06	0.049535	0.054367	Bacteria(100);Proteobacteria(100);Alphaproteobacteria(100);Rhizobiales(100);Beijerinckiaceae(100);Bosea(97);	0.012505	0.006186	0.039979	0.023661
K3 / K4	0.016864	Otu10	0.036904	0.054367	Bacteria(100);Proteobacteria(100);Gammaproteobacteria(100);Pseudomonadales(100);Moraxellaceae(100);Acinetobacter(100);	0.027423	0.007042	0.000000	0.000000
K3 / K4	0.016599	Otu08	0.049535	0.054367	Bacteria(100);Actinobacteriota(100);Actinobacteria(100);Micrococcales(100);Microbacteriaceae(100);Microbacteriaceae_unclassified(84);	0.030731	0.014375	0.003508	0.001603
K3 / K4	0.012075	Otu16	0.046302	0.054367	Bacteria(100);Proteobacteria(100);Gammaproteobacteria(100);Burkholderiales(100);Comamonadaceae(100);Ideonella(62);	0.021082	0.019667	0.001393	0.001157
K3 / K4	0.011726	Otu17	0.049535	0.054367	Bacteria(100);Bacteroidota(100);Bacteroidia(100);Flavobacteriales(100);Flavobacteriaceae(100);Flavobacterium(100);	0.020506	0.013357	0.001156	0.001194
K3 / K4	0.010544	Otu27	0.036904	0.054367	Bacteria(100);Bacteroidota(100);Bacteroidia(100);Chitinophagales(100);Chitinophagaceae(100);Edaphobaculum(100);	0.000000	0.000000	0.017107	0.012023

CHAPITRE 3

RESPONSE OF HYPOLIMNETIC MICROBIAL COMMUNITIES TO FRESHWATER SALINIZATION – A MICROCOSM EXPERIMENT

3.1 Introduction

The salinization of freshwater is a problem that is growing with human development and is increasingly being promoted with studies attempting to detect its short- and long-term effects, such as the freshwater salinization syndrome (Kaushal *et al.,* 2018). While freshwater habitats possess a plethora of different species that can vary from one region to another, what defines and unites them is the salinity level of their environment (1 ppt ; WSS, 2018). Many studies have focused on prokaryotic communities in estuaries (Herlemann *et al.,* 2011 ; Webster *et al.,* 2015 ; Gao *et al.,* 2018 ; Paver *et al*., 2018), and these habitats benefit from a salinity gradient that allows species to gradually acclimate and settle in areas that are adequate to their survival. As a general trend, part of the transition in estuaries is driven by the change in dominance of Betaproteobacteria in freshwater to Alphaproteobacteria as salinity increases. But community composition is not the only factor affected by salinity. While transitions occur along estuarine salinity gradients, a study by Webster *et al*. (2015) reported higher archaeal 16S rRNA abundance in low-salinity brackish sediments than in higher-salinity samples, while representing a larger proportion of the prokaryotic communities at higher salinity. Also, while some lineages proved to be found in a wide array of salinity, some methanogens and ammonia oxidizers were more localized, showing a need for a more specific niches, of which salinity played an important role.

Freshwater lake communities, on the other hand, are accustomed to very little variation in salinity, and a change in ion concentration can trigger an environmental stress that can be hard to overcome, especially in lakes with longer residency time (Chapra *et al.,* 2012). The response of epilimnion procaryotic communities exposed to sodium chloride (NaCl) intrusion, the most used de-icing salt, has been previously explored (Gagnon *et al.,* 2022). However, hypolimnetic prokaryotes are not safe from the adverse effect of a salinity rise. Being major contributors to nutrient cycling (e.g. nitrogen, methane, carbon dioxide, phosphorus ; Santoro, 2010 ; Pernthaler *et al.,* 2013 ; Anderson,

2018), as well as being involved in various food webs, procaryotic communities present in hypolimnetic water and sediments constitute key players of any freshwater habitat. A study by Edmonds *et al*. (2009) on the effect of seawater intrusion on freshwater sediment community structure concluded that salinity had an effect on gene expression and metabolic activity rather than on the general community composition, stating that it did not become "marine-like" over time. However, other studies (Dang *et al*., 2019 ; Zhang *et al*., 2014 ; DeVilbiss *et al*., 2022 ; Rocca *et al*., 2019) showed that changes in community composition and richness can occur following salinization of freshwater, but also important loss of taxa, and that long periods of time could be necessary for ecosystemic function equilibration. This disparity in results goes to show that more intensive efforts are necessary to understand the effect of NaCl introduction in freshwater.

Now, as deicing in northern latitudes is promoting salt use that leads to a rise to its drainage into nearby habitats (Kaushal *et al*., 2005), freshwater communities are now facing seasonal salt intrusion pulses (Kaushal *et al.*, 2016). But as the effect of a rise in salinity is well documented for eukaryotes (Environment Canada, 2001), its impact on prokaryotic species remains unclear. It is therefore essential to understand the effect generated by NaCl on hypolimnetic and sedimentary bacteria and archaea in a freshwater Laurentian Lake, as the loss of α-diversity and/or abundance could have an effect on other species that depend on procaryote grazing and/or on nutrients made bioavailable by microbial communities. Thus, through a microcosm setup, sequencing of bacterial and archaeal 16S and eukaryotic 18S rRNA genes, and digital polymerase chain reactions (dPCR), we aimed to investigate the effect of increasing salinities (0.01 – 3.22 ppt / 10 – 3220 mg/L^{-1} NaCl) on the abundance and α- and ß-diversity of benthic sedimentary and hypolimnetic Archaea and Bacteria, after three and six weeks of exposure.To better consider the biotic influences, and to get a better global view of hypolimnetic and sedimentary microbial communities' sensitivity to NaCl, we considered eukaryotic diversity and community composition as an explanatory variable. We also sought to determine if a salinity threshold could be determined, from which a significant transition of the communities can be observed, for comparison purposes with the regulations in place regarding the introduction of NaCl into freshwaters. Transitional salinity values for eukaryotes were assessed as well, to verify and compare their sensitivity to NaCl to prokaryotic communities and see if a domain showed a high level of sensitivity, which would require more monitoring efforts.

We hypothesized that bacterial abundance and diversity would be affected at salinity levels lower than archaea, and that a partial recovery of both abundances and diversities would be possible for both prokaryotic domains after a six-week incubation compared to values observed after a three-week incubation, both in sediments and hypolimnetic water samples. We also hypothesized that a significant transition of bacterial communities would be seen at salinity levels lower than for archaea, for both sampling media, but that eukaryotic community's transitional threshold will be lower than both prokaryotic domains. Combined with the previously observed effect on the epilimnion, understanding the impact of NaCl on bacterial and archaeal communities in the hypolimnion and sediments, following exposure for up to six weeks, will allow to understand the possible long-term repercussions of its intrusion into freshwater lake habitats.

3.2 Material et methods

3.2.1 Experimental setup

During the spring of 2019, sampling was carried out at Lac Croche (Saint-Hippolyte, Quebec, Canada – 45°59'17.34" N / 74°0'20.75" W; May 2019), to collect sediments from the lake, as well as water from the hypolimnion. We first established the depth of the lake to be at 6.3 m. Subsequently, a Van Dorn type sampler was used and submerged to a depth of 5.5 m in order to triple rinse it and collect hypolimnetic water, which was then poured into glass bottles of 1.14L previously autoclaved. Then, a YSI multiparameter probe (model 10102030 ; Yellow Springs Inc.) was used to measure initial conductivity, pH and temperature in the hypolimnion. Finally, a corer was used to extract sedimentary sludge from the lake, resulting in three cores approximately 30 cm deep, topped with water from the hypolimnion. The water and the harvested cores were collected and divided in the laboratory.

In five autoclaved 1.14 L glass bottles, a volume of 300 mL of sediment was transferred from the core, divided into 250 mL of compact muddy sediment (composing the mass present in the deeper part of the core) deposited at the bottom of the microcosms, as well as 50 mL of muddy sediment (present in the top layer of cores) deposited on top of the compacted sediments in the microcosms. Subsequently, a volume of 814 mL of water from the collected hypolimnion was introduced into the bottles, taking care to limit the mixing of the sediments, and making sure not to leave air at the

level of the neck. A waiting period of two hours was then applied to allow the sediments which had been suspended to descend, to limit a possible bias caused by the binding of the sodium or chloride to the particles in suspension and therefore its precipitated sedimentation. Following the waiting period, the sodium chloride concentrations corresponding to a previously carried out mesocosm experiment using water from the epilimnion of lake Croche (Astorg *et al.,* 2022) - S0 (control treatment with no salt addition ; 0.01 ppt or 10 mg/L^{-1}), S5 (0.16 ppt or 160 mg/L^{-1}), S11 (0.93 ppt or 930 mg/L^{-1}), S15 (1.93 ppt or 1930 mg/L^{-1}) and S20 (3.22 ppt or 3220 mg/L^{-1}) - was introduced into the different microcosms. Finally, the bottles were wrapped with aluminum foil to reproduce the absence of light characterizing the hypolimnion and were placed at a temperature of 4°C to reproduce the temperature of 4.5°C measured at the sampling site. Salinities and sample names were selected in association with a mesocosmal experiment within the same lake (see Gagnon *et al.,* 2022 and Astorg *et al.,* 2022), in relation to short- and long-term water quality guidelines in Canada and US, and investigating the effect of NaCl on epilimnion procaryotic and eukaryotic communities and thus consolidating the effect of NaCl within the different stratified layers of the lake environment.

3.2.2 DNA extraction

Sediment (~10 g), and water (100 ml) samples were extracted from each microcosm using sterile serological pipettes (sediment) and 0.2 µm filter syringes (water) after 3- and 6-weeks exposure to the NaCl. However, a first sampling of water and sediments was made from the S0 treatment following the creation of the microcosms, thus representing the initial sampling control (T0). The volumes of water extracted from the microcosms were replaced with 100 ml of ultrapure water with adequately adapted salinity to not disturb the incubations from 3 to 6 weeks. DNA was extracted from the collected sediment samples using the DNeasy PowerMax® kit (Qiagen, 2018), while water samples were processed using the DNeasy PowerWater® kit by Qiagen ™ (Qiagen, 2017). All DNA samples were stored at −20 °C.

3.2.3 16S and 18S rRNA gene sequencing and dPCR

16S and 18S rRNA sequencing was performed using the Illumina Miseq platform of the Center of Excellence in Research on Orphan Diseases (CERMO, Department of Biological Sciences,

UQAM). Primers A340F (5'-CCCTAYGGGGYGCASCAG-3') and A915R (5'-GTGCTCCCCCGCCAATTCCT-3') (Lazar *et al.,* 2017) were used for archaeal amplification, while primers B341F (5'-CCTACGGGIGGCIG -3') and B785R (5'-GACTACHVGGGTATCTAATCC-3') (Sun *et al.,* 2020) were used for bacteria. Finally, primers E960Fc (3′-RYRGGCTTAATTTGACTCAACRCG-5’) and NSR1438 (5’-GGGCATCACAGACCTGTTAT-3’) (Capo *et al.,* 2016) were used to amplify the 18S eukaryotic genes. The raw sequence data was deposited in NCBI Sequence Read Archive, (https://www.ncbi.nlm.nih.gov/sra), under BioProject ID number PRJNA701941, under accession numbers SAMN17917569 to SAMN17917634.

The absolute abundance, determined by measuring the copy numbers of the archaeal and bacterial 16S rRNA genes in the different samples, was measured by digital polymerase chain reaction (dPCR) (Applied biosystems by Life technologies), with a QuantStudio ™ 3D device (ThermoFisher Scientific, N.D) using SYBR® Green dye, with a volume of 1 µl DNA sample per chip, following the manufacturer’s instructions (ThermoFisher Scientific, 2014). Dilutions (1/10, 1/50) were carried out for certain samples whose absolute abundance was greater than the reading capacity of the device. The final number of 16S rRNA gene copies was then adjusted to represent the number of copies present per liter for water samples, and per gram of humid soil for sediment samples. The pairs of bacterial and archaeal primers used in the dPCR were the same as those used for sequencing (B341F - B785R ; A340F - A915R). Details about chip loading mixture, primers, and cycles steps are provided in Tables 3.7.S1 and 3.7.S2.

3.2.4 Bioinformatic and statistical analyses

The obtained sequences were processed using the mothur software (v.1.44.3 ; Schloss *et al.,* 2009). Archaeal sequences were taxonomically identified using the SILVA v.138 database (Glöckner, Bremen, Germany) to which reference sequences were supplemented to refine the classification (see Liu *et al.,* 2018 and Zhou *et al.*, 2018), while bacterial and eukaryotic sequences were associated using the SILVA v.138 database. During the rarefaction process, samples with sequence counts too low (≤500) were removed (archaeal initial water sample; T0_Wat). Other sequences were then grouped by Operational Taxonomic Units (OTUs) using a 97% similarity threshold. The

OTU tables were ultimately processed using Rstudio (Team, 2020) and PAST 4.03 software (Hammer, 2020).

Raw OTU tables were used to obtain bacterial, archaea and eukaryotic α-diversity indices (Shannon H) using the phyloseq package in R software(Bioconductor v3.12, McMurdie & Holmes, 2013). The obtained α diversities, as well as absolute abundance were used as the dependent variable in linear regressions, with the NaCl concentrations as the independent variable, and a regression was carried out using the *lm* function. A rarefaction (0.9 × min) as well as a transformation (Hellinger) were performed on the raw OTU tables, using the vegan (v2.5-7, Oksanen *et al.*, 2013) and phyloseq packages. The tables thus obtained were used to produce Principal Coordinate Analysis (PCoA) of bacterial, archaeal and eukaryotic communities, using a Bray-Curtis dissimilarity index. The two first axes from the PCoAs (Table 3.7.S3) were then used as a variable for further analysis, as a proxy for community structure. Distance-based redundancy analysis (db-RDA) was applied to the distance matrices using the capscale function from the vegan package, with explanatory variables (salinity, bacterial and archaeal abundance, archaeal, bacterial and Eukaryotic diversity) and the addition of the two first PCoA axes from the other domains, following a normalization on all variables to approach normal distribution. The significance of constraints was assessed using the anova function from the vegan package, with 200 permutations. The most significant variables were then used as an input within the framework of a variance partitioning analysis (varpart function, vegan package) to assess their unique and shared contributions on the different communities' compositional changes. The significant variables obtained within the db-RDA were also used to produce linkage tree analysis (LINKTREE), using the PRIMER v.6 software package (Clarke & Gorgley, 2006) to associate thresholds of imputed significant variables with the differentiation of communities.

Clusters of samples were created based on β-diversity's repartition obtained within the framework of the PCoA and LINKTREE analysis and were subjected to a one-way permutational analysis of variance (one-way PERMANOVA), using normalized and transformed tables, the Bray-Curtis dissimilarity index and 9999 permutations on the PAST4.03 software. A similarity percentage analysis (SIMPER) between the different clusters, with Bray-Curtis for dissimilarity index, paired with a Kruskal-Wallis test, were performed on rarefied and transformed OTU tables, using the

vegan package and the Simper_pretty and R_krusk functions (Steinberger, 2020). The SIMPER aimed at identifying the OTUs that differed significantly between clusters. Finally, correlations (Spearman) between the most abundant classes and orders and the salinity values were carried out using the Phylosmith function (Smith, 2019).

3.3 Results

3.3.1 Absolute abundance and correlation with salinity concentrations

Planktonic archaea (Table 3.6.1, Fig. 3.7.S1a) showed an increase across the salinity gradient after three weeks at salinity up to 1.9 ppt NaCl, varying between 4×10^6 and 63×10^6 gene copies/L^{-1}, followed by a decrease to 63×10^6 gene copies/L^{-1} at 3.22 ppt NaCl. After six weeks, the S0 sample showed an absolute abundance of 14×10^6 gene copies/L^{-1}, while the other samples fluctuated between 587.25 and 17×10^5 gene copies/L^{-1}. For sedimentary archaea the absolute abundance decreased from 63×10^4 to 21×10^4 gene copies/g^{-1} across the salinity gradient at T3, while at T6 it varied between 16×10^4 and 40×10^4 gene copies/g^{-1} between 0.01 and 1.9 ppt NaCl, with 10×10^5 gene copies/g^{-1} at 3.22 ppt NaCl (Table 3.6.1, Fig. 3.7.S1b). No relationship proved to be significant. All absolute abundance raw values are available in Table 3.7.S4. All regressions statistics are supplied in Tableau Annexe A2.

For the planktonic bacteria, after three weeks the abundances varied between 36×10^6 and 21×10^7 gene copies/L^{-1} between 0.01 and 1.9 ppt NaCl, and 13×10^8 gene copies/L^{-1} at 3.22 ppt, while absolute abundances varied from 25×10^6 to 13×10^8 gene copies/L^{-1} after 6 weeks. (Table 3.6.1, Fig. 3.7.S2a,). No significant relation was found for water or sedimentary bacteria (Table 3.6.1, Fig. 3.7.S2a and 3.7.S2b,) with the lowest absolute abundance in sediments being 13×10^4 gene copies/g^{-1} at 0.16 ppt NaCl exposure, and the highest point at 51×10^5 gene copies/g^{-1} at 1.9 ppt NaCl, both after a three-week exposure.

3.3.2 Alpha diversity indices and correlation with salinity concentrations

After three weeks, the lowest diversity for planktonic archaeal indices (2.86) was at 0.01 ppt NaCl, and was then followed by fluctuations from 2.96 to 3.05, the highest point being at 1.9 ppt NaCl.

Values after six weeks were consistently lower than at T3 across the salinity gradient except for the sample at 0.01 ppt NaCl, where it reached its highest diversity (3.09), while the lowest diversity index 2.74 (0.93 ppt NaCl). After three weeks, sedimental archaeal diversity varied from 2.68 (0.01 ppt NaCl) to 2.29 (0.93 ppt NaCl) but the reach of the lowest point was followed by a rise to indices of 2.45 at 1.9 ppt NaCl and 2.61 at 3.22 ppt NaCl. At T6, the diversity indices were consistently higher than at T3 from 0.01 ppt NaCl to 1.9 ppt NaCl, with H diversity values located between 2.45 and 2.83. At 3.22 ppt, however, diversity was lower than after three weeks for the same salinity, with a value of 2.44. The relationship between NaCl concentrations and planktonic archaeal α-diversity (Table 3.6.2, Fig. 3.7.S3a) was not significant after three or six weeks. In sediments (Table 3.6.2, Fig. 3.7.S3b), all relationships were not found to be significant as well. All calculated Shannon's H values are made available in Table 3.7.S4. All regressions statistics are supplied in Tableau Annexe A2.

Planktonic bacterial diversity showed low levels of variations throughout the salinity gradient after three weeks, with the highest value at 0.93 ppt NaCl (3.99), while a gradual diversity loss was present after six weeks, from 4.05 to 3, at salinities ranging from 0.16 to 3.22 ppt NaCl. In sediment, bacterial diversity was at its highest at 0.01 ppt NaCl at both sampling times. Diversity values ranged between 5.97 and 5.66 after three weeks, with the lowest value observed at 1.9 ppt NaCl. After six weeks, diversity values were between 6.08 and 5.71, with the lowest value at 1.9 ppt NaCl as well. For planktonic bacteria (Table 3.6.2, Fig. 3.7.S4a), relationships were significant after six weeks (positive) but not in sediments (Table 3.6.2, Fig. 3.7.S4b). These results demonstrate the effect that the presence of NaCl may have on bacterial α-diversity in the lacustrine hypolimnion.

3.3.3 β-diversity and correlation with environmental variables

3.3.3.1 Archaea

The db-RDA plot (Fig. 3.6.1) shows that the spatial distribution of samples was divided between water and sediment samples on the first axis, while salinity was an important factor influencing the β-diversity for both the water and sediment samples on the second axis. The ANOVA (Table 3.7.S5) showed that salinity, bacterial absolute abundances, bacterial α-diversity and bacterial ß-diversity were significant variables explaining archaeal variance, with salinity explaining 3.7% of

the variance, and bacterial abundance and bacterial ß-diversity taken together explained 48.2% (Fig. 3.7.S5a).

Within the archaeal LINKTREE (Fig. 3.7.S6), node A separates the archaeal water from sediment samples. In the water samples, a first division (H) separates samples S0/S05 from S11-S20 for both T3 and T6, with salinity as the main explanatory variable. Lower salinity samples (S0/S05) were further subdivided (I) with salinity, bacterial abundance and ß-diversity explaining the differentiation. S11, S15 and S20 samples for both times were distinct (J and K). In the sediment samples, a first node (B) separates S0 and S05 of all sampling times from the S11, S15 and S20 samples, with salinity as the main driver. At higher salinities, sample S20 at T3 was separated from all S11, S15 and S20 (T6) samples (E) explained by bacterial β-diversity, while S11 from T6 was split from other samples (F) also explained by bacterial β-diversity. Finally, split G divided S11 and S15 of T3 from S15 and S20 from T6, with the bacterial abundance as the main explanatory variable.

3.3.3.2 Bacteria

The db-RDA plot (Fig. 3.6.3) shows a separation of the sediment and water samples on the first axis. While there was little to no spatial distribution along any explanatory variables for the sediment samples, the plot shows a linear repartition of water samples following the salinity gradient on the second axis. The ANOVA (Table 3.7.S5) showed that salinity, bacterial absolute abundance, archaeal α-diversity, eukaryotic α-diversity, archaeal ß-diversity and eukaryotic ß-diversity were significant variables explaining bacterial variance. Salinity, eukaryotic α-diversity and archaeal ß-diversity were selected for variance partitioning, globally explaining 56% of the bacterial variance (Fig. 3.7.S5b). By itself, the archaeal ß-diversity explained 54% of the variance.

Within the LINKTREE analysis (Fig. 3.7.S7), a first division (A) separated water and sediment samples. A first division within the water samples (B) separated the initial water sample (T0) from all other samples, with the archaeal and eukaryotic α-diversity, as well as archaeal β-diversity as the main explanatory variables. The S0 and S05 at T3 and T6 were shown to be separated from S11 and S15 at both sampling time, as well as S20 at T3 (D), with the salinity, eukaryotic and archaeal β-diversity as the main drivers. Finally, both S11 were separated from both S15 and S20

at T3 (F), with the salinity and bacterial α-diversity as the main explanatory variables. For the sediment samples, S0 at T3 and T6, as well as S05 at T3 were grouped (H), with the archaeal α-diversity as the main variable. Both S15 and the S20 samples at T6 were separated (I), with eukaryotic α- and β-diversity for explanatory variables. Finally, a last division separated S20 at T3 from both S11 and T05 at T6 (J), explained by salinity, eukaryotic α- and β-diversity, and archaeal α- and β-diversity.

3.3.4 Microbial community structures (ß-diversity)

For the archaeal communities (Fig. 3.6.5a), we observed five main clusters on the PCoA plot. Clusters K1 (S0-S05, and S11 at T6) and K2 (S11 at T3, and S15-S20) comprised sedimentary samples, while clusters K3 (S0/S05), K4 (S15) and K5 (S11 and S20) consisted of the aquatic samples.

For the bacterial communities (Fig. 3.6.5b) we identified four clusters. The first cluster (Y1) grouped together all the sediment samples. Clusters Y2 (S0 at T0/T3/T6 and S05 at T6), Y3 (S11, S05 and S15 at T3), and Y4 (S15 at T6 and S20) contained all the water samples.

Finally, for the eukaryotic communities (Fig. 3.6.5c) we identified four clusters. The first two Z1 (S0, S15 and S20 at T3) and Z2 (S05, S11, and S20 at T3) were composed of sediment samples, while Z3 (S0 and S05) and Z4 (S11-S20) contained the water samples.

All the clusters obtained on the PCoA graph, both in archaea and bacteria as well as in eukaryotes, underwent permutational analysis of variance (Permanova). The results thus obtained are presented in Table 3.7.S6, demonstrating that in archaea, only the fourth cluster (K4) was not significantly different compared to the other clusters. In bacteria, however, all clusters were significantly different.

3.3.5 Correlations between the most abundant taxa and NaCl concentrations

Correlation analyses (Spearman) between the 500 most abundant taxa within the archaeal (Fig. 3.7.S8) and bacterial (Fig. 3.7.S7) OTU matrices, and salinity levels, were performed at the class

and order levels. Several classes within archaeal communities (Fig. 3.7.S8) demonstrated a significant correlation with NaCl concentrations. In sediments, Methanosarcinia was positively correlated ($p \leq 0.05$), while Methanomethylicia was negatively correlated ($p \leq 0.05$), after three weeks. After six weeks, however, only the Woesearchaeota subgroup 5a was negatively correlated ($p \leq 0.05$). In the water samples, Woesearchaeota 22b ($p \leq 0.001$) and Woesearchaeota 24 ($p \leq 0.05$) showed a positive correlation after three weeks, while the Bathyarchaeota subgroup 18, Bathyarchaeota 5bb, Methanosarcinia and Woesearchaeota 5b classes showed a negative correlation ($p \leq 0.05$) after three weeks. After six weeks, only the Micrarchaeia and Woesearchaeota 22a classes showed significant negative correlations ($p \leq 0.05$).

In sedimentary bacteria (Fig. 3.7.S9), the Bacteroidia and Cyanobacteriia classes showed significant positive correlations with the NaCl concentrations ($p \leq 0.05$), and Dehalococcoidia a negative correlation ($p \leq 0.05$), after three weeks. After six weeks, however, the uncultured TA06 class was positively correlated ($p \leq 0.05$) while Spirochaetia was negatively correlated. In the hypolimnetic water, the Gammaproteobacteria and Alphaproteobacteria showed a negative relationship with NaCl ($p \leq 0.001$). After six weeks, Desulfobacteria and Gammaproteobacteria exhibited a negative relationship ($p \leq 0.05$), while Kryptonia and Syntrophia had a positive relationship ($p \leq 0.05$).

3.3.6 Differential significance of microbial taxa

The juxtaposed SIMPER and Kruskal-Wallis analyzes carried out on archaeal and bacterial matrices are presented in Table 3.7.S7, showing which taxa best explained the differences in community structure observed on the PCoA plot (clusters). Only the water-water and sediment-sediment cluster analysis were kept, to emphasize the differences brought by salinity rather than by the difference in environment. In the sedimentary archaeal samples, 12 OTUs presented a *p*-value below the threshold (p=0.05), with four of them belonging to the Thermoplasmatota phylum (all Thermoplasmata), three being from the Halobacterota phylum (Methanomicrobia and Methanosarcinia), four from the Woesearchaeota phylum (Woese-24 and Woese-5b) and one unclassified. In the water samples, the comparison of cluster K3 and K5 showed seven OTUs as significatively varying, with three being from the Bathyarchaeota phylum (Bathy-5b, Bathy 18 and

Bathy-5bb), two from Woesarchaeota (Woese-24 and Woese-5a), one from the Halobacterota phylum (Methanosarcinia) and one being unclassified archaea. The K3 and K4 clusters showed two OTUs, both being from the Woesearchaeota class (both Woese-24). Finally, the SIMPER for clusters K5 and K4 showed three OTUs affiliated with unclassified archaea, three as Woesearchaeota (Woese-13, Woese-24 and Woese-5a), two as Halobacterota (Methanosarcinia, Methanomicrobia) and one Iainarchaeota (Iainarchaeia).

As for the bacterial clusters, only one sedimental cluster was created and thus no comparison could be made. However, from the Y2 and Y3 water sample clusters, four were of the Proteobacteria phylum (all being Gammaproteobacteria, three of them Burkholderiales), one being from the Bacteroidota phylum (Bacteroidia) and one being from the Sva0485 phylum. Clusters Y2 and Y4 showed three Bacteroidota (Bacteroidia and Kryptonia) , one Actinobacteriota (Actinobacteria), one Proteobacteria (Gammaproteobacteria and Burkholderiales) and one of the Desulfobacterota phylum (Syntrophia). Finally, the SIMPER on clusters Y3 and Y4 showed four OTUs from the Actinobacteriota phylum (Actinobacteria and Acidimicrobiia), two Bacteroidota (Bacteroidia and Kryptonia) amd two Proteobacteria (Methylococcales and Burkholderiales). These results demonstrate that, overall, a differentiation took place between the compared clusters, particularly in water samples.

3.4 Discussion

In spring 2018, we carried out a study on the effect generated by the introduction of NaCl on the abundance and α- and ß-diversity of prokaryotic communities in the freshwater epilimnion of lake Croche (Gagnon *et al.,* 2022 ; Astorg *et al.,* 2022). However, as it was also important for us to understand how the introduction of salt could affect the hypolimnion and benthic communities in the same lake, we explored the effect generated on the absolute and relative abundance of archaeal and bacterial 16S rRNA genes, in hypolimnetic water and sediments from the same lake. As a whole, this study, combined with those produced in the epilimnion, aims to see the effect produced by the intrusion of NaCl in the Laurentian lacustrine systems, which are prey to salinization. Taking into consideration the extent of the impact produced will make it possible to see whether remedial measures are necessary to undertake to ensure the well-being of these habitats.

3.4.1 Aquatic procaryotic abundance and diversity

In aquatic archaea, we did not observe a significant effect of salinity on absolute abundance. However, a decrease was seen at 3.22 ppt (3220 mg/L^{-1}) NaCl, the saltiest environment applied in our study, raising the possible existence of a limit to their resilience. After six weeks of incubation, the supplemented microcosms all had extremely low absolute abundance values compared to the third week. While our results could indicate an effect generated by the incubations in a closed environment,the presence of a relatively high abundance in the microcosm without NaCl supplementation suggests a drastic effect of NaCl on the archaeal biomass.

A similar effect was observed with archaeal α-diversity indices. The observed decrease in α-diversity between the two exposure times implies that the introduction of even a low level of NaCl had an effect on archaeal α-diversity after a six-week incubation. Other factors, such as viruses (lysis, lysogeny ; Cooper, 2012) cannot be ruled out, seeing it can influence prokaryotic (Tang *et al.*, 2020) and eukaryotic α-diversity (Weynberg, 2018). However, the variance partitioning analysis highlighted the bacterial communities composition and absolute abundance as important explanatory variables in the general archaeal community composition transition, and consequently its diversity. Indeed, when combined with salinity, the α-diversity and composition of bacterial communities explained 56.66% of archaeal variation seen through the salinity gradient. Such an influence of the interaction between the two domains is not surprising considering that the bacteria-archaea co-occurrence is an important element shaping the structure of planktonic prokaryotic communities (Wang, 2021), even more so than salinity, although the latter may constitute the main environmental variable to this effect. Through the LINKTREE analysis, we observed a major separation between aquatic samples with low salinity (<0.93 ppt / 930 mg/L^{-1}) and those with higher salinity (≥0.93 ppt / 930 mg/L^{-1}), which was explained by salinity. Nevertheless, in addition to salinity, bacterial composition, α-diversity and abundance also explained these subdivisions. Subsequent analysis would be necessary to see the instances of co-occurrence, particularly within the dominating archaeal groups in the hypolimnion.

As for bacteria, an increase in absolute abundance in water samples was observed across the salinity gradient after 6 weeks compared with results after three weeks, with a strong increase at 3.22 ppt

(3220 mg/L^{-1}) NaCl at both sampling times, suggesting the capacity of some taxa to cope with higher levels of salinity. Although it would be possible for autochthonous hypolimnetic species to show plasticity towards higher ion concentration in their environment, samples dispersion on the second axis of the db-RDA as well as the overall composition would be indicative of a transition effect rather than a simple change in relative abundance. Some species, previously shown to be halotolerant, are only present in water samples at higher salinity, such as Syntrophia (Ma *et al.*, 2020) and Desulfosporosinus (Thajudeen *et al.*, 2017 ; Pester *et al.*, 2010), implying that changes in environmental conditions led to the creation of new niches.

Despite there being taxa to substitute the loss of indigenous freshwater bacteria, the increase in salinity resulted in a significant detrimental effect on planktonic bacterial α-diversity, after 6 weeks. Our results agree with those obtained by Vidal-Durà *et al.* (2018), reporting similar results to those obtained by Campbell and Kirchman (2013) and Liu *et al*. (2014) and may attribute the variation in diversity to the influence of riparian inputs in estuaries. However, our study in microcosms did not have any freshwater intrusion and would therefore limit the variations to a few possible causes. Among these could be the direct effect of NaCl on abundant and rare taxa (<2%), the lack of potential metabolic pathways needed to cope with this environmental change (Tee *et al.*, 2021), or changes in the bioavailability of certain nutrients brought about by the increase in salinity (Nielsen *et al.*, 2003).

In addition, and as highlighted previously, microbial interrelation should be considered. By combining salinity with the matrix of archaeal communities as well as eukaryotic α-diversity to measure variance partitioning, it was possible to explain 56% of the bacterial communities' variance. The bacteria-archaea relationship seems most important for the former, since the archaeal community matrix alone explained 54% of the variance in bacterial communities. Moreover, the LINKTREE analysis presented salinity as a dividing factor between the major division, with archaeal and eukaryotic β-diversity as essential drivers for bacterial β-diversity through the salinity gradient. The loss of certain archaeal groups could have an influence on nutrients cycling and availability (e.g. Bathyarchaeota ; nitrogen and sulfur ; Pan *et al*., 2020) , and the Bathy-6 subgroup, one of the most common taxa in our samples, was shown to be sensitive to salinity when in a freshwater environment (Zou *et al*., 2020). Additionally, the Bathy-6 subgroup was shown to

contribute to the biosynthesis of cobalamin (vitamin B12) (Zou *et al.*, 2020), as well as the presence of rocF genes (nitrogen metabolism) in Bathy-6 and Bathy-15, both subgroups present in our study. The drop in the relative abundance of these two subgroups in the water samples, although not significant, could have had an unfavorable effect on the maintenance of bacterial α-diversity. Similarly, the significant decrease in the methanogenic Methanomicrobia in sediments and Methanosarciniales in the water column, despite a significant increase in Methanosarcinia in sediments, may have affected carbon recycling in the microcosms (Ling *et al.*, 2022), an element that is also essential for bacterial metabolism (Laskar *et al.*, 2018 ; Wang *et al.*, 2019). Our results on the effect of NaCl on the hypolimnetic water microbial communities show that, overall, an effect is present on the bacterial α-diversity, although possibly more intricate than a simple physiological effect. Considering nutrient fluctuations and microbial co-occurrence network in subsequent studies could shed light on the dynamics at play in archaeal and bacterial α-diversity variations.

3.4.2 Sediment procaryotic abundance and α-diversity

The results obtained for the sediment samples showed a decrease in archaeal absolute abundance, and 67% of the variation was significantly explained by the NaCl concentration after three weeks, thus demonstrating an effect of NaCl on the archaeal abundance in the sediments.

No clear effect of NaCl on the archaeal abundance in the sediments was seen within our study. Such an effect was not surprising since the introduction of sodium chloride into the sediments would be limited. Indeed, only 1 to 2% of the chloride and sodium dissolved in water should penetrate the sediment (Lerman & Weiler, 1970), typically remaining in solution in water and thus limiting the effect that can be achieved on sedimentary organisms. Many of the most abundant classes and orders in sediment samples, including Methanosarcinia, Methanomicrobia, and Thermoplasmata exhibit high plasticity with respect to the presence of NaCl in their environment. Methanosaeta (Methanosarcinia) can adapt to salinities up to 1.2 M NaCl (70 ppt / 70 000 mg/L^{-1} NaCl) and are able to produce biofilms (Gagliano *et al.*, 2017 ; Sudmalis *et al.*, 2018 ; Gagliano *et al.*, 2020). Methanomicrobiaceae (Methanomicrobiales), as well as Thermoplasmata and Woese-5b, are found in a variety of sediments whether freshwater, estuarine and even saline environments (Chen *et al.*, 2020 ; Liu *et al.*, 2016 ; Liu *et al.*, 2018). However, despite their ability to be

halotolerant, salinity remains to be known as an important regulator of certain archaeal groups, particularly methanogens (Tong *et al.*, 2017). But with many archaeal taxa being tolerant to salinity, and a low penetration potential of NaCl in sediments, archaeas remain sensitive to potential fluctuations in nutrient availability, as well as bacterial community variations (diversity, abundance and composition), as shown by the LINKTREE. Factors external to salinity sould be considered as influential in our study, rather than a single impact of NaCl on archaeal absolute abundance, particularly in view of the presence of variations in absolute abundance but the absence of linearity with salinity.

Another aspect to consider is the phenomenon of endosymbiosis with eukaryotic, such as protists producing H_2 in freshwater sediments. This is the case for some Methanomicrobials (Bertrand *et al.*, 2015), including Methanoregula (Takeshita *et al.*, 2019) previously shown to associate with Intramacronucleata (Ciliophora), both coincidentally found in all the sediment samples, but which would be most found in tripartite symbiosis with Holosporaceae, a family found in the water sample at T0, and of which several members are endosymbiotic. Although only a small portion of the NaCl would be able to reach the sediments, it can reach the pore waters of surface sediments (CCME, 2011) and thus affect benthic eukaryotes, which are generally more sensitive, particularly micro-invertebrates (Schuler *et al.*, 2019), although organisms inhabiting environments with fluctuating salinity (e.g. estuaries) are capable of greater resistance (Stefanidou *et al.*, 2018). Hence, endosymbiosis with sensitive sedimental eukaryotic species would likely have an influence on archaeal communities upon NaCl intrusion in the environment.

There was no significant relation between salinity and sedimentary bacterial abundance. Only a slight increase in absolute abundance between 0.93 and 1.9 ppt (930 – 1900 mg/L^{-1}) NaCl was noticeable after three weeks, thus not being a clear indicator of an effect of salinity. The distribution of the samples on the second axis of the db-RDA suggested the absence of differentiation, without a clear distinction of the effect of NaCl in the dissimilarity. Its effect on sedimental bacterial α-diversity also remains elusive, showing no clear relation with salinity, despite α-diversity values lower than the microcosm without NaCl supplementation in all the microcosms with addition. Although several studies demonstrate a negative effect of salinity on bacterial α-diversity in freshwater sediment (Baldwin *et al.*, 2006), estuaries (Vidal-Durà *et al.*, 2018), saline (Yang *et al.*,

2016) and hypersaline lakes (Jiang *et al.*, 2006), some studies have been able to observe an increase (Jackson & Valaire, 2009) or the absence of an effect (Nielsen *et al.*, 2003 ; Ikenaga *et al.*, 2010 ; Freitag *et al.*, 2006) in freshwater and estuarine environments. Overall, our results show that despite there being variation in archaeal and bacterial α-diversity and absolute abundance throughout the NaCl gradient in sediment, those variations could not be directly linked to NaCl. It would be interesting to see if a higher salinity range could induce more variations in further studies.

3.4.3 Salinity threshold for microbial community transition

As diversity and abundance have been investigated, we also we tested if certain salinity levels induced significant transitions in microbial community composition, to determine potential salinity thresholds and if one of the microbial domains was more sensitive to NaCl intrusion in sediment and hypolimnetic water. We observed a difference between sediment and water samples. Such a distinction can be explained by several factors, including the difference in environment (Walsh *et al.*, 2016) and the limited capacity of chloride to penetrate the sediments. The oxygen levels, the available nutrients, the associated metabolic pathways, the presence of phytoplankton and the favored osmoregulatory pathways (Tee *et al.*, 2021) could have led to the creation of niches within which organisms were adapted (Vidal-Durà *et al.*, 2018). Thus, it was not so surprising to observe such levels of variation within the framework of the PCoA carried out, being able to lead to a first axis explaining as much as 53.2% of the variation in bacteria, and up to 46.8% in archaea, showing the disparity between planktonic microbial communities and the underlying benthic communities.

For aquatic microbial communities, differentiation appeared to be present in all kingdoms at salinities of 0.93 ppt (930 mg/L^{-1}) NaCl and above. The effect achieved on the bacterial communities showed an initial differentiation of samples ranging from 0.93 to 1.9 ppt (930 to 1900 mg/L^{-1}) NaCl. A PERMANOVA performed between clusters, however, did not conclude to a significative differentiation. Seeing that there was graduality to the sample differentiation throughout the salinity gradient that was reflected by the β-diversity, such results were not surprising, and are a demonstration that despite their level of dissimilarity part of the community remained and tolerated NaCl intrusion. Eukaryotes in water samples showed a sensitivity similar than that of archaea, with a significant transition seen at 0.93 ppt (930 mg/L^{-1}) NaCl. Further

analysis would be necessary to determine exactly where the transitional threshold is, between 0.16 ppt (0.160 mg/L^{-1}) and 0.93 ppt (930 mg/L^{-1}) NaCl. Located in-between, organisms present in the sediment-water interface are subject to a higher osmotic pressure than sedimentary organisms (Schuler *et al.*, 2019), and these can therefore affect the results of sediment samples, despite a low chloride penetration potential. Thus, although the sedimentary samples have a proximal distribution, variations were present, particularly for archaeal and eukaryotic communities. In addition, while eukaryotes, even fungi (Yan *et al.*, 2015), are more sensitive to chloride than prokaryotes, studies have shown that bacteria are more sensitive to chlorides (Mani *et al.*, 2020) and to environmental variations (Lv *et al.*, 2021) than archaea. Thus, a small proportion of the chloride entering the sediment would have a stronger effect on these domains than on the archaea. However, our results demonstrate that sedimentary archaeal communities differentiated as early as 0.93 ppt (930 mg/L^{-1}) NaCl after three weeks of exposure, while very little variation was observed in bacteria. This effect could be mediated by a lower archaeal richness, which would limit the possibility of intolerant species to remain above a certain salinity threshold (Elliott & Whitfield, 2011) and for "seed banks" taxa (Wisnoski & Lennon, 2021) to thrive in the available niche. Nonetheless, an effect was observed in archaea leading to a significant differentiation of communities, and the LINKTREE analysis for archaeal communities intrinsically link such transition to salinity. While there was little variation in β-diversity in bacteria, the clustering observed within the bacterial LINKTREE does, however, imputes the presented shift to other factors, such as archaeal and eukaryotic α-diversity, thus emphasizing the fragile balance between species dynamics and co-occurrences.

Taken together, these results demonstrate that in hypolimnion and freshwater sediments, archaeal communities could prove be more sensitive than the bacterial communities in freshwater sediments, and that the introduction of sodium chloride at concentrations as low as 0.93 ppt (930 mg/L^{-1}) NaCl would have the potential to lead to a differentiation of microbial communities, particularly in the hypolimnetic layer in the context of our study. Such concentrations would correspond to an approximate introduction of 564.13 mg/L^{-1} Cl^-, which is above chronic exposure regulations. Established at 120 mg/L^{-1} Cl^- in Canada and 230 mg/L^{-1} Cl^- in the United States (Schuler *et al*., 2019), compliance with regulations regarding chronic exposure to Cl^- should ensure the sustainability of microbial communities in freshwater hypolimnion and sediments.

3.4.4 Contributors to the transition

As we have seen that a transition occurs, different species are at play in this dynamic. Certain archaeal classes appeared only after 6 weeks incubation (e.g., Woese-8, Woese-22b, Micrarchaeia), and could be a demonstration of the sustainability of said class within the environment provided inthe microcosm. However, the negative relationship that these classes have with salinity are a good representation of the multiplicity of factors influencing their establishment. Other species, like Woese-5a, show that not only the level of salinity is to be considered to understand its effect but also the exposition time. If after three weeks only a negative relationship was present between Woese-5a and salinity, that relationship turns significant after six weeks. Orders, such as Methanomicrobial showed a significant decline throughout the salinity gradient after three weeks but end up having a positive relationship after six weeks and could then demonstrate either the order's long-term resilience to NaCl introduction, or the substitution to different families within the same order. Many taxa contributed to the observed significant differentiation starting at 0.93 ppt (930 mg/L^{-1}) NaCl in sedimental archaea communities. The SIMPER uncovered a significant shift of relative abundance for Methanomicrobia, decreasing as the salinity rose, while Methanosarcinia's abundance increased with salinity. These results were surprising, considering that Methanomicrobiaceae, the concerned Methanomicrobia, is known to be a salt-tolerant methanogen (Chen *et al.*, 2020) that can be found in estuarine mixing zones. While competition for nutrients could occur between dominant methanogenic subpopulation, the incapacity of Methanomicrobiales to use acetate as a carbon source (Angelidaki *et al.*, 2011), while dominant in Methanosaetaceae (Methanosarcinia) (Karakashev *et al.*, 2006 ; Tian *et al.*, 2018), could be an influential factor, especially the level of acetate bioavailable for methanogenic pathways. As acetoclastic methanogenesis is a dominating pathway in freshwater sediments, composing up to two-thirds of the methane formed (Fenchel *et al.*, 2012), a rise in acetate brought on by the fermentation of particulate organic carbon (POC) by bacteria (Zheng *et al.*, 2022) is possible, following eukaryotic, bacterial and archaeal salt-induced death and lysis (Bianchi & Bauer, 2011). While decaying process could bring higher levels of acetate, taxa like Methanosarcina would be predominant in high-acetate environments (Pavlostathis, 2011) and is shown to be present in all salt-supplemented sedimental samples but are absent from the microcosms without NaCl addition at all sampling times. Conversely, the Methanosaeta taxa is present in all sample and has been

shown to benefit from lower acetate bioavailability (Smith & Ingram-Smith, 2007 ; Chen & He, 2015 ; Pierangeli *et al.*, 2021). As Methanosarcinia was shown to be correlated with salinity in our experiment, these results highlight the importance of nutrients analysis in further studies. The loss of eukaryotic species could be an important driver for taxa such as Methanomassilicocales, which was shown to contribute to community transition, and are dependent on methanol production by phytoplankton (Fischer *et al.*, 2021) but also to aerobic and anoxic microbial demethoxylation of pectin, lignin and galactans in which phytoplankton assimilates their carbon.

Conversely, as highlighted by the SIMPER analysis, whether for the Methylophilaceae or the Oxalobacteraceae family, the Burkholderiales order was very strongly and negatively correlated with the salinity gradient in the water samples after three weeks. As those results go hand in hand with those of the study carried out on epilimnion communities (Gagnon *et al*., 2022), even more similarities were present. The increase in Bacteroidia at higher salinity, also observed in mesocosms, was reminiscing of that observed in estuaries (Webster *et al.*, 2015; Liu *et al.*, 2016). In the epilimnion, the observed variations could have been influenced by the increase in NaCl concentration but also by the reduction in predation pressure, the eukaryotic α-diversity loss, and the associated decomposition. Although the composition of the bacterial communities between the upper and lower strata of the freshwater environment that makes up lake Croche may vary, the similarity of variation between some of the major groups composing them suggests that they could be subjected to similar influences, despite lower predation pressure in the anoxic layer (Pedrós-Alió *et al.*, 2000).

3.5 Conclusion

The effect of sodium chloride introducing in freshwater on microbial communities is a growing area of research. Our study provided an insight on the effect generated on prokaryotic α-diversity and abundance by different NaCl concentrations. The introduction of NaCl was shown to have a negative effect on hypolimnetic bacterial α-diversity after six weeks. However, the archaeal community’s composition was seen to be an important driving factor in the variation encountered.

In sediments, our results indicated that despite a weak penetration potential of NaCl, variations were seen for archaeal communities' absolute abundance after three weeks, and on its α-diversity after six weeks, despite no direct linearity with NaCl. Consideration for the major taxa leads to believe in a high level of tolerance for salinity that was reflected in low β-diversity values. In subsequential experiments, nutrients analysis as well as a deeper analysis of rare taxa and a co-occurrence network would provide a better understanding of the dynamics at play.

We also sought to find if a salinity threshold leading to a significant microbial community differentiation was present within the salinity limits of our experiments, for bacteria and archaea, but also for eukaryotes, to check if a domain exhibited a higher level of sensitivity towards salinity. In hypolimnetic water samples, our results indicate that the lowest salinity threshold encountered for microbial communities was 0.93 ppt (930 mg/L^{-1}) NaCl. As this would represent an approximate introduction of 564.13 mg/L^{-1} Cl-, and that the chronic exposure regulations limits are set to 120 mg/L^{-1} Cl^- in Canada and 230 mg/L^{-1} Cl^- in the United States, compliance with regulations should suffice to avoid significant hypolimnetic freshwater archaeal, bacterial or eukaryotic communities from a dire and potentially irreversible transition.

3.6 Figures and tables

Table 3.6.1. Values associated with regression between salinity and archaeal and bacterial absolute abundance in water and sediment samples. Sampling times, R^2 and *p* values are shown. Visual representations are available in Fig. 3.7.S1 and 3.7.S2.

Variables	**Time**	**R^2**	***p value***
Water archaea absolute abundance × Salinity	T3	0.2342	0.4088
	T6	0.1831	0.4723
Sediment archaea absolute abundance × Salinity	T3	0.6703	0.09011
	T6	0.5589	0.1463
Water bacterial absolute abundance × Salinity	T3	0.5555	0.1482
	T6	0.4064	0.2473
Sediment bacterial absolute abundance × Salinity	T3	0.0336	0.0768
	T6	0.0613	0.688

Table 3.6.2. Values associated with regression between salinity and archaeal or bacterial α diveristy (Shannon's H) in water and sediment samples. Sampling times, R^2 and *p* values are shown. Visual representations are available in Fig. 3.7.S3 and 3.7.S4.

Variables	**Time**	**R^2**	***p value***
Water archaeal α diversity × Salinity	T3	0.2637	0.3762
	T6	0.2605	0.3796
Sediment archaeal α diversity × Salinity	T3	0.0088	0.8808
	T6	0.5186	0.1701
Water bacterial α diversity × Salinity	T3	0.0418	0.7414
	T6	0.9196	0.00992
Sediment bacterial α diversity × Salinity	T3	0.0893	0.62525
	T6	0.0004	0.97385

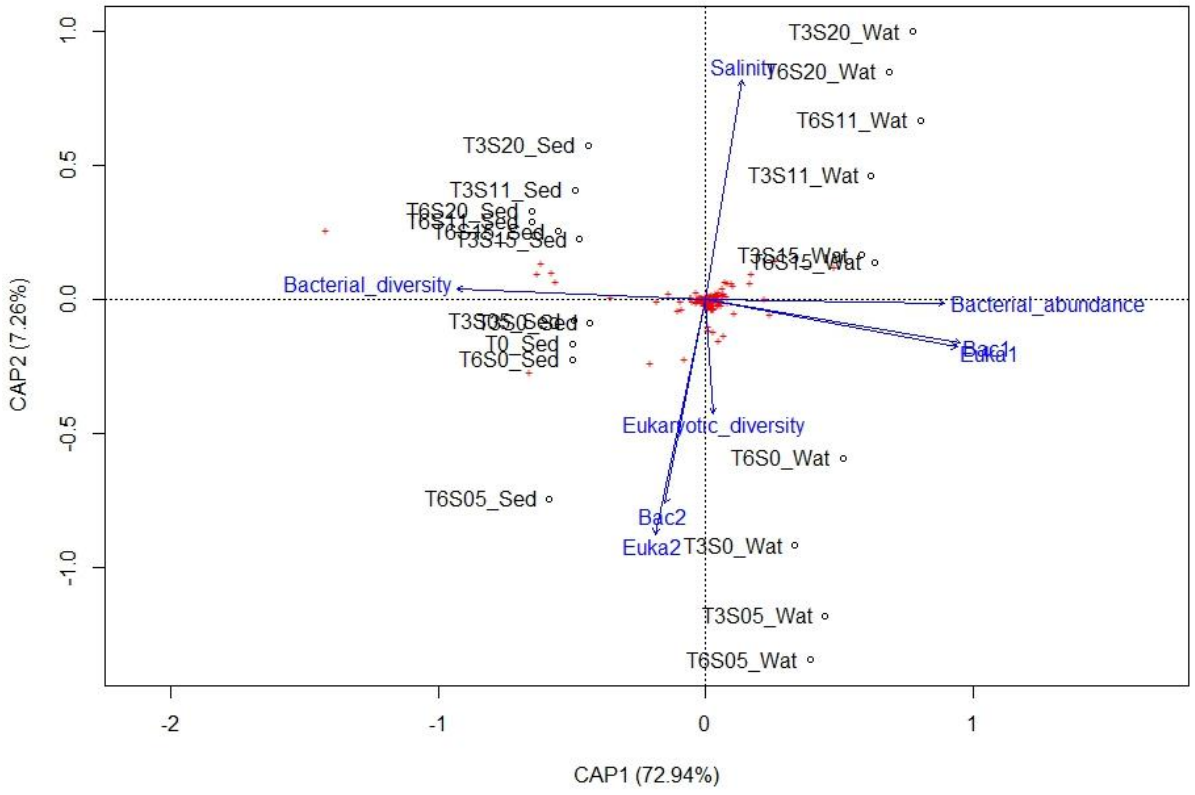

Figure 3.6.1. Distance-based redundancy analysis (db-RDA) used to correlate archaeal communities from water and sediment samples with explanatory factors. OTUs are represented as red points. T3, samples taken after a thre-weeks incubation; T6, samples taken after a six-week incubation; Sed, sedimentary samples; Wat, Water samples Bac1, bacterial community composition represented by the first axis of a PCoA (see Table S3 for PCoA axes values); Bac2, bacterial community composition represented by the second axis of a PCoA; Euka1, eukaryotic community composition represented by the first axis of a PCoA; EukA2, eukaryotic community composition represented by the second axis of a PCoA; Diveuc, eukaryotic diversity.

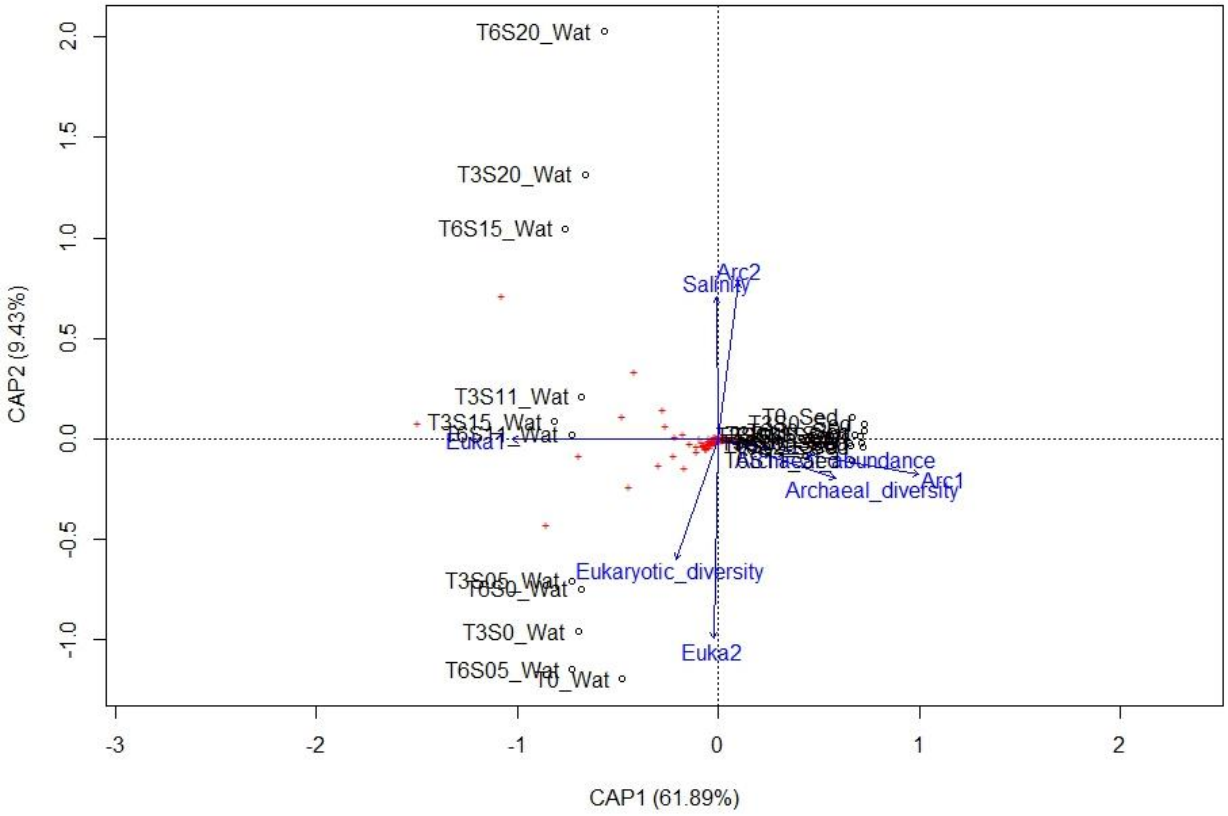

Figure 3.6.2. Distance-based redundancy analysis (db-RDA) used to correlate bacterial communities from water and sediment samples with explanatory factors. OTUs are represented as red points. T3, samples taken after a three-weeks incubation in microcosms; T6, samples taken after a six-week incubation; Sed, sedimentary samples; Wat, water samples; arc1, archaeal community composition represented by the first axis of a PCoA (see Table S3 for PCoA axes values); Arc2, archaeal community composition represented by the second axis of a PCoA; Euka1, eukaryotic community composition represented by the first axis of a PCoA; EukA2, eukaryotic community composition represented by the second axis of a PCoA; Diveuc, eukaryotic diversity.

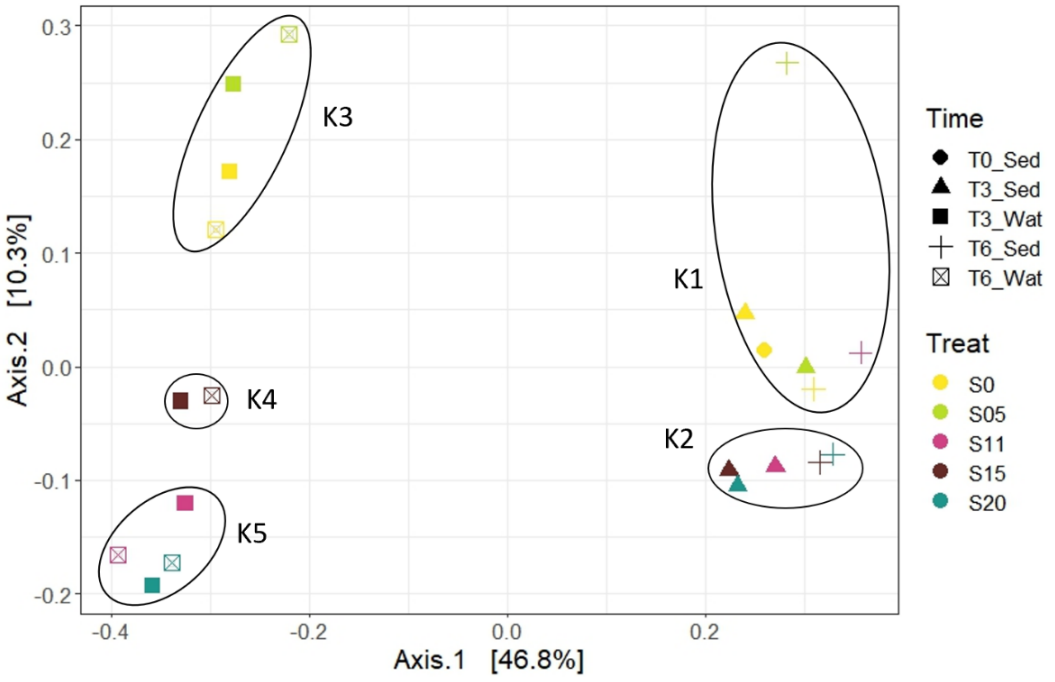
K3
K1
K4
K2
K5
Axis.2 [10.3%]
Axis.1 [46.8%]
0.3
0.2
0.1
0.0
-0.1
-0.2
-0.4
-0.2
0.0
0.2
Time
T0_Sed
T3_Sed
T3_Wat
T6_Sed
T6_Wat
Treat
S0
S05
S11
S15
S20

(a)

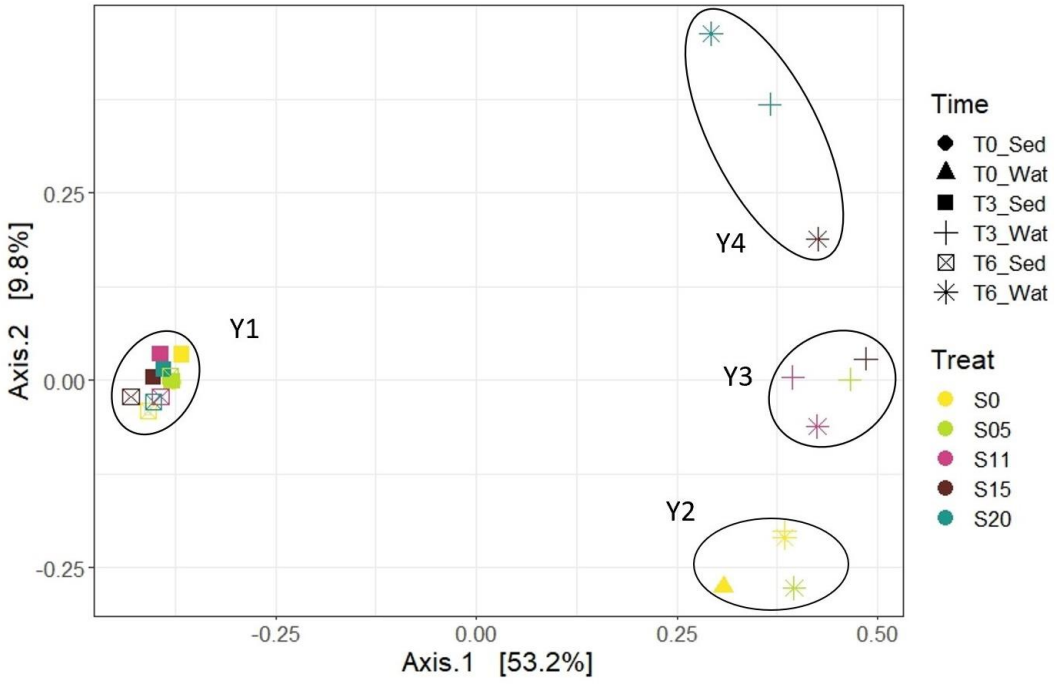
Y4
Y1
Y3
Y2
Axis.2 [9.8%]
Axis.1 [53.2%]
0.25
0.00
-0.25
-0.25
0.00
0.25
0.50
Time
T0_Sed
T0_Wat
T3_Sed
T3_Wat
T6_Sed
T6_Wat
Treat
S0
S05
S11
S15
S20

(b)

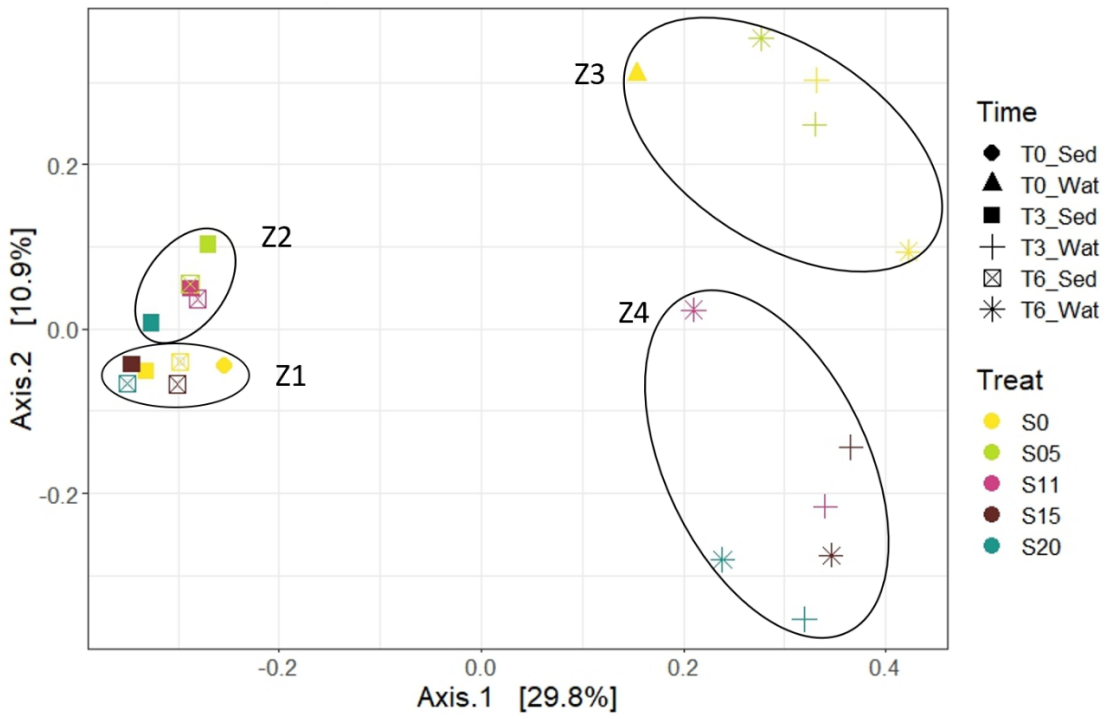

(c)

Figure 3.6.3. Principal coordinate analysis based on dissimilarity matrices (Bray-Curtis) for the microcosm's communities. **(a)** Archaeal communities. **(b)** Bacterial communities. **(c)** Eukaryotic communities. For each PCoA, the two first axes of variance are shown. The different type of medium and sampling times are shown within the "Time" section. Treatments are shown under "Treat". The different microcosms treatment represents salinities as follow: S0 (0.01 ppt or 10 mg/L^{-1}), S5 (0.16 ppt or 160 mg/L^{-1}), S11 (0.93 ppt or 930 mg/L^{-1}), S15 (1.93 ppt or 1930 mg/L^{-1}) and S20 (3.22 ppt or 3220 mg/L^{-1}). Clusters created for further analysis are shown (circles) and identified.

3.7 Supplementary figures and tables

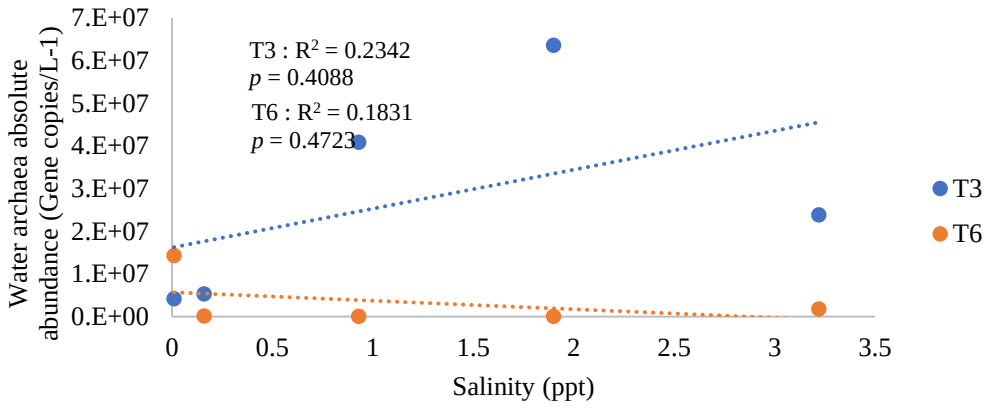

(a)

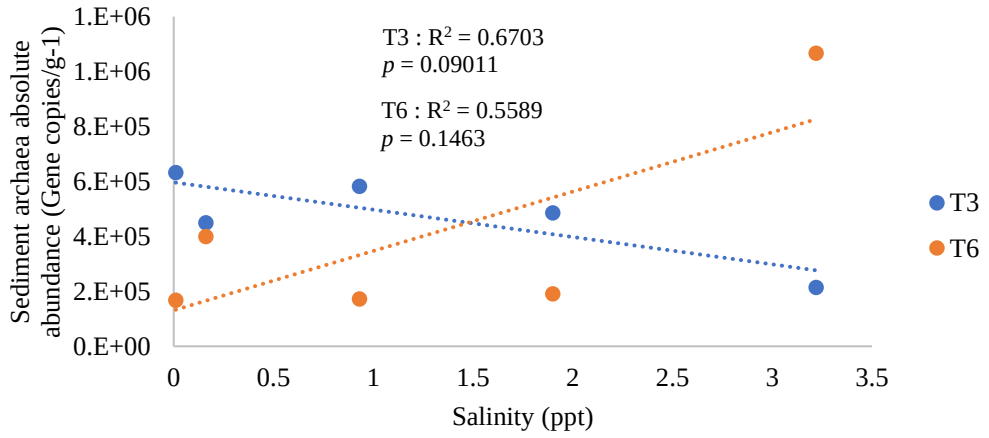

(b)

Supplementary figure 3.7.S1. **(a)** Planktonic and **(b)** sedimentary archaeal absolute abundance regression analysis, with salinity as the independent variable. Values are shown through the gradient after a three- (T3) and six-week (T6) incubation. All abundance values were obtained by digital polymerase chain reactions (dPCR). R2 and *p*-values are displayed.

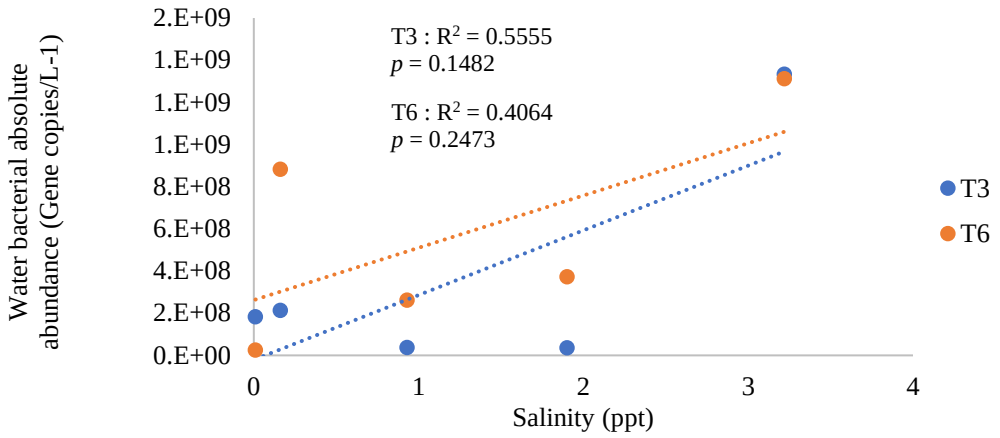

(a)

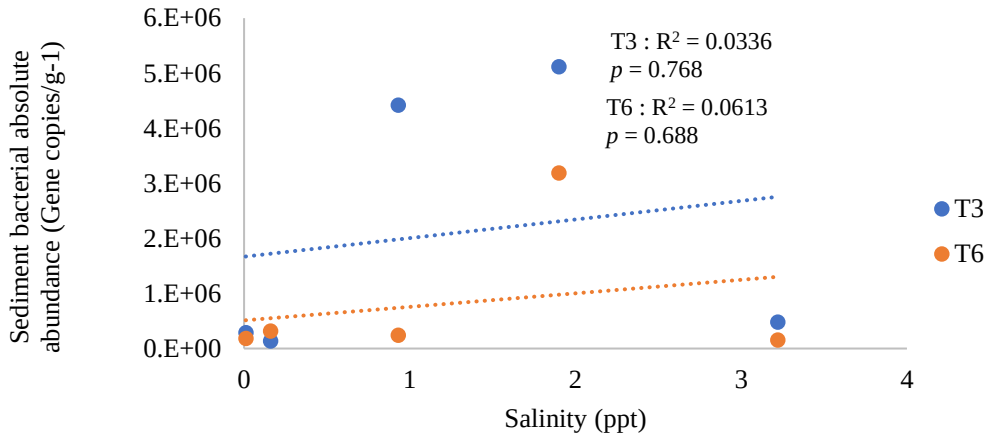

(b)

Supplementary figure 3.7.S2. **(a)** Planktonic and **(b)** sedimentary bacterial absolute abundance regression analysis, with salinity as the independent variable. Values are shown through the gradient after a three- and six-week incubation in microcosms. All abundance values were obtained by digital polymerase chain reactions (dPCR). R2 and *p*-values are displayed.

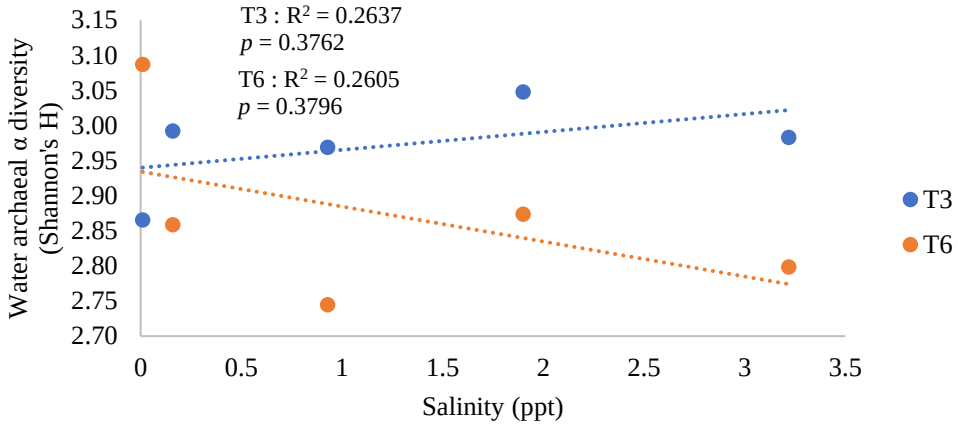

(a)

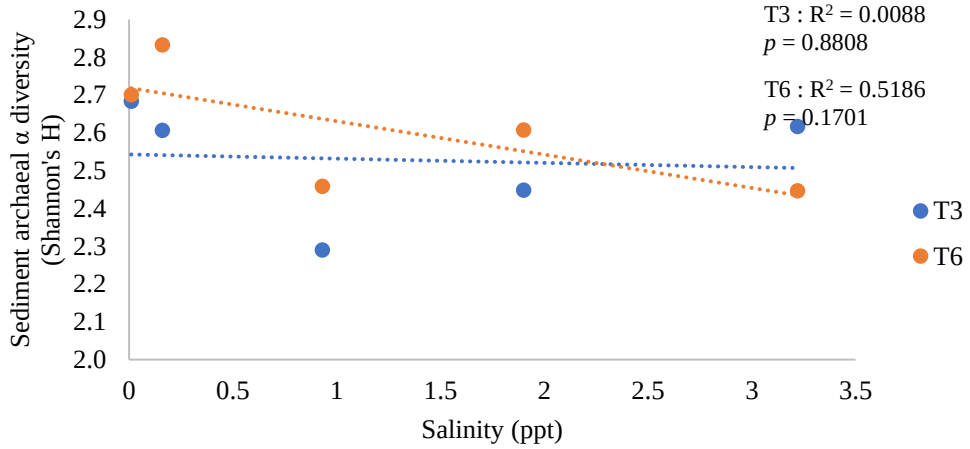

(b)

Supplementary figure 3.7.S3. **(a)** Regression for archaeal α diversity (Shannon's H) in water samples and salinity after a three- and six-week incubation in microcosms. **(b)** Regression for archaeal α diversity in sediment samples and salinity after a three- and six-week incubation in microcosms. All Shannon index values were calculated from raw OTU tables. R2 and *p*-values for both sampling times are shown.

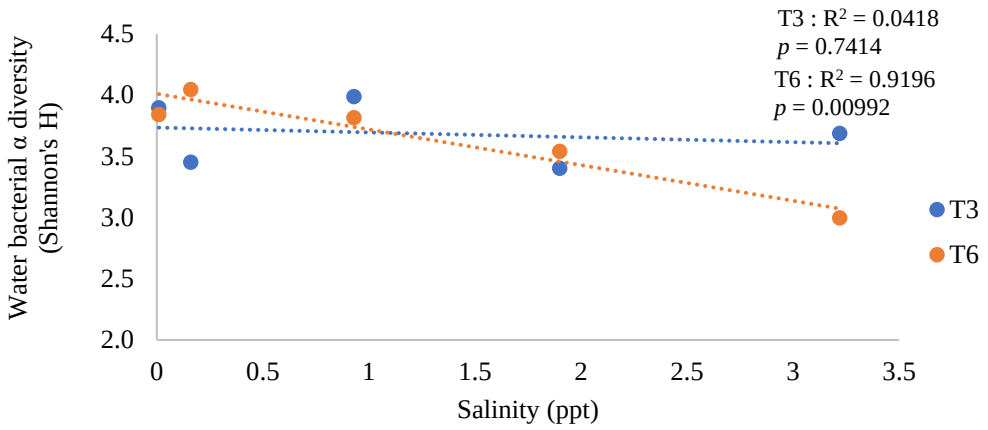

(a)

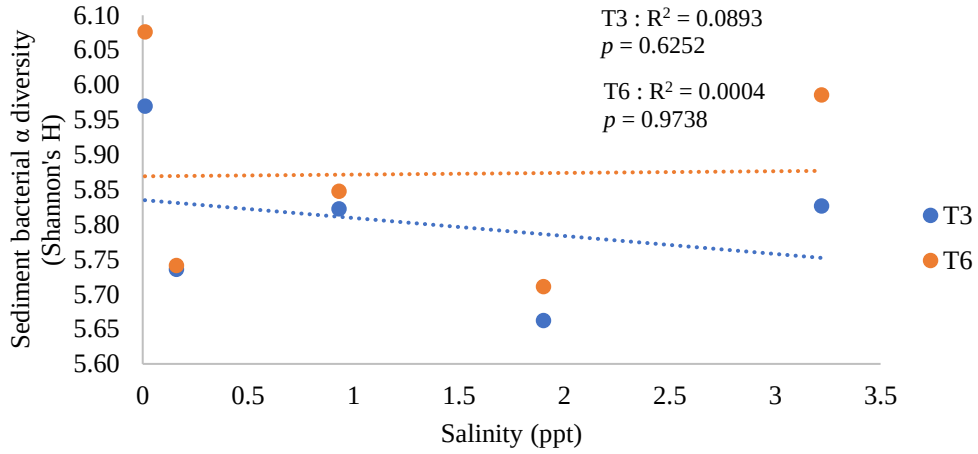

(b)

Supplementary figure 3.7.S4. **(a)** Regression for bacterial α diversity (Shannon's H) in water samples, with salinity as the independent variable after a three- and six-week incubation in microcosms. **(b)** Regression for bacterial α diversity in sediment samples and salinity after a three- and six-week incubation in microcosms. Shannon indexes were obtained from raw OTU tables. R2 and *p*-values for both sampling times are shown.

(a)

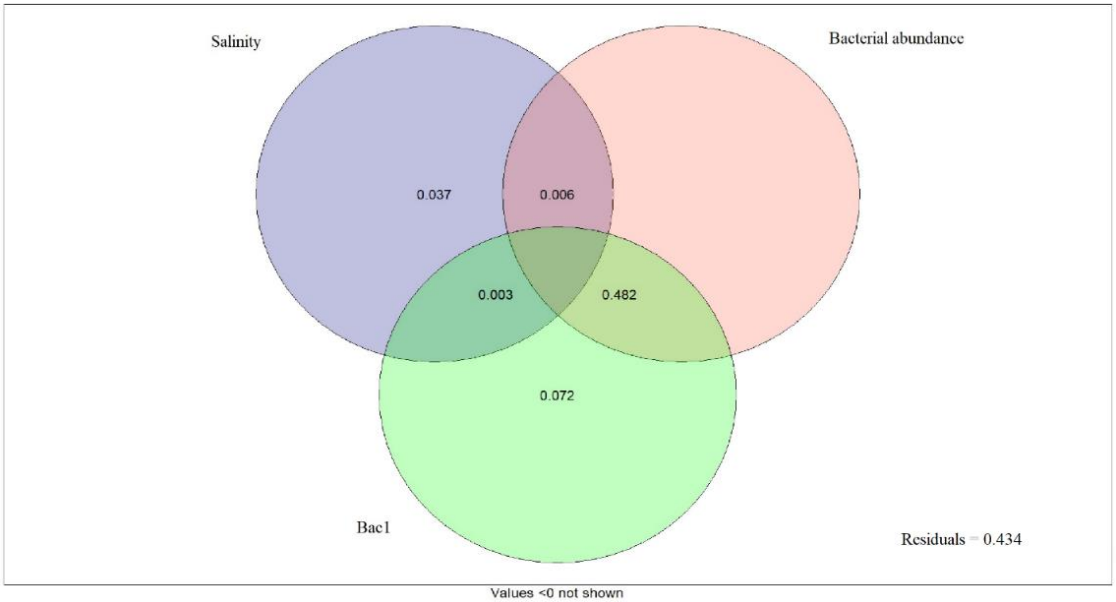

(b)

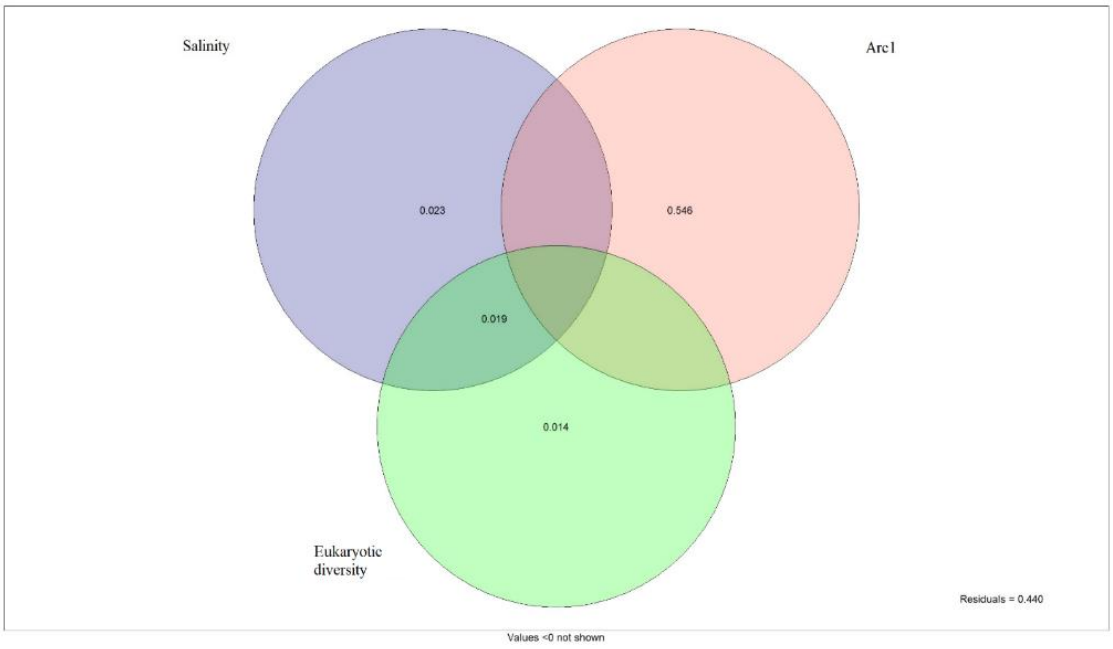

Supplementary figure 3.7.S5. **(a)** Variance partitioning analysis explaining variation in archaeal communities for three explanatory factors, separately and together: salinity, bacterial abundance and the bacterial community composition's first PCoA axis (Bac1). Residual variance is shown (bottom right). **(b)** Variance partitioning analysis explaining variation in bacterial communities for three explanatory factors, separately and together: salinity, archaeal community composition's first PCoA axis (Arc1) and eukaryotic diversity. Residual variance is shown (bottom right).

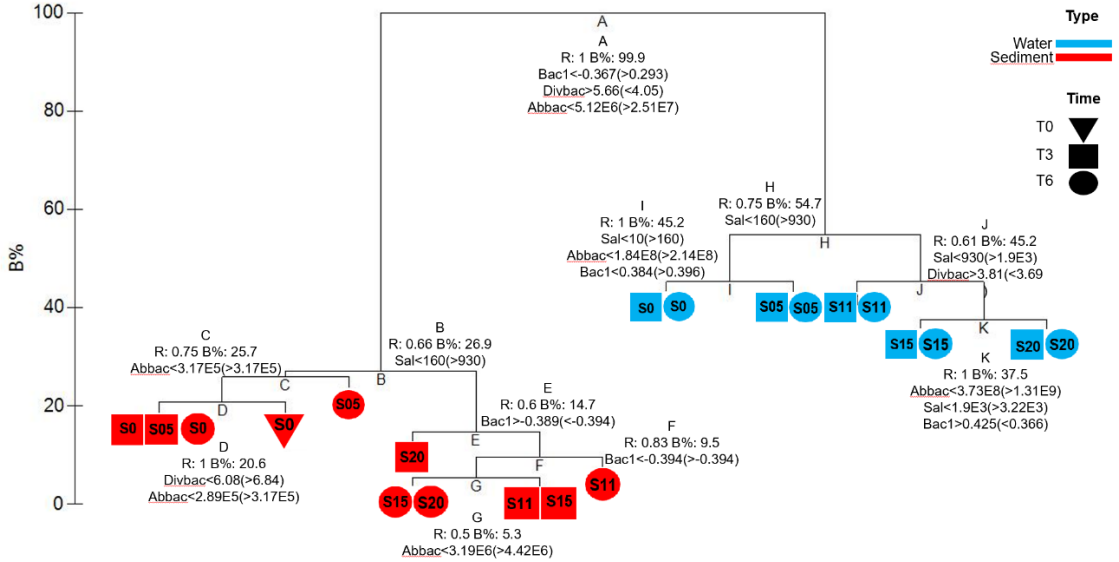

Supplementary figure 3.7.S6. Linkage tree (LINKTREE) analysis showing the clustering of archaeal samples constrained by explanatory factors. R represents the optimal ANOSIM R value. B% represents the absolute difference (Bray-Curtis). Abbac, bacterial abundance; Divbac, bacterial diversity; Bac1, bacterial community composition represented by the first axis of a PCoA; Sal, salinity; T0, initial sampling; T3, sampling after three weeks; T6, sampling after six weeks.

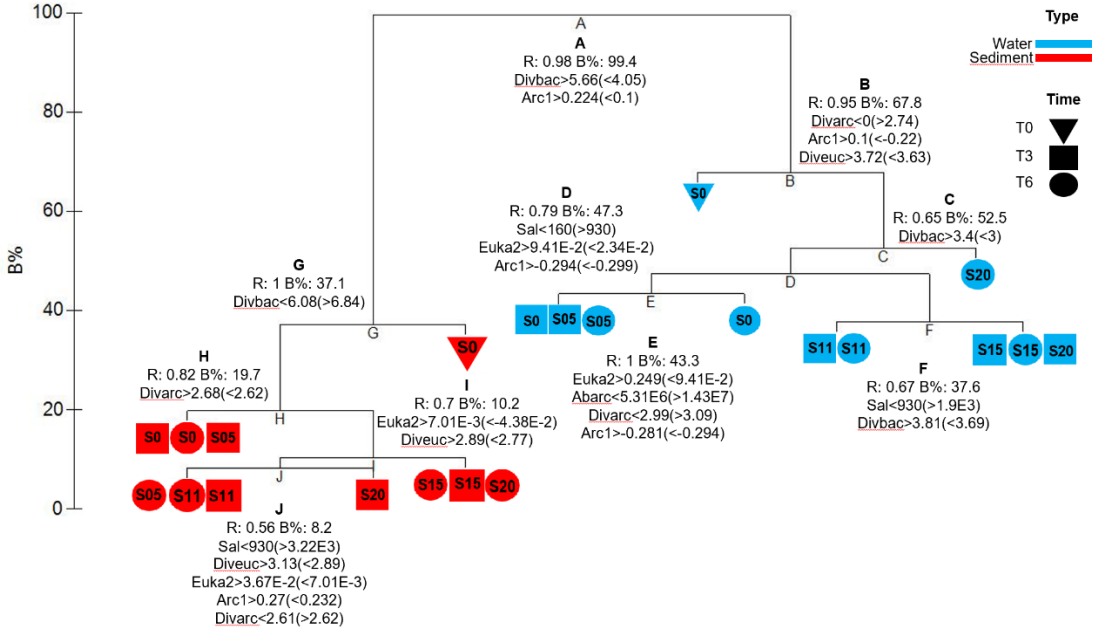

Supplementary figure 3.7.S7. Linkage tree (LINKTREE) analysis showing the clustering of bacterial microcosm samples constrained by explanatory factors. R represents the optimal ANOSIM R value. B% represents the absolute difference (Bray-Curtis). Sal, salinity; Diveuc, eukaryotic diversity; Euka2, eukaryotic community composition represented by the second axis of a PCoA; arc1, archaeal community composition represented by the first axis of a PCoA; Divarc, archaeal diversity; Divbac, bacterial diversity; T0, initial sampling; T3, sampling after three weeks; T6, sampling after six weeks.

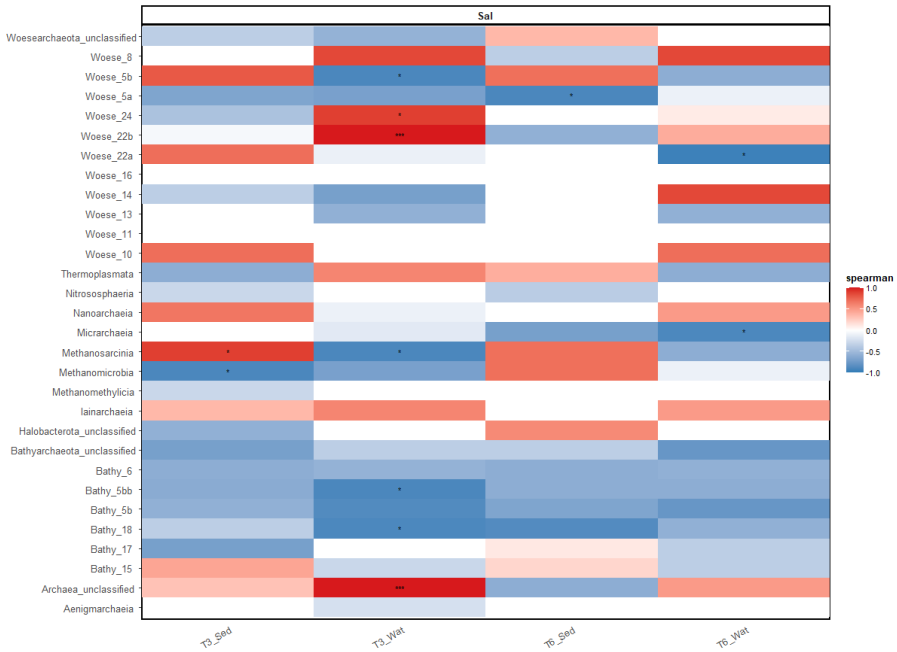

(a)

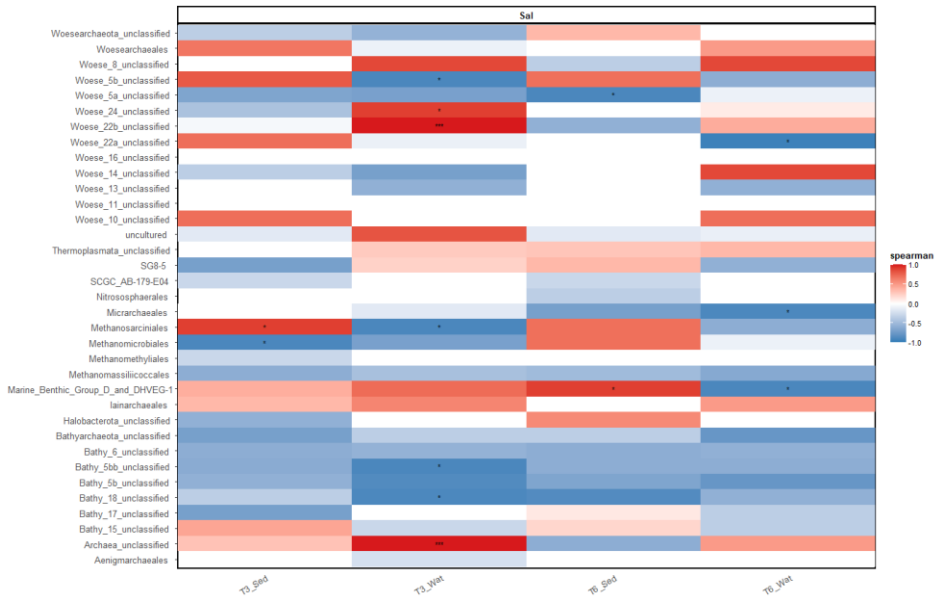

(b)

Supplementary figure 3.7.S8. Spearman correlations between the 500 most abundant archaeal taxa present in the microcosm samples and the salinity values. Time and sampling media is shown at the base of the column. The correlation coefficients are shown on the color scale, with a positive relation being in shown in red, while negative relations are shown in blue. Absence of the taxa or absence of relation (Spearman $\rho \approx 0$) is shown in white. The level of significance is shown by asterisks (0.001 =”***”, 0.01=”**”, 0.05=”*”). **(a)** Correlations of the 500 most abundant archaeal taxa, presented at the class taxonomic rank. **(b)** Correlations of the 500 most abundant archaeal taxa, presented at the order taxonomic rank.

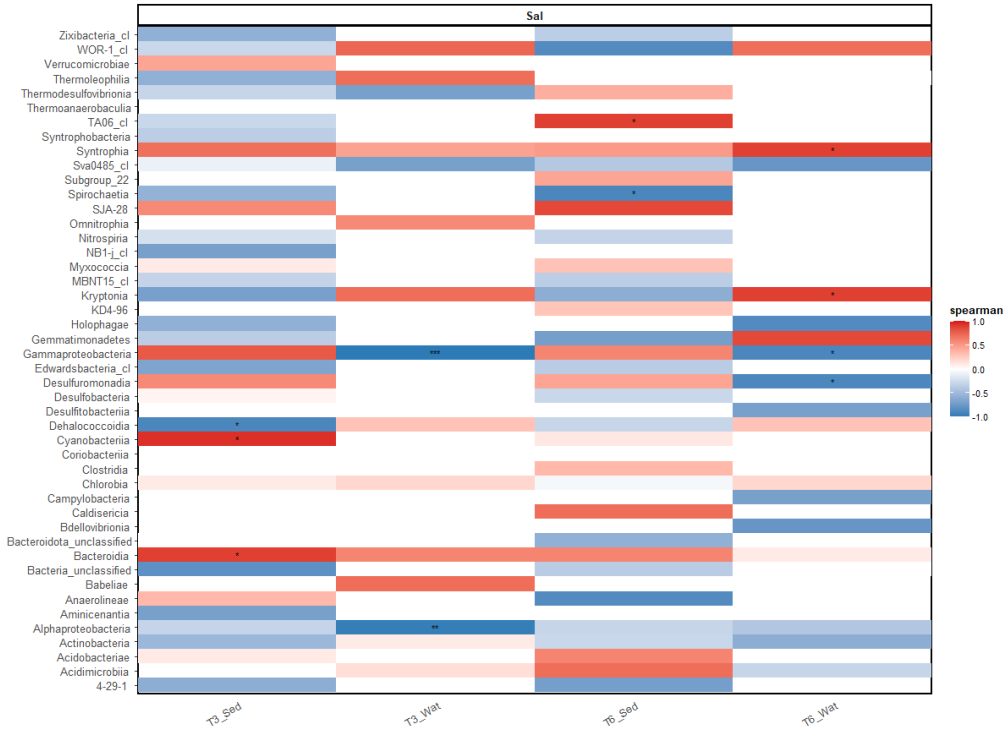

(a)

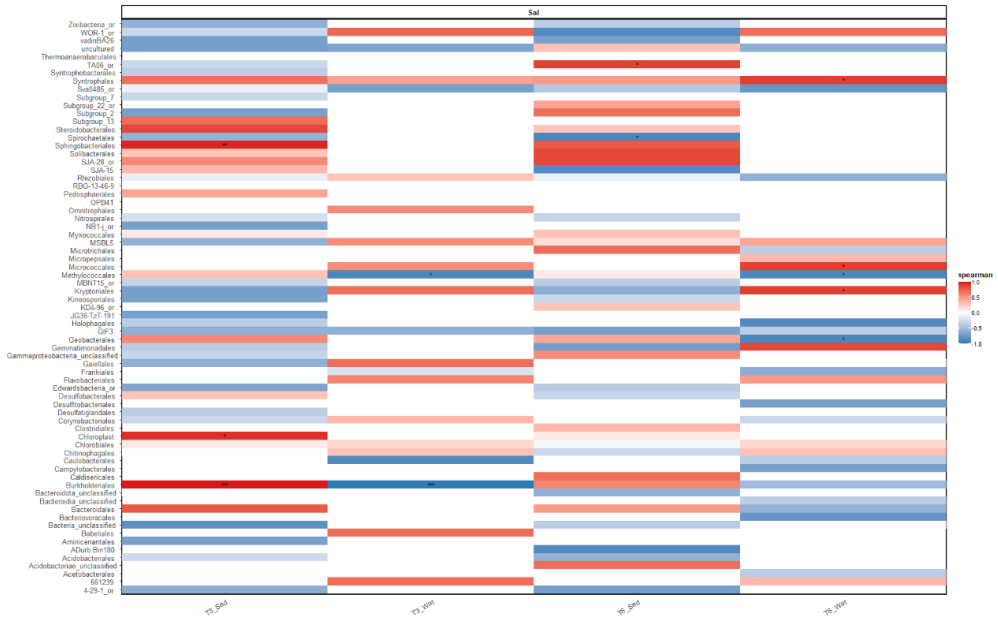

(b)

Supplementary figure 3.7.S9. Spearman correlations between the 500 most abundant bacterial taxa present in the microcosm samples and the salinity values. Time and sampling media is shown at the base of the column. The correlation coefficient is shown on the color scale, with a positive relation being in shown in red, while negative relations are shown in blue. Absence of the taxa or

absence of relation (Spearman ρ ≈ 0) is shown in white. The level of significance are shown by asterisks (0.001 =”***”, 0.01=”**”, 0.05=”*”). **(a)** Correlations of the 500 most abundant bacterial taxa, presented at the class taxonomic rank. **(b)** Correlations of the 500 most abundant bacterial taxa, presented at the order rank.

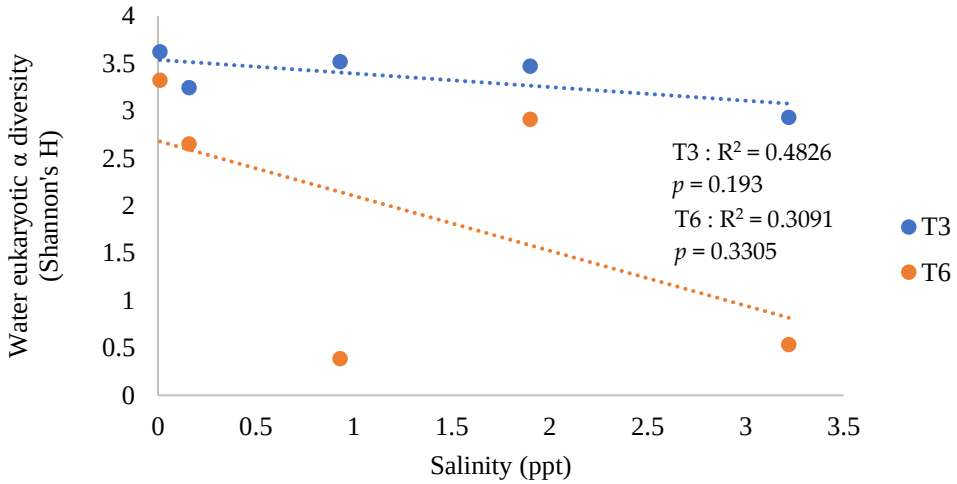

(a)

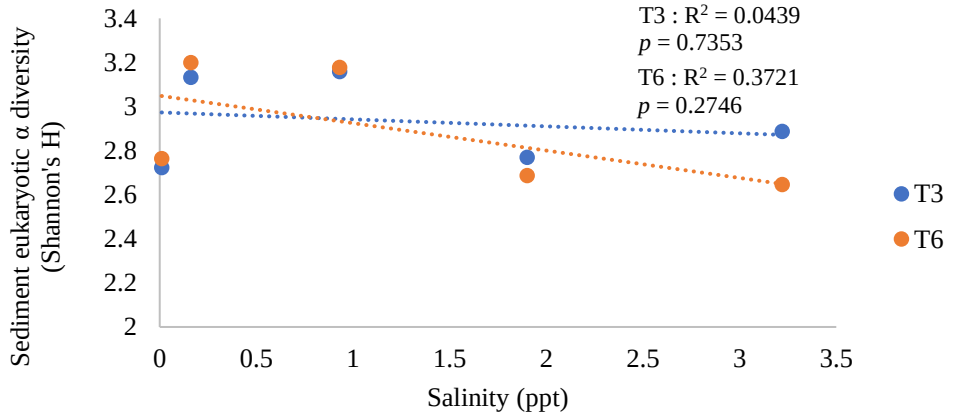

(b)

Supplementary figure 3.7.S10. **(a)** Regression for eukaryotic α diversity (Shannon’s H) in water samples, with salinity as the independent variable after a three- and six-week incubation in microcosms. **(b)** Regression for eukaryotic α diversity in sediment samples and salinity after a three-and six-week incubation in microcosms. Shannon indexes were obtained from raw OTU tables. R2 and *p*-values for both sampling times are shown.

Supplementary table 3.7.S1. Reaction mixture used for each chip in the context of dPCR.

Material	Volume per chip (µL)	Final concentration
QuantStudio™ 3D Digital PCR Master Mix	7.25	1X
20X SYBR Green 1 dye in TE buffer, pH 8	1.45	2X
Forward and reverse primer	0.3	200nM
cDNA sample	1	50ng total
Water	Bring to 14.5	-

Supplementary table 3.7.S2. Steps carried out during dPCR, depending on the primers used. The phases, temperatures, times and number of cycles are presented.

Eukaryotic primers E960F - NSR1438R

	Phase	Temperature	Number of cycles	Number of cycles
Step 1	Initial denaturation	96°C	00:10:00	1X
Step 2	Denaturation	58°C	00:02:00	39X
	Hybridization	98°C	00:00:30	
	Elongation60°C	00:02:00		
Step 3	Conservation	10°C	∞	1X

Bacterial primers B341F - B785R

	Phase	Temperature	Number of cycles	Number of cycles
Step 1	Initial denaturation	96°C	00:10:00	1X
Step 2	Denaturation	56°C	00:02:00	39X
	Hybridization	98°C	00:00:30	
	Elongation	60°C	00:02:00	
Step 3	Conservation	10°C	∞	1X

Archaeal primers A340F - A915R

	Phase	Temperature	Number of cycles	Number of cycles
Step 1	Initial denaturation	96°C	00:10:00	1X
Step 2	Denaturation	58°C	00:02:00	39X
	Hybridization	64°C	00:00:30	
	Elongation	60°C	00:02:00	
Step 3	Conservation	10°C	∞	1X

Supplementary table 3.7.S3. Following a Principal coordinate analysis (PCoA) on bacterial, archaeal and eukaryotic OTU tables, the first two axes values from the computed PCoA were kept as environmental variables.

Sample	Bacterial PCoA axis 1	bacterial PCoA axis 2	Archaeal PCoA axis 1	Archaeal PCoA axis 2	Eukaryotic PCoA axis 1	Eukaryotic PCoA axis 2
T0_S0_Wat	0.307796694	-0.27572654	NA	NA	0.153706711	0.309126148
T0_S0_sed	-0.377388628	-0.00252214	0.259920645	0.01426841	-0.253285947	-0.044437553
T3_S0_Wat	0.384439585	-0.201759959	-0.280692271	0.17134219	0.331250071	0.302464517
T3_S0_sed	-0.367324461	0.033852242	0.239374895	0.046279897	-0.33184383	-0.051629225
T3_S05_Wat	0.465647186	0.001299766	-0.276762302	0.248450318	0.329686465	0.248870541
T3_S05_sed	-0.379116902	-0.00075318	0.300602046	-0.001150038	-0.27020099	0.102532429
T3_S11_Wat	0.394297993	0.003615985	-0.325023832	-0.120304129	0.339874913	-0.215633806
T3_S11_sed	-0.39360944	0.034460331	0.270321333	-0.08814901	-0.286490814	0.048651198
T3_S15_Wat	0.485721071	0.028483252	-0.329511725	-0.030412476	0.365361199	-0.144014077
T3_S15_sed	-0.402634141	0.003544931	0.223547024	-0.09176392	-0.345551825	-0.043808834
T3_S20_Wat	0.365797408	0.36810822	-0.357933632	-0.192990713	0.319288677	-0.353384759
T3_S20_sed	-0.389499992	0.013791675	0.232126252	-0.104737386	-0.326561845	0.007014065
T6_S0_Wat	0.383870678	-0.210178666	-0.294200437	0.120947271	0.422059684	0.094052016
T6_S0_sed	-0.409095506	-0.040762843	0.308447244	-0.019703595	-0.297891428	-0.039755915
T6_S05_Wat	0.396007494	-0.277131485	-0.220390888	0.292664086	0.276451916	0.353865848
T6_S05_sed	-0.381355192	0.005434295	0.28198017	0.267284622	-0.288126655	0.054660819
T6_S11_Wat	0.425114044	-0.06117766	-0.393312373	-0.165513929	0.209987822	0.023362201
T6_S11_sed	-0.393553191	-0.02231498	0.356270181	0.012243155	-0.280563286	0.036718131
T6_S15_Wat	0.425221748	0.188428594	-0.298762251	-0.024985577	0.345870744	-0.275268559
T6_S15_sed	-0.430501721	-0.022294033	0.315276435	-0.084046244	-0.301177341	-0.066978793
T6_S20_Wat	0.292707604	0.462200472	-0.339148053	-0.17257337	0.238446081	-0.280498328
T6_S20_sed	-0.40254233	-0.028598276	0.327871541	-0.077149562	-0.350290321	-0.065908064

Supplementary table 3.7.S4. All abiotic and biotic values used for multivariate analyses, for all samples at all sampling time in microcosms.

Sample	Salinity - ppt	Bacteria; abundance - Wat: Gene copies/L^{-1}, Sed: Gene copies/g^{-1}	Archaeal abundance - Wat: Gene copies/L^{-1}, Sed: Gene copies/g^{-1}	Archaeal diversity - Shannon's H	Eukaryotic diversity - Shannon's H	Bacterial diversity - Shannon's H	Bacterial PCoA axis 1	Bacterial PCoA axis 2	Archaeal PCoA axis 1	Archaeal PCoA axis 2	Eukaryotic PCoA axis 1	Eukaryotic PCoA axis 2
T0_Wat	10	942412.5	51750	NA	3.72457	3.86817	0.30780	-0.27573	NA	NA	0.15371	0.30913
T0_Sed	10	316995	301402.5	2.53122	2.88417	6.83883	-0.37739	-0.00252	0.25992	0.01427	-0.25329	-0.04444
T3S0_Wat	10	183705000	4137375	2.86548	3.62671	3.89639	0.38444	-0.20176	-0.28069	0.17134	0.33125	0.30246
T3S0_Sed	10	289125	632572.5	2.68399	2.72300	5.96927	-0.36732	0.03385	0.23937	0.04628	-0.33184	-0.05163
T3S05_Wat	160	213915000	5312925	2.99235	3.24685	3.45301	0.46565	0.00130	-0.27676	0.24845	0.32969	0.24887
T3S05_Sed	160	137392.5	449865	2.60651	3.13255	5.73524	-0.37912	-0.00075	0.30060	-0.00115	-0.27020	0.10253
T3S11_Wat	930	36808500	40820250	2.96901	3.51993	3.98747	0.39430	0.00362	-0.32502	-0.12030	0.33987	-0.21563
T3S11_Sed	930	4420050	582975	2.28984	3.15770	5.82205	-0.39361	0.03446	0.27032	-0.08815	-0.28649	0.04865
T3S15_Wat	1900	36421500	63594750	3.04764	3.47481	3.40317	0.48572	0.02848	-0.32951	-0.03041	0.36536	-0.14401
T3S15_Sed	1900	5115375	485977.5	2.44822	2.76998	5.66184	-0.40263	0.00354	0.22355	-0.09176	-0.34555	-0.04381
T3S20_Wat	3220	1333500000	23782500	2.98316	2.93404	3.68789	0.36580	0.36811	-0.35793	-0.19299	0.31929	-0.35338
T3S20_Sed	3220	478972.5	214200	2.61676	2.88685	5.82650	-0.38950	0.01379	0.23213	-0.10474	-0.32656	0.00701
T6S0_Wat	10	25086750	14295000	3.08687	3.32550	3.84130	0.38387	-0.21018	-0.29420	0.12095	0.42206	0.09405
T6S0_Sed	10	182010	167692.5	2.70056	2.76306	6.07580	-0.40910	-0.04076	0.30845	-0.01970	-0.29789	-0.03976
T6S05_Wat	160	882000000	92700	2.85856	2.65344	4.04657	0.39601	-0.27713	-0.22039	0.29266	0.27645	0.35387
T6S05_Sed	160	317002.5	400072.5	2.83264	3.19951	5.74080	-0.38136	0.00543	0.28198	0.26728	-0.28813	0.05466
T6S11_Wat	930	261675000	600.75	2.74487	0.38922	3.81483	0.42511	-0.06118	-0.39331	-0.16551	0.20999	0.02336
T6S11_Sed	930	243000	172252.5	2.45894	3.17764	5.84745	-0.39355	-0.02231	0.35627	0.01224	-0.28056	0.03672
T6S15_Wat	1900	373140000	587.25	2.87377	2.91202	3.54178	0.42522	0.18843	-0.29876	-0.02499	0.34587	-0.27527
T6S15_Sed	1900	3185100	191017.5	2.60719	2.68583	5.71069	-0.43050	-0.02229	0.31528	-0.08405	-0.30118	-0.06698
T6S20_Wat	3220	1312012500	1772100	2.79822	0.53609	2.99779	0.29271	0.46220	-0.33915	-0.17257	0.23845	-0.28050
T6S20_Sed	3220	155707.5	1067775	2.44706	2.64544	5.98566	-0.40254	-0.02860	0.32787	-0.07715	-0.35029	-0.06591

Supplementary table 3.7.S5. ANOVA table for explanatory variables used in archaeal, bacterial and eukaryotic db-RDA. Bac1, bacterial community composition represented by the first axis of a PCoA (see Table 3.3 for PCoA axes values); Bac2, bacterial community composition represented by the second axis of a PCoa. Arc1, archaeal community composition represented by the first axis of a PCoA; Arc2, archaeal community composition represented by the second axis of a PCoA; Euka1, community composition represented by the first axis of a PCoA; EukA2, eukaryotic community composition represented by the second axis of a PCoA.

Archaea	**Df**	**SumOfSqs**	**F**	**Pr(>F)**
Salinity	1	0.14793	6.1659	0.006
Bacterial abundance	1	1.29456	53.96	0.001
Bacterial diversity	1	0.15396	6.4175	0.009

Eukaryotic diversity	1	0.03758	1.5663	0.206
Bac1	1	0.09201	3.8353	0.035
Bac2	1	0.0622	2.5927	0.091
Euka1	1	0.02763	1.1519	0.288
Euka2	1	0.0322	1.3421	0.257
Residual	12	0.28789		

Bacteria	**Df**	**SumOfSqs**	**F**	**Pr(>F)**
Salinity	1	0.27801	4.5849	0.02
Archaeal abundance	1	0.2563	4.2268	0.019
Archaeal diversity	1	1.02472	16.8995	0.001
Eukaryotic diversity	1	0.485	7.9986	0.001
Arc1	1	1.82127	30.0362	0.001
Arc2	1	0.13033	2.1494	0.108
Euka1	1	0.12672	2.0899	0.106
Euka2	1	0.21127	3.4842	0.042
Residual	13	0.78827		

Eukaryotes	**Df**	**SumOfSqs**	**F**	**Pr(>F)**
Sal	1	0.3172	2.1825	0.059 .
Abbac	1	2.07899	14.3044	0.001
Abarc	1	0.31589	2.1734	0.046
Divarc	1	0.33627	2.3137	0.055
Divbac	1	0.46834	3.2224	0.007
Bac1	1	0.42793	2.9444	0.013
Bac2	1	0.23151	1.5929	0.122
Arc1	1	0.31911	2.1956	0.057
Arc2	1	0.15068	1.0368	0.342
Residual	12	1.74407		

Supplementary table 3.7.S6. PERMANOVA realized on the different archaeal, bacterial and eukaryotic clusters obtained from PCoA and LINKTREE analysis, and separating the different sampling mediums (water / sediment) and salinity groups.

Archaea

	K1	K2	K3	K4	K5
K1		0.0162	0.0058	0.0364	0.0047
K2	0.0162		0.0096	0.0506	0.0083
K3	0.0058	0.0096		0.1327	0.0282
K4	0.0364	0.0506	0.1327		0.1392
K5	0.0047	0.0083	0.0282	0.1392	

Bacteria

	Y1	Y2	Y3	Y4
Y1		0.0007	0.001	0.0029
Y2	0.0007		0.0856	0.0298
Y3	0.001	0.0856		0.0294
Y4	0.0029	0.0298	0.0294	

Eukaryotes

	Z1	Z2	Z3	Z4
Z1		0.0039	0.0074	0.0041
Z2	0.0039		0.0012	0.0008
Z3	0.0074	0.0012		0.0027
Z4	0.0041	0.0008	0.0027	

Supplementary table 3.7.S7. Results of the similarity percentage (SIMPER) analysis and Kruskal-Wallis test on the different clusters obtained by the PCoA for the archaeal, bacterial and eukaryotic communities of Croche lake microcosms. Only clusters from same-mediums (water-water / sediment-sediment) were kept.

Clusters	SIMPER	OTU	Krusk p.val	fdr_krus k p.val	Taxonomy	Left mean abund	Left stdev	Right mean abund	Right stdev
K1 / K2	0.017585 227	Otu020	0.0051 67391	0.103219 141	Archaea(100);Halobacterota(100);Methanomicrobia(100);Methanomicrobiales(100);Methanomicrobiaceae(86);uncultured(85);	0.0204 59137	0.0027 85053	0.0107 79313	0.0063 47304
K1 / K2	0.016116 394	Otu004	0.0058 24908	0.103219 141	Archaea(100);Halobacterota(100);Methanosarcinia(100);Methanosarciniales(10 0);Methanosaetaceae(100);Methanosaeta(100);	0.0382 83454	0.0062 43291	0.0290 44861	0.0025 59686
K1 / K2	0.015214 903	Otu047	0.0088 28761	0.103219 141	Archaea(100);Woesearchaeota(100);Woese_5b(100);Woese_5b_unclassified(10 0);Woese_5b_unclassified(100);Woese_5b_unclassified(100);	0	0	0.0082 09427	0.0045 92006
K1 / K2	0.013339 465	Otu080	0.0452 01353	0.111222 867	Archaea(100);Archaea_unclassified(62);Archaea_unclassified(62);Archaea_unc lassified(62);Archaea_unclassified(62);Archaea_unclassified(62);	0.0015 2144	0.0037 26752	0.0080 98271	0.0045 34123
K1 / K2	0.013267 098	Otu065	0.0452 01353	0.111222 867	Archaea(100);Thermoplasmatota(100);Thermoplasmata(100);uncultured(100);u ncultured_fa(100);uncultured_ge(100);	0.0016 68762	0.0040 87616	0.0081 19777	0.0045 4697
K1 / K2	0.013014 408	Otu034	0.0347 18599	0.110551 33	Archaea(100);Thermoplasmatota(100);Thermoplasmata(100);Marine_Benthic_ Group_D_and_DHVEG-1(100);Marine_Benthic_Group_D_and_DHVEG-1_fa(100);Marine_Benthic_Group_D_and_DHVEG-1_ge(100);	0.0075 43396	0.0060 75765	0.0141 40706	0.0023 8952
K1 / K2	0.012578 395	Otu050	0.0290 96332	0.109367 394	Archaea(100);Woesearchaeota(100);Woese_5b(100);Woese_5b_unclassified(10 0);Woese_5b_unclassified(100);Woese_5b_unclassified(100);	0.0034 76388	0.0053 8576	0.0101 64801	0.0002 69637
K1 / K2	0.012578 395	Otu129	0.0290 96332	0.109367 394	Archaea(100);Thermoplasmatota(100);Thermoplasmata(100);Methanomassiliic occales(100);Methanomassiliicoccaceae(100);uncultured(100);	0.0068 48593	0.0053 6425	0	0
K1 / K2	0.012449 883	Otu009	0.0328 57128	0.109367 394	Archaea(100);Thermoplasmatota(100);Thermoplasmata(100);Marine_Benthic_ Group_D_and_DHVEG-1(100);Marine_Benthic_Group_D_and_DHVEG-1_fa(100);Marine_Benthic_Group_D_and_DHVEG-1_ge(100);	0.0199 95641	0.0045 33432	0.0260 38839	0.0024 74087
K1 / K2	0.012400 843	Otu062	0.0290 96332	0.109367 394	Archaea(100);Woesearchaeota(100);Woese_24(100);Woese_24_unclassified(10 0);Woese_24_unclassified(100);Woese_24_unclassified(100);	0.0066 40991	0.0051 63532	0	0
K1 / K2	0.011373 809	Otu040	0.0338 94854	0.109367 394	Archaea(100);Woesearchaeota(100);Woese_24(100);Woese_24_unclassified(10 0);Woese_24_unclassified(100);Woese_24_unclassified(100);	0	0	0.0061 16729	0.0055 84869
K1 / K2	0.011369 816	Otu167	0.0338 94854	0.109367 394	Archaea(100);Halobacterota(100);Methanosarcinia(100);Methanosarciniales(10 0);Methanosaetaceae(100);Methanosaeta(100);	0	0	0.0061 14602	0.0055 87792
K3 / K5	0.017205 819	Otu014	0.0338 94854	0.109367 394	Archaea(100);Archaea_unclassified(89);Archaea_unclassified(89);Archaea_unc lassified(89);Archaea_unclassified(89);Archaea_unclassified(89);	0.0088 71436	0.0061 56098	0.0224 02571	0.0017 48785
K3 / K5	0.013714 386	Otu040	0.0192 54406	0.103219 141	Archaea(100);Woesearchaeota(100);Woese_24(100);Woese_24_unclassified(10 0);Woese_24_unclassified(100);Woese_24_unclassified(100);	0	0	0.0111 6426	0.0019 21538
K3 / K5	0.012696 039	Otu004	0.0323 12911	0.109367 394	Archaea(100);Halobacterota(100);Methanosarcinia(100);Methanosarciniales(10 0);Methanosaetaceae(100);Methanosaeta(100);	0.0222 30055	0.0032 71716	0.0109 20644	0.0040 41767
K3 / K5	0.012619 469	Otu033	0.0307 53561	0.109367 394	Archaea(100);Bathyarchaeota(99);Bathy_5b(92);Bathy_5b_unclassified(92);Bat hy_5b_unclassified(92);Bathy_5b_unclassified(92);	0.0130 18846	0.0030 35797	0.0021 16358	0.0036 65639
K3 / K5	0.011935 411	Otu029	0.0307 53561	0.109367 394	Archaea(100);Bathyarchaeota(100);Bathy_18(100);Bathy_18_unclassified(100); Bathy_18_unclassified(100);Bathy_18_unclassified(100);	0.0124 33531	0.0036 7916	0.0021 16358	0.0036 65639
K3 / K5	0.011888 239	Otu010	0.0323 12911	0.109367 394	Archaea(100);Bathyarchaeota(100);Bathy_5bb(99);Bathy_5bb_unclassified(99); Bathy_5bb_unclassified(99);Bathy_5bb_unclassified(99);	0.0188 73245	0.0033 27611	0.0083 36625	0.0018 08395
K3 / K5	0.010412 993	Otu006	0.0307 53561	0.109367 394	Archaea(100);Woesearchaeota(100);Woese_5a(100);Woese_5a_unclassified(10 0);Woese_5a_unclassified(100);Woese_5a_unclassified(100);	0.0209 61565	0.0023 47774	0.0284 6971	0.0052 4754
K3 / K4	0.011915 841	Otu040	0.0284 59737	0.109367 394	Archaea(100);Woesearchaeota(100);Woese_24(100);Woese_24_unclassified(10 0);Woese_24_unclassified(100);Woese_24_unclassified(100);	0	0	0.0080 05288	0.0020 25207
K3 / K4	0.011483 374	Otu040	0.0455 00264	0.111222 867	Archaea(100);Woesearchaeota(100);Woese_24(100);Woese_24_unclassified(10 0);Woese_24_unclassified(100);Woese_24_unclassified(100);	0	0	0.0094 76258	NA
K5 / K4	0.010068 262	Otu020	0.0455 00264	0.111222 867	Archaea(100);Halobacterota(100);Methanomicrobia(100);Methanomicrobiales(100);Methanomicrobiaceae(86);uncultured(85);	0	0	0.0066 23223	7.07E-05
K5 / K4	0.010068 262	Otu093	0.0455 00264	0.111222 867	Archaea(100);Archaea_unclassified(95);Archaea_unclassified(95);Archaea_unc lassified(95);Archaea_unclassified(95);Archaea_unclassified(95);	0	0	0.0066 23223	7.07E-05
K5 / K4	0.010068 262	Otu100	0.0455 00264	0.111222 867	Archaea(100);Archaea_unclassified(99);Archaea_unclassified(99);Archaea_unc lassified(99);Archaea_unclassified(99);Archaea_unclassified(99);	0.0065 09447	0.0003 25955	0	0
K5 / K4	0.010068 262	Otu110	0.0455 00264	0.111222 867	Archaea(100);Woesearchaeota(100);Woese_13(100);Woese_13_unclassified(10 0);Woese_13_unclassified(100);Woese_13_unclassified(100);	0	0	0.0066 23223	7.07E-05
K5 / K4	0.010068 262	Otu112	0.0455 00264	0.111222 867	Archaea(100);Halobacterota(100);Methanosarcinia(100);Methanosarciniales(10 0);Methanosaetaceae(100);Methanosaeta(100);	0	0	0.0066 23223	7.07E-05
K5 / K4	0.010068 262	Otu138	0.0455 00264	0.111222 867	Archaea(100);Woesearchaeota(100);Woese_24(100);Woese_24_unclassified(10 0);Woese_24_unclassified(100);Woese_24_unclassified(100);	0	0	0.0066 23223	7.07E-05

K5 / K4	0.010068262	Otu194	0.045500264	0.111222867	Archaea(100);Woesearchaeota(98);Woese_5a(98);Woese_5a_unclassified(98);Woese_5a_unclassified(98);Woese_5a_unclassified(98);	0	0	0.006623223	7.07E-05
K5 / K4	0.010068262	Otu200	0.045500264	0.111222867	Archaea(100);Iainarchaeota(100);Iainarchaeia(100);Iainarchaeales(100);Iainarchaeales_fa(100);Candidatus_Iainarchaeum(100);	0.006509447	0.000325955	0	0
K5 / K4	0.010068262	Otu239	0.045500264	0.111222867	Archaea(100);Archaea_unclassified(95);Archaea_unclassified(95);Archaea_unclassified(95);Archaea_unclassified(95);Archaea_unclassified(95);	0	0	0.006623223	7.07E-05
Y2 / Y3	0.033892306	Otu002	0.042066412	0.105522526	Bacteria(100);Proteobacteria(100);Gammaproteobacteria(100);Burkholderiales(100);Methylophilaceae(100);Methylotenera(85);	0.045897232	0.031685777	0.092458586	0.022096865
Y2 / Y3	0.020808982	Otu049	0.047220904	0.110931648	Bacteria(100);Proteobacteria(100);Gammaproteobacteria(100);Methylococcales(100);Methylomonadaceae(100);uncultured(96);	0.020106881	0.017870372	0	0
Y2 / Y3	0.015784867	Otu013	0.028429536	0.089522794	Bacteria(100);Bacteroidota(100);Bacteroidia(100);Chitinophagales(100);Chitinophagaceae(100);Sediminibacterium(99);	0.012153409	0.009232436	0.032562804	0.009656226
Y2 / Y3	0.013015853	Otu152	0.045500264	0.108917948	Bacteria(100);Proteobacteria(100);Gammaproteobacteria(100);Burkholderiales(100);Methylophilaceae(100);MM1(70);	0.012416122	0.008818879	0	0
Y2 / Y3	0.011436019	Otu121	0.040423979	0.104960508	Bacteria(100);Proteobacteria(100);Gammaproteobacteria(100);Burkholderiales(100);Methylophilaceae(100);Candidatus_Methylopumilus(54);	0	0	0.013158441	0.00880206
Y2 / Y3	0.011434837	Otu023	0.040423979	0.104960508	Bacteria(100);Sva0485(100);Sva0485_cl(100);Sva0485_or(100);Sva0485_fa(100);Sva0485_ge(100);	0.010909822	0.007354632	0	0
Y2 / Y4	0.067247157	Otu003	0.033894854	0.091207969	Bacteria(100);Bacteroidota(100);Bacteroidia(100);Flavobacteriales(100);Flavobacteriaceae(100);Flavobacterium(100);	0.020695508	0.016167976	0.123263208	0.041422828
Y2 / Y4	0.040641112	Otu007	0.032312911	0.090232028	Bacteria(100);Actinobacteriota(100);Actinobacteria(100);Micrococcales(100);Micrococcales(100);Microbacteriaceae(100);Microbacteriaceae_unclassified(53);	0.013409753	0.010594523	0.077460979	0.046326113
Y2 / Y4	0.025685043	Otu011	0.030753561	0.090232028	Bacteria(100);Proteobacteria(100);Gammaproteobacteria(100);Burkholderiales(100);Oxalobacteraceae(96);Oxalobacteraceae_unclassified(82);	0.018392134	0.006449756	0.059445869	0.007569017
Y2 / Y4	0.014505628	Otu013	0.030753561	0.090232028	Bacteria(100);Bacteroidota(100);Bacteroidia(100);Chitinophagales(100);Chitinophagaceae(100);Sediminibacterium(99);	0.012153409	0.009232436	0.035692638	0.005953755
Y2 / Y4	0.014314297	Otu014	0.041586341	0.105522526	Bacteria(100);Desulfobacterota(100);Syntrophia(100);Syntrophales(100);Syntrophales_unclassified(75);Syntrophales_unclassified(75);	0.003302502	0.006605004	0.024934845	0.008169821
Y2 / Y4	0.01247809	Otu101	0.014305878	0.046027609	Bacteria(100);Bacteroidota(100);Kryptonia(100);Kryptoniales(100);BSV26(100);BSV26_ge(100);	0	0	0.017879695	0.002980133
Y3 / Y4	0.074346422	Otu003	0.033894854	0.091207969	Bacteria(100);Bacteroidota(100);Bacteroidia(100);Flavobacteriales(100);Flavobacteriaceae(100);Flavobacterium(100);	0.046831684	0.031451639	0.123263208	0.041422828
Y3 / Y4	0.062402134	Otu007	0.032312911	0.090232028	Bacteria(100);Actinobacteriota(100);Actinobacteria(100);Micrococcales(100);Micrococcales(100);Microbacteriaceae(100);Microbacteriaceae_unclassified(53);	0.013985341	0.009568154	0.077460979	0.046326113
Y3 / Y4	0.052698103	Otu001	0.032312911	0.090232028	Bacteria(100);Proteobacteria(100);Gammaproteobacteria(100);Methylococcales(100);Methylomonadaceae(100);Methylobacter(54);	0.093641889	0.032222135	0.045873091	0.014529852
Y3 / Y4	0.043126071	Otu004	0.049745991	0.115037604	Bacteria(100);Actinobacteriota(100);Actinobacteria(100);Frankiales(100);Sporichthyaceae(100);Sporichthyaceae_unclassified(76);	0.067747142	0.027021739	0.028722452	0.010749229
Y3 / Y4	0.035196712	Otu011	0.030753561	0.090232028	Bacteria(100);Proteobacteria(100);Gammaproteobacteria(100);Burkholderiales(100);Oxalobacteraceae(96);Oxalobacteraceae_unclassified(82);	0.024349588	0.009281917	0.059445869	0.007569017
Y3 / Y4	0.022028366	Otu021	0.045627789	0.108917948	Bacteria(100);Actinobacteriota(100);Acidimicrobiia(100);uncultured(100);uncultured_fa(100);uncultured_ge(100);	0.025575846	0.008337713	0.005170292	0.008955209
Y3 / Y4	0.019625831	Otu017	0.045627789	0.108917948	Bacteria(100);Actinobacteriota(100);Actinobacteria(100);Corynebacteriales(100);Mycobacteriaceae(98);Mycobacterium(98);	0.023749109	0.006355562	0.005634152	0.009758638
Y3 / Y4	0.018362773	Otu101	0.014305878	0.046027609	Bacteria(100);Bacteroidota(100);Kryptonia(100);Kryptoniales(100);BSV26(100);BSV26_ge(100);	0	0	0.017879695	0.002980133
Z1 / Z2	0.022246251	Otu04	0.029387286	0.051904816	Eukaryota(100);Dinoflagellata(99);Dinophyceae(85);Dinophyceae_unclassified(85);Dinophyceae_unclassified(85);Dinophyceae_unclassified(85);	0.050118488	0.005148348	0.061157371	0.008058418
Z1 / Z2	0.014809865	Otu0114	0.006757852	0.024182651	Eukaryota(100);Eukaryota_unclassified(90);Eukaryota_unclassified(90);Eukaryota_unclassified(90);Eukaryota_unclassified(90);Eukaryota_unclassified(90);	0.012184718	0.002789157	0.001204303	0.003186287
Z1 / Z2	0.013718919	Otu15	0.003012305	0.019363291	Eukaryota(100);Ciliophora(99);Intramacronucleata(99);Spirotrichea(99);Choreotrichia(90);Choreotrichia_unclassified(80);	0	0	0.009436846	0.001283473
Z1 / Z2	0.013024303	Otu09	0.027555875	0.049310513	Eukaryota(100);Protalveolata(61);Protalveolata_unclassified(61);Protalveolata_unclassified(61);Protalveolata_unclassified(61);Protalveolata_unclassified(61);	0.029189703	0.004063037	0.018786151	0.005163463
Z1 / Z2	0.012886451	Otu20	0.012739427	0.029295763	Eukaryota(100);Eukaryota_unclassified(100);Eukaryota_unclassified(100);Eukaryota_unclassified(100);Eukaryota_unclassified(100);Eukaryota_unclassified(100);Eukaryota_unclassified(100);	0.009454455	0.006610532	0.017528634	0.002905113
Z1 / Z2	0.011431479	Otu76	0.036682774	0.061590831	Eukaryota(100);Ochrophyta_ph(100);Chrysophyceae(95);Chrysophyceae_unclassified(89);Chrysophyceae_unclassified(89);Chrysophyceae_unclassified(89);	0	0	0.007788622	0.005677821
Z3 / Z4	0.035244326	Otu05	0.005938707	0.023754827	Eukaryota(100);Ochrophyta_ph(98);Chrysophyceae(90);Chrysophyceae_unclassified(83);Chrysophyceae_unclassified(83);Chrysophyceae_unclassified(83);	0.049211057	0.020095164	0.010997287	0.010592518
Z3 / Z4	0.023986153	Otu13	0.025625209	0.046467046	Eukaryota(100);Cryptophyceae_ph(93);Cryptophyceae_cl(93);Cryptomonadales(93);Cryptomonadales_fa(93);Cryptomonas(88);	0.032086295	0.016723521	0.007191032	0.010435788
Z3 / Z4	0.013514532	Otu48	0.011163994	0.027112558	Eukaryota(100);Eukaryota_unclassified(96);Eukaryota_unclassified(96);Eukaryota_unclassified(96);Eukaryota_unclassified(96);Eukaryota_unclassified(96);	0.016024654	0.011704214	0	0

Z3 / Z4	0.012083 88	Otu55	0.0111 63994	0.027112 558	Eukaryota(100);Ochrophyta_ph(82);Chrysophyceae(82);uncultured(63);uncultur ed_fa(63);uncultured_ge(63);	0.0150 44997	0.0135 74431	0	0
Z3 / Z4	0.010662 981	Otu46	0.0366 27535	0.061590 831	Eukaryota(100);Eukaryota_unclassified(93);Eukaryota_unclassified(93);Eukary ota_unclassified(93);Eukaryota_unclassified(93);Eukaryota_unclassified(93);	0.0131 29058	0.0142 67765	0	0
Z3 / Z4	0.010297 716	Otu67	0.0025 33803	0.019363 291	Eukaryota(100);Ochrophyta_ph(78);Chrysophyceae(75);Chrysophyceae_unclas sified(75);Chrysophyceae_unclassified(75);Chrysophyceae_unclassified(75);	0.0121 21108	0.0069 35402	0	0
Z3 / Z4	0.010244 218	Otu53	0.0146 47882	0.029295 763	Eukaryota(100);Eukaryota_unclassified(100);Eukaryota_unclassified(100);Euka ryota_unclassified(100);Eukaryota_unclassified(100);Eukaryota_unclassified(10 0);	0.0149 59971	0.0063 31774	0.0033 2362	0.0054 44083
Z3 / Z4	0.010179 676	Otu70	0.0027 48407	0.019363 291	Eukaryota(100);Eukaryota_unclassified(100);Eukaryota_unclassified(100);Euka ryota_unclassified(100);Eukaryota_unclassified(100);Eukaryota_unclassified(10 0);	0.0123 61642	0.0064 84887	0	0

CHAPITRE 4
DISCUSSION

Au cours des deux derniers chapitres, nous avons exploré l'impact produit par l'introduction de NaCl en eaux douces dans l'épilimnion et au niveau de l'hypolimnion. Tandis que des résultats différents peuvent être expliqués par la différence de méthodologie empruntée pour explorer l'influence de l'halocline sur les communautés microbiennes dulcicoles laurentiennes, la différence d'habitats que composent ces deux milieux partiellement superposés en explique sûrement grandement la disparité. Séparés par le métalimnion, les sédiments et les eaux de surface possèdent des caractéristiques physico-chimiques et biogéochimiques différentes, et bénéficiant tous deux des brassages saisonniers. Si l'épilimnion fournit un apport plus grand en oxygène aux strates inférieures lors de ces évènements (Rowe, 2001), elle obtient en échange de la part de l'hypolimnion un apport en nutriments bénéfique au maintien des communautés planctoniques (Guo *et al.*, 2020). Cependant, l'introduction de NaCl en eaux douces peut avoir une incidence non seulement sur les espèces dulcicole, mais également sur les échanges stratigraphiques, pouvant ainsi transformer un milieu polymictique ou dimictique en milieu monomictique, et ainsi induire des changements anthropique dans la dynamique des assises dulcicoles. Hors de ces événements, les communautés microbiennes composant ces strates se différencient d'autant plus dans leurs rôles que leur composition. L'étude en microcosmes précédemment abordée en a partiellement démontré l'étendue, avec jusqu'à 53 % de la variation rencontrée entre les échantillons ayant pu être expliquée par leur milieu (eau / sédiments). Il n'est donc pas surprenant d'observer une différence de composition des communautés bactériennes et archées entre l'étude réalisée en épilimnion (mésocosmes) et et hypolimnion (microcosmes).

4.1 Sensibilité des différents domaines et relation avec les régulations en place

La décomposition d'organismes eucaryotes, tout comme les fluctuations biogéochimiques et physico-chimiques du milieu ont le potentiel d'influencer la composition des communautés microbiennes, et ces variations sont à même de contribuer aux changements d'espèces dominantes dans les environnements d'eaux douces, tout comme la présence potentielle de « seed bank »

pouvant soutenir partiellement la transition communautaire observée. Par-dessus tout, ce que nos résultats indiquent, tout comme avancé par la littérature (Fournier *et al.*, 2021) est que les eucaryotes seraient plus sensibles que les bactéries dans l'épilimnion lacustre, mais de façon plus importante, il semblerait que les eucaryotes des eaux de surfaces soient plus sensibles à la salinité que les organismes microbiens habitant les sédiments et la couche d'eau les surmontant. Tandis que l'étude produite par Astorg *et al.* (2022) montre que les eucaryotes épilimniales voient une première scission de communauté à partir de ≈0.4 ppt NaCl, les groupements/clusters basés sur la dissimilarité induite par la salinisation et réalisées pour les communautés bactériennes et archées, aussi bien en mésocosmes qu'en microcosmes, montrent qu'une première différentiation significative de ces communautés n'est opérée qu'à partir de 0.93 ppt NaCl. Bien que les bactéries et archées fassent partie intégrante des réseaux trophiques, leur transition vers des communautés acclimatées ou adaptées à la salinité, démontrée dans l'épilimnion comme partiellement similaire à celle opérée au sein des estuaires, montre que l'augmentation de la salinité et de la conductivité s'ensuivant ne serait pas à même de rendre les habitats lacustres dépourvus de diversité ou abondance bactérienne et/ou archée. Ainsi, bien qu'il était attendu que les bactéries soient plus sensibles que les archées au NaCl, nos résultat démontrent que la sensibilité microbienne à la salinité serait dans l'ordre eucaryote > archée > bactéries lorsque sont considérés l'ensemble des niches abordés. Comprendre l'impact global et à long terme d'une telle transition sur l'environnement nécessitera des études plus approfondies, mais considérant qu'il nous est maintenant possible d'établir que les communautés eucaryotes sont affectées par la salinité à des niveaux bien inférieurs au niveau de salinité capable d'induire une transition significative des communautés microbiennes, il nous est au moins possible de nous positionner par rapport aux normes en place. Placé à 640 mg/L^{-1} Cl^- pour une exposition aigüe, et à 120 mg/L^{-1} Cl^- pour une exposition chronique au Canada, le seuil de 185 mg/L^{-1} Cl^- (≈0.4 ppt NaCl) menant à la scission des communautés eucaryotes représente une valeur surpassant les normes d'exposition chronique au Cl^- et donc, le respect des régulations en place permettrait de limiter l'effet réalisé par l'introduction du sel en eaux douces sur les organismes y étant exposé. Toutefois plusieurs pays ont pour normes des valeurs supérieures à celles-ci. Parmi ceux-ci peut-on compter les États-Unis, avec 230 mg/L^{-1} Cl^- comme norme d'exposition chronique, alors que la World Health Organization recommande des concentrations en chlorure variant entre 200 et 300 mg/L^{-1} Cl^- (Schuler *et al.*, 2019), principalement basé sur la potabilité et le goût de l'eau. Dans une optique de protection des

milieux aquatiques, une révision de ces normes s'avère nécessaire, car réduire les seuils de salinité tolérés aurait le potentiel de réduire l'impact du développement humain sur les habitats naturels, particulièrement les habitats vierges. Également, bien que les recommandations canadiennes d'exposition aigüe au Cl^- surpassent la valeur seuil observée pour les eucaryotes, l'apport en eaux de la source en amont du bassin touché par la salinisation constitue l'élément clef dans la dilution des concentrations en ions. Dans le cadre d'un plan d'eau recevant un flux entrant limité (i. e : un bassin versant affecté par une sècheresse), les concentrations en ions qui initialement constituaient une exposition aigüe pour les organismes présents dans l'exutoire peuvent rapidement devenir une exposition chronique à même concentration si un effet de dilution n'est pas réalisé. Si le site d'étude utilisé au cours de cette étude, le lac Croche (Saint-Hippolyte, Québec, Canada), n'est présentement pas en proie à l'impact d'une forte introduction de NaCl, possède un niveau de salinité basale faible et sois sans historique de salinisation, d'autres facteurs tel que la morphologie du lac engendre naturellement une anoxie morphométrique au cours de l'été, dû à son faible volume hypolimnétique (Carignan *et al*., 2003). De ce fait, bien que la seule présence de sel à concentration inférieure au seuil recommandé soit en mesure d'assurer la présence de communautés procaryotes et eucaryotes, la salinisation et densification de l'eau du lac pourrait affecter sa stratification et retarder, voir inhiber, son brassage. Bien que d'autres lacs puissent posséder des charges ioniques naturellement ou anthropiquement plus élevées, abritant des communautés procaryotes y étant adaptées, celles-ci ne sont pas à l'abri d'une augmentation de la salinité. Même les espèces halotolérantes sont pas à l'écart de l'impact de l'isolation stratigraphique et de l'absence d'échange en nutriments et oxygène pouvant s'ensuivre. Si mené à être méromictique, les milieux lacustres pourraient voir se développer des communautés procaryotes entièrement distinctes des communautés indigènes, aussi bien dans l'épilimnion que l'hypolimnion, et de tels changements au niveau des producteurs primaires pourraientt cascader sur l'ensemble des réseaux trophiques. Dès lors, l'alteration des échanges naturels entre les strates emmené par la salinisation pourrait ainsi avoir des répercussions sur l'ensemble de l'écosystème à plus long terme, faisant de la salinisation des eaux douces une problématique plus grande que la somme de ses ions. Ainsi, afin de mieux encadrer la salinisation des eaux douces et son effet réalisé dans l'environnement, il serait nécessaire d'adapter les normes d'exposition chronique et aigüe afin de prendre en considération d'autres facteurs, tels que le type de plan d'eau, sa morphologie, le temps de résidence des eaux, les conditions climatiques et le niveau de salinité naturel du milieu. Car prendre en considération la complexité de la dynamique

de la salinisation des eaux douces constitue une première étape essentielle à son suivi, et permettra peut-être un jour aussi sa remédiation.

4.2 Alternatives au chlorure de sodium comme sel de voiries

Au cours de notre étude, il nous a été possible d'observer des variations au sein des communautés microbiennes suite à l'introduction de NaCl, et ce, à tous les niveaux. Tandis que la présence de sel en milieu peu ou pas affecté par le développement humain peut induire des changements au niveau du pH, la dynamique et le cycle de certains nutriments, la sédimentation de la matière en suspension et la libération d'autres ions, en plus d'affecter les différentes strates des réseaux trophiques (Lin *et al.*, 2017 ; Golubkov *et al.*, 2018), son impact pourrait s'avérer encore plus grand dans les environnements à proximité des développements humains. Pouvant interagir avec certains organophosphorés (e.g., Atrazine, Molinate, Chlorphyrifos) ou éléments trace métalliques (e.g., cadmium, chromium, mercure), l'augmentation de la salinité pourrait avoir des conséquences des plus désastreuses sur la faune, la flore ou le microbiote des milieux où ces composés sont présents. Comme ces contaminants peuvent être emmenés par le développement et l'exploitation anthropique (Kalita et Baruah, 2020), emmenant du même coup le développement de routes et le salage de route s'ensuivant, il est impératif de considérer des solutions alternatives à l'utilisation de sel de route et à son ampleur.

4.2.1 Chlorure de calcium, magnésium et CMA

L'une des contraintes majeures dans l'implantation de solution alternative est, bien évidemment, de trouver la balance entre le coût d'utilisation, la gamme de températures d'utilisation et l'impact environnemental possible. Parmi les options de déglaçage existantes, notons le chlorure de calcium et le chlorure de magnésium, lesquels peuvent permettre la fonte glaciale à des températures de -31°C et -25°C, respectivement (Boehm, 2011). Ces composés, bien que permettant d'atteindre une température de fonte bien inférieure aux -21°C permis par l'utilisation d'une saumure à base de chlorure de sodium (23%) (Abbas *et al.*, 2021), sont plus dispendieux et contiennent deux fois plus de chlorure que le NaCl traditionnellement utilisé. Leur utilisation à grande échelle serait donc décommandée. L'acétate de calcium et magnésium (CMA), pour sa part, possèderait un impact environnemental différent que les composés à base de chlorure et sodium (Boehm, 2011). Bien

qu'efficace, le CMA prendrait non seulement plus de temps que le NaCl à mener à bien le déglaçage routier, il serait également inefficace à des températures inférieures à -5°C, et son introduction dans les cours d'eau aurait pour effet la déplétion de l'oxygène dissout, limitant ainsi ses bienfaits et son utilité.

4.2.2 Sous-produits agriculturels

L'utilisation de produits de l'agriculture comme adjuvant aux saumures montre des résultats positifs. Une alternative explorée est l'utilisation de jus de betterave. Tandis qu'un mélange à ratio 15/85 jus de betterave/NaCl s'est démontré efficace à la fonte glaciale à une température de -6.7°C (Gerbino-Bevins *et al.*, 2012) et permettrait ainsi d'alléger partiellement la charge en sel utilisé dans le déglaçage routier, en plus d'offrir une meilleure adhérence routière et de permettre au sel d'adhérer plus aisément à la route (Boehm, 2011). Bien que cette alternative permettrait de réduire partiellement la charge en sel de route utilisée annuellement, en plus de constituer une option économique, celle-ci contiendrait des concentrations en phosphore supérieures aux recommandations émises par le Pacific Northwest Snowfithers (Robitaille, 2011), pouvant alors mener un débalancement négatif de l'assimilation et reminéralisation de certains nutriments par les bactéries (Phillips *et al.*, 2017) et/ou à l'eutrophisation des plans d'eau en cas de mauvaise gestion (Ortiz-Reyes & Anex, 2018).

D'autres produits dérivés de l'agriculture sont toutefois encore explorés. Parmi ceux-ci peut-on compter des polyols dérivés du maïs, soit le sorbitol, maltitol et mannitol. Permettant également d'augmenter l'adhérence routière et la viscosité du chlorure de sodium utilisé, les polyols permettent de doubler la capacité de fonte moyenne à une température de -20°C (Sajid *et al.*, 2021), en plus d'abaisser le point de congélation des saumures (23% NaCl) à une température aussi basse que -38°C. Leur utilisation augmenterait toutefois le coût d'épandage, et s'est démontré induire une déplétion du taux d'oxygène dissout de 33%, ce qui pourrait être néfaste à long terme sur les communautés bactériennes et archées aérobiques habitant la zone aquatique oxique.

4.2.3 Abrasifs

Comme des études plus approfondies sur l'impact environnemental de composés alternatifs de déglaçage sont nécessaires avant d'en généraliser leur utilisation, d'autres options sont présentement utilisées et permettent d'amoindrir l'utilisation de NaCl sur les routes. L'un des moyens les plus couramment empruntés pour rendre les routes plus sécuritaires est l'épandage d'abrasifs. Composés principalement de sable et de 5% de sel, les abrasifs permettent de réduire efficacement l'utilisation de sel de voiries (Robitaille, 2011), tout en permettant l'adhérence routière. Bien que son utilisation soit favorisée à proximité des environnements peu affectés par le développement, son utilisation à grande échelle est contrainte par son introduction en milieu aquatique, laquelle peut affecter la qualité de l'eau et les sédiments, sans compter l'augmentation potentielle des particules en suspension et sa capacité de blocage des systèmes de drainages routiers. Néanmoins, le défi principal à contourner pour considérer son utilisation sur de plus grands réseaux routiers se trouve à être sa dispersion hors route à plus haute vitesse (60 – 80 km/h ; Klein-Paste & Dalen, 2018) et son effet de roulement à billes une fois la chaussée séchée. Pour contourner la première de ces deux problématiques majeures, l'utilisation de gravier est favorisée par plusieurs municipalités puisqu'une fois trouvé en bordure de route, il peut être partiellement récupéré et réutilisé, rendant cette pratique plus écologique.

Bien évidemment, plusieurs autres solutions permettant le déglaçage existent (voir Environment Canada, 2001 pour une liste plus détaillée). Mais dans son ensemble, les différentes alternatives à l'utilisation de NaCl montrent qu'il est ardu de balancer le coût d'exploitation, la sécurité routière et l'amoindrissement de l'impact écologique de leur utilisation. Il est donc essentiel de mettre en place des structures décisionnelles prenant en considération ces éléments, mais particulièrement la sensibilité des milieux aquicoles à proximité des réseaux routiers. Si nos études en mésocosmes et microcosmes ont permis d'observer qu'une transition significative des communautés microbiennes n'était présente qu'à des niveaux de salinités surpassant 0.93 ppt NaCl, l'étude réalisée par Astorg *et al.* (2022) montre que les communautés eucaryotes planctoniques sont pour leur part beaucoup plus sensibles à la hausse de salinité dans un environnement vierge. Afin de protéger ces environnements, une option proposée est le développement de routes blanches. Conjuguant l'utilisation d'abrasifs à 5% de NaCl, son épandage se limite aux pentes, tournants et autres endroits

stratégiques, et bien qu'il nécessite une adaptation des occupants routiers et des municipalités, elles permettraient de réduire efficacement le coût d'entretien routier et l'impact anthropique de ces procédures dans les municipalités implantant une telle pratique. Ainsi, cette adaptation serait à favoriser pour certains types de routes (e.g., routes d'accès aux ressources), et sa popularisation à l'échelle provinciale, voir nationale, aurait le pouvoir de diminuer l'impact de l'épandage de sel de voirie sur les communautés dulcicoles plus sensibles, et ne démontrant pas la plasticité d'acclimatation et de transition que les communautés bactériennes et archées ont su démontrer au cours de cette étude.

CONCLUSION

La salinisation des eaux douces est sans contredit un problème d'actualité, son importance ayant été soulevée au cours des dernières années (e.g., études sur le syndrome de salinisation des eaux douces). Toutefois, malgré l'avancement des connaissances liées à ce sujet, le nombre d'études relatives à l'effet engendré sur les organismes procaryotes reste limité.

À travers la littérature, nous avons pu voir que l'utilisation de sel dans le cadre du déglaçage routier a pu être liée à la salinisation des plans d'eaux douces aux latitudes supérieures au 39°N (Kaushal *et al*., 2005), et est maintenant reconnue comme contributeur majeur à la hausse d'ions dans les habitats dulcicoles. Ainsi, nous avons exploré au cours du premier chapitre les caractéristiques du NaCl et de ses composantes, mais également l'effet généré par son introduction dans l'environnement sur les bactéries et archées, à travers des problématiques comme le syndrome de salinisation des eaux douces. Afin de comprendre l'influence de salinité sur les communautés procaryotes, une revue des études existantes portant principalement sur les estuaires a pu être faite, avec pour emphase la transition des communautés procaryotes à travers le gradient de salinité.

Nous avons toutefois cherché à déterminer l'effet réalisé par le NaCl sur les communautés procaryotes des habitats dulcicoles, afin d'entrevoir l'effet réalisé sur cette part essentielle des réseaux trophiques. À l'aide du séquençage des gènes ARNr 16S et 18S, et de dPCR, il nous a été possible d'entrevoir l'impact de l'introduction de NaCl en eaux douces sur l'abondance et la diversité bactérienne et archée dans l'épilimnion, l'hypolimnion et les sédiments. Nous avons également investigué la relation entre la transition des communautés microbiennes et les régulations en place, tout en tentant d'entrevoir les contributeurs majeurs d'une telle transition.

Nous avons pu, au cours du second chapitre, investiguer l'effet du NaCl sur les communautés bactériennes de l'épilimnion. D'une part aucun effet sur la diversité n'a pu être observé. Toutefois, une hausse de l'abondance absolue liée à la salinité était présente après trois semaines, et amplifiée après six semaines. Toutefois, d'autres facteurs sont crus être en jeu dans les variations observées, dont la baisse potentielle de prédation emmenée par la baisse de diversité

eucaryote, ainsi que l'implication possible des communautés bactériennes dans les processus de décomposition des organismes eucaryotes affectés par l'introduction de NaCl. De façon intéressante, la transition de dominance des Burkholderiales (anciennement Betaprotéobactéries) et Actinobactéries vers les Bacteroidia et Alphaprotéobactéries à travers le gradient de salinité se trouve à être similaire à la transition bactérienne observée lors d'études réalisées en estuaires (Herlemann *et al.*, 2011 ; Cottrell et Kirchman, 2004 ; Bouvier et del Giorgio, 2002).

Ensuite, à l'aide de microcosmes, nous avons pu explorer l'effet réalisé par le NaCl sur les bactéries et archées de l'hypolimnion et les sédiments. Dans l'hypolimnion, nos résultats montrent que bien que l'introduction de NaCl puisse influencer les communautés procaryotes, d'autres facteurs tels que la co-occurrence d'espèces composeraient des facteurs importants dans l'effet engendré par la salinité sur l'abondance absolue archée. Chez les bactéries, un effet positif sur leur abondance absolue a pu être observé, alors qu'un effet négatif était présent au niveau de leur diversité α. Dans les sédiments, la salinité s'est démontré avoir un effet sur l'abondance absolue archée après trois semaines, et ce, malgré le faible potentiel de pénétration du NaCl dans les sédiments. Un effet synergique de l'abondance et de la composition des communautés bactériennes serait toutefois en jeu dans les variations rencontrées, tout comme la possibilité ade symbiose et/ou endosymbiose (e.g., Methanoregula avec Intramacronucleata et Holosporacées). Néanmoins, un suivi de la biodisponibilité des nutriments dans le cadre d'une expérience en microcosmes serait de mise lors d'études subséquentes afin de mieux comprendre la dynamique en jeu lors d'événements d'introduction de sel en eaux douces, particulièrement au niveau des taxons rares. Mesurer les niveaux d'acétate et de carbone organique particulaires permettrait d'élucider les variations en méthanogènes acétoclastiques (e.g., Methanosarcina et Methanosaeta) et leur relation avec les bactéries fermentatives. Bien qu'aucun effet du NaCl n'ait pu être observé chez les bactéries dans les sédiments, l'interdépendance des espèces et des domaines est toutefois mise de l'avant, et la réalisation d'un réseau d'interaction serait à même de nous éclairer sur la multiplicité des cascades engendrées par l'introduction de sel en eaux douces.

Nous cherchions à déterminer quels organismes démontraient la plus grande sensibilité à l'introduction de NaCl dans l'environnement, et les niveaux de salinités entrainant une première transition significative des communautés microbiennes. Un premier élément surprenant s'est avéré

l'absence de différentiation des communautés bactériennes dans les sédiments, et un seuil de transition à 1.9 ppt NaCl (1900 mg/L^{-1}), démontrant ainsi un niveau de sensibilité inférieur à celui des archées, lesquels se sont différentiées à partir de 0.93 ppt NaCl (930 mg/L^{-1}) aussi bien dans l'hypolimnion que dans les sédiments, alors qu'une sensibilité supérieure des bactéries avait été mise en hypothèses. Dans l'épilimnion, une exposition à 420 mg/L^{-1} Cl^-, représentative d'une salinité de 0.93 ppt NaCl (930 mg/L^{-1}) a mené à une première transition significative des communautés bactériennes. Toutefois, l'étude jointe produite par Astorg *et al.* (2022) sur les communautés eucaryotes montre qu'une scission est opérée dès ≈0.4 ppt NaCl (>185 mg/L^{-1} Cl^-), entrainant la perte des groupes majeurs à l'exception d'*Ochrophyta*, et démontrant ainsi la plus forte sensibilité des eucaryotes à la salinité. En considérant ces résultats, il nous a donc été possible d'établir un ordre de sensibilité d'eucaryotes > archées > bactéries. Heureusement, les concentrations en chlorure entrainées par une telle salinité surpassent les normes canadiennes d'exposition chroniques, étant établies à 120 mg/L^{-1} Cl^-, et ainsi le respect des normes en place devrait assurer la sauvegarde à long terme d'une part importante des communautés eucaryotes et procaryotes autochtones des environnements lacustres affectés par le drainage du sel utilisé pour le déglaçage. Néanmoins, prendre en considération d'autres facteurs, tel que le type de plan d'eau affecté par la salinisation et sa morphologie ne devrait pas être négligé et pourrait contribuer à en améliorer le suivi.

Alors que le respect des recommandations gouvernementales d'introduction de Cl^- en eaux douces permettrait de limiter l'effet engendré sur les organismes aquatiques, il peut être ardu de trouver une balance adéquate entre sécurité routière, économie et protection des milieux naturels. Toutefois, certaines pratiques peuvent être adoptées et permettraient de réduire de façon globale l'utilisation de NaCl sur les routes, et donc les probabilités d'introduction de celui-ci dans les habitats dulcicoles. L'utilisation généralisée d'abrasifs, comportant 5% de NaCl, sur les routes à vitesse modérée (60 – 80 km/h) permettrait d'amoindrir l'épandage, alors que la popularisation des routes blanches dans les arrondissements à proximité de milieux vierges aurait le potentiel de contribuer à leur protection.

L'instauration de telle pratique sur l'ensemble des territoires faisant usage de sel de déglaçage hivernal nécessiterait la participation des municipalités et des populations pour adapter les

pratiques de conduites (e.g., réduction des limites de vitesse). La baisse d'introduction du NaCl dans les habitats dulcicoles emmené par ces changements aurait le potentiel d'amoindrir le développement de problématiques tel que le syndrome de salinisation des eaux douces, tout en promouvant la protection des communautés microbiennes, et de façon plus généralisée, des milieux naturels pour les générations à venir.

ANNEXE A

Tableau Annexe A1. Tableau des analyse de variance à un facteur (ANOVA) réalisé sur les regressions linéaires dans les mésocosmes. *p.values :* 0 '***' 0.001 '**' 0.01 '*' 0.05 '.' 0.1 ' ' 1.

Fig. 2.6.1a lm(formula = Abondbact3 ~ ClT3, data = dataset) Residuals: Min 1Q Median 3Q Max -104588494 -56264000 -9181644 70405461 99975273	Coefficients: Estimate Std. Error t value Pr(>|t|) (Intercept) 79080300 39983148 1.978 0.0885 . ClT3 172599 59376 2.907 0.0228 * Residual standard error: 80090000 on 7 degrees of freedom Multiple R-squared: 0.5469, Adjusted R-squared: 0.4822 F-statistic: 8.45 on 1 and 7 DF, *p*-value: 0.02276
Fig. 2.6.1a lm(formula = AbondbacT6 ~ ClT6, data = dataset) Residuals: Min 1Q Median 3Q Max -264401809 -105662021 -9035403 97978969 400120028	Coefficients: Estimate Std. Error t value Pr(>|t|) (Intercept) 302690887 108774723 2.783 0.0272 * ClT6 32869 189006 0.174 0.8669 Residual standard error: 218500000 on 7 degrees of freedom Multiple R-squared: 0.004302, Adjusted R-squared: -0.1379 F-statistic: 0.03024 on 1 and 7 DF, *p*-value: 0.8669
Fig. 2.6.1b lm(formula = DivbacT3 ~ ClT3, data = dataset) Residuals: Min 1Q Median 3Q Max -0.43291 -0.07807 -0.01782 0.10165 0.29907	Coefficients: Estimate Std. Error t value Pr(>|t|) (Intercept) 3.4367063 0.1173017 29.298 1.39e-08 *** ClT3 -0.0002057 0.0001742 -1.181 0.276 Residual standard error: 0.235 on 7 degrees of freedom Multiple R-squared: 0.1661, Adjusted R-squared: 0.04695 F-statistic: 1.394 on 1 and 7 DF, *p*-value: 0.2763
Fig. 2.6.1b lm(formula = DivbacT6 ~ ClT6, data = dataset) Residuals: Min 1Q Median 3Q Max -0.78111 -0.14973 -0.00306 0.46679 0.57344	Coefficients: Estimate Std. Error t value Pr(>|t|) (Intercept) 2.9503441 0.2630478 11.216 9.99e-06 *** ClT6 0.0005404 0.0004571 1.182 0.276 Residual standard error: 0.5285 on 7 degrees of freedom Multiple R-squared: 0.1664, Adjusted R-squared: 0.04736 F-statistic: 1.398 on 1 and 7 DF, *p*-value: 0.2757
Fig. 2.7.S2a lm(formula = AbarcT3 ~ ClT3, data = dataset) Residuals: Min 1Q Median 3Q Max -299.39 -191.25 14.62 114.32 354.92	Coefficients: Estimate Std. Error t value Pr(>|t|) (Intercept) 538.7115 117.3560 4.590 0.00251 ** ClT3 -0.1172 0.1743 -0.672 0.52290 Residual standard error: 235.1 on 7 degrees of freedom Multiple R-squared: 0.06067, Adjusted R-squared: -0.07352 F-statistic: 0.4521 on 1 and 7 DF, *p*-value: 0.5229

Fig. 2.7.S2a

lm(formula = AbarcT6 ~ ClT6, data = dataset)

Residuals:

Min	1Q	Median	3Q	Max
-1072.8	-793.1	-640.1	-119.7	3542.7

Coefficients:

	Estimate	Std. Error	t value	Pr(>|t|)	
(Intercept)	1498.5399	772.1297	1.941	0.0934	.
ClT6	-0.6122	1.3416	-0.456	0.6620	

Residual standard error: 1551 on 7 degrees of freedom

Multiple R-squared: 0.02888, Adjusted R-squared: -0.1098

F-statistic: 0.2082 on 1 and 7 DF, *p*-value: 0.662

Fig. 2.7.S2b

lm(formula = DivarcT3 ~ ClT3, data = dataset)

Residuals:

Min	1Q	Median	3Q	Max
-0.7855	-0.4831	-0.1575	0.6065	1.0420

Coefficients:

	Estimate	Std. Error	t value	Pr(>|t|)	
(Intercept)	1.316329	0.336018	3.917	0.00577	**
ClT3	0.001140	0.000499	2.285	0.05621	.

Residual standard error: 0.673 on 7 degrees of freedom

Multiple R-squared: 0.4273, Adjusted R-squared: 0.3454

F-statistic: 5.222 on 1 and 7 DF, *p*-value: 0.05621

Fig. 2.7.S2b

lm(formula = DivarcT6 ~ ClT6, data = dataset)

Residuals:

Min	1Q	Median	3Q	Max
-0.88572	-0.12844	0.07903	0.32520	0.48323

Coefficients:

	Estimate	Std. Error	t value	Pr(>|t|)	
(Intercept)	1.6884016	0.2304014	7.328	0.000159	***
ClT6	0.0007764	0.0004003	1.939	0.093626	.

Residual standard error: 0.4629 on 7 degrees of freedom

Multiple R-squared: 0.3495, Adjusted R-squared: 0.2566

F-statistic: 3.761 on 1 and 7 DF, *p*-value: 0.09363

Fig. 2.7.S3a

lm(formula = AbarcT3 ~ DiveucT3, data = dataset)

Residuals:

Min	1Q	Median	3Q	Max
-259.03	-238.63	23.32	58.74	385.62

Coefficients:

	Estimate	Std. Error	t value	Pr(>|t|)	
(Intercept)	467.745	124.101	3.769	0.00699	**
DiveucT3	6.631	51.131	0.130	0.90046	

Residual standard error: 242.2 on 7 degrees of freedom

Multiple R-squared: 0.002397, Adjusted R-squared: -0.1401

F-statistic: 0.01682 on 1 and 7 DF, p-value: 0.9005

Fig. 2.7.S3a

lm(formula = AbarcT6 ~ DiveucT6, data = dataset)

Residuals:

Min	1Q	Median	3Q	Max
-1114.5	-753.3	-595.2	-46.4	3530.2

Coefficients:

	Estimate	Std. Error	t value	Pr(>|t|)
(Intercept)	707.8	1261.6	0.561	0.592
DiveucT6	276.5	601.3	0.460	0.660

Residual standard error: 1551 on 7 degrees of freedom

Multiple R-squared: 0.02932,Adjusted R-squared: -0.1094

F-statistic: 0.2114 on 1 and 7 DF, p-value: 0.6596

Fig. 2.7.S3b

lm(formula = DivarcT3 ~ DiveucT3, data = dataset)

Residuals:

Min	1Q	Median	3Q	Max
-0.7043	-0.6284	-0.1898	0.6078	0.9146

Coefficients:

	Estimate	Std. Error	t value	Pr(>|t|)	
(Intercept)	2.4814	0.3469	7.153	0.000185	***
DiveucT3	-0.3220	0.1429	-2.253	0.058965	.

Residual standard error: 0.6771 on 7 degrees of freedom

Multiple R-squared: 0.4203, Adjusted R-squared: 0.3374

F-statistic: 5.075 on 1 and 7 DF, p-value: 0.05897

Fig. 2.7.S3b

Coefficients:

lm(formula = DivarcT6 ~ DiveucT6, data = dataset)

Residuals:

Min	1Q	Median	3Q	Max
-0.91393	-0.18107	0.01767	0.29898	0.53113

Coefficients:

	Estimate	Std. Error	t value	Pr(>|t|)	
(Intercept)	2.6818	0.3779	7.097	0.000194	***
DiveucT6	-0.3457	0.1801	-1.919	0.096439	.

Residual standard error: 0.4646 on 7 degrees of freedom
Multiple R-squared: 0.3448, Adjusted R-squared: 0.2512
F-statistic: 3.683 on 1 and 7 DF, p-value: 0.09644

Fig. 2.7.S5a
lm(formula = Abondbact3 ~ DiveucT3, data = dataset)

Residuals:

Min	1Q	Median	3Q	Max
-133883800	-42819973	-18401774	37087133	182768994

Coefficients:

	Estimate	Std. Error	t value	Pr(>|t|)	
(Intercept)	221228989	54301728	4.074	0.00472	**
DiveucT3	-30179554	22372797	-1.349	0.21936	

Residual standard error: 1.06e+08 on 7 degrees of freedom
Multiple R-squared: 0.2063, Adjusted R-squared: 0.09293
F-statistic: 1.82 on 1 and 7 DF, *p*-value: 0.2194

Fig. 2.7.S5a
lm(formula = AbondbacT6 ~ DiveucT6, data = dataset)

Residuals:

Min	1Q	Median	3Q	Max
-277807266	-118473916	-26323145	108821081	374999118

Coefficients:

	Estimate	Std. Error	t value	Pr(>|t|)
(Intercept)	297964000	177981359	1.674	0.138
DiveucT6	9810485	84833812	0.116	0.911

Residual standard error: 218800000 on 7 degrees of freedom
Multiple R-squared: 0.001907, Adjusted R-squared: -0.1407
F-statistic: 0.01337 on 1 and 7 DF, *p*-value: 0.9112

Fig. 2.7.S5b
lm(formula = DivbacT3 ~ DiveucT3, data = dataset)

Residuals:

Min	1Q	Median	3Q	Max
-0.43888	-0.10669	0.01339	0.10854	0.32953

Coefficients:

	Estimate	Std. Error	t value	Pr(>|t|)	
(Intercept)	3.23249	0.12182	26.535	2.77e-08	***
DiveucT3	0.05486	0.05019	1.093	0.311	

Residual standard error: 0.2378 on 7 degrees of freedom
Multiple R-squared: 0.1458, Adjusted R-squared: 0.02377
F-statistic: 1.195 on 1 and 7 DF, *p*-value: 0.3106

Fig. 2.7.S5b
lm(formula = DivbacT6 ~ DiveucT6, data = dataset)

Residuals:

Min	1Q	Median	3Q	Max
-0.7534	-0.1576	0.1981	0.2526	0.6212

Coefficients:

	Estimate	Std. Error	t value	Pr(>|t|)	
(Intercept)	3.8231	0.3886	9.839	2.38e-05	***
DiveucT6	-0.3354	0.1852	-1.811	0.113	

Residual standard error: 0.4777 on 7 degrees of freedom
Multiple R-squared: 0.319, Adjusted R-squared: 0.2217
F-statistic: 3.279 on 1 and 7 DF, *p*-value: 0.1131

Tableau Annexe A2. Tableau des analyse de variance à un facteur (ANOVA) réalisé sur les régressions linéaires dans les microcosmes. *p.values* : 0 '***' 0.001 '**' 0.01 '*' 0.05 '.' 0.1 ' ' 1.

Fig. 3.7.S1a
lm(formula = AbarcT3Eau ~ NaCl, data = dataset2)

Coefficients:

	Estimate	Std. Error	t value	Pr(>|t|)
(Intercept)	16185597	16417833	0.986	0.397

Residuals:

1	2	3	4	5
-12139412	-12331703	16154037	30083165	-21766087

NaCl 9118941 9520504 0.958 0.409

Residual standard error: 25420000 on 3 degrees of freedom

Multiple R-squared: 0.2342,Adjusted R-squared: -0.02108

F-statistic: 0.9174 on 1 and 3 DF, *p*-value: 0.4088

Fig. 3.7.S1a

lm(formula = AbarcT6Eau ~ NaCl, data = dataset2)

Residuals:

1	2	3	4	5
8598954	-5303851	-3858541	-1921817	2485255

Coefficients:

	Estimate	Std. Error	t value	Pr(>|t|)
(Intercept)	5716013	4198780	1.361	0.267
NaCl	-1996636	2434822	-0.820	0.472

Residual standard error: 6502000 on 3 degrees of freedom

Multiple R-squared: 0.1831, Adjusted R-squared: -0.08919

F-statistic: 0.6725 on 1 and 3 DF, *p*-value: 0.4723

Fig. 3.7.S1b

lm(formula = AbarcT3Sed ~ NaCl, data = dataset2)

Residuals:

1	2	3	4	5
36728	-131062	78628	78102	-62396

Coefficients:

	Estimate	Std. Error	t value	Pr(>|t|)
(Intercept)	596839	69452	8.594	0.00331 **
NaCl	-99455	40274	-2.469	0.09011 .

Residual standard error: 107600 on 3 degrees of freedom

Multiple R-squared: 0.6703, Adjusted R-squared: 0.5603

F-statistic: 6.098 on 1 and 3 DF, *p*-value: 0.09011

Fig. 3.7.S1b

lm(formula = AbarcT6Sed ~ NaCl, data = dataset2)

Residuals:

1	2	3	4	5
34503	234480	-159678	-350456	241151

Coefficients:

	Estimate	Std. Error	t value	Pr(>|t|)
(Intercept)	131029	191070	0.686	0.542
NaCl	216024	110799	1.950	0.146

Residual standard error: 295900 on 3 degrees of freedom

Multiple R-squared: 0.5589, Adjusted R-squared: 0.4119

F-statistic: 3.801 on 1 and 3 DF, *p*-value: 0.1463

Fig. 3.7.S2a

lm(formula = AbbacT3Eau ~ NaCl, data = dataset2)

Residuals:

1	2	3	4	5
201576023	185747811	-227688177	-525788946	366153290

Coefficients:

	Estimate	Std. Error	t value	Pr(>|t|)
(Intercept)	-20940237	273337513	-0.077	0.944
NaCl	306921412	158505144	1.936	0.148

Residual standard error: 423300000 on 3 degrees of freedom

Multiple R-squared: 0.5555, Adjusted R-squared: 0.4074

F-statistic: 3.749 on 1 and 3 DF, *p*-value: 0.1482

Fig. 3.7.S2a

lm(formula = AbbacT6Eau ~ NaCl, data = dataset2)

Residuals:

1	2	3	4	5
-239744013	579978951	-231256184	-360288368	251309614

Coefficients:

	Estimate	Std. Error	t value	Pr(>|t|)
(Intercept)	262351411	298332679	0.879	0.444
NaCl	247935241	172999541	1.433	0.247

Residual standard error: 4.62e+08 on 3 degrees of freedom

Multiple R-squared: 0.4064, Adjusted R-squared: 0.2085

F-statistic: 2.054 on 1 and 3 DF, *p*-value: 0.2473

Fig. 3.7.S2b

lm(formula = AbbacT3Sed ~ NaCl, data = dataset2)

Residuals:

Coefficients:

	Estimate	Std. Error	t value	Pr(>|t|)
(Intercept)	1668035	1804271	0.924	0.423
NaCl	337739	1046275	0.323	0.768

1 2 3 4 5	Residual standard error: 2794000 on 3 degrees of freedom
-1382288 -1584681 2437917 2805635 -2276583	Multiple R-squared: 0.03357, Adjusted R-squared: -0.2886
	F-statistic: 0.1042 on 1 and 3 DF, *p*-value: 0.768
Fig. 3.7.S2b	Coefficients:
lm(formula = AbbacT6Sed ~ NaCl, data = dataset2)	Estimate Std. Error t value Pr(>|t|)
	(Intercept) 510843 957612 0.533 0.631
Residuals:	NaCl 245757 555308 0.443 0.688
1 2 3 4 5	Residual standard error: 1483000 on 3 degrees of freedom
-331290 -233161 -496396 2207320 -1146472	Multiple R-squared: 0.06129, Adjusted R-squared: -0.2516
	F-statistic: 0.1959 on 1 and 3 DF, *p*-value: 0.688
Fig. 3.7.S3a	Coefficients:
lm(formula = DivarcT3Eau ~ NaCl, data = dataset2)	Estimate Std. Error t value Pr(>|t|)
	(Intercept) 2.93978 0.04246 69.235 6.64e-06 ***
Residuals:	NaCl 0.02552 0.02462 1.036 0.376
1 2 3 4 5	Residual standard error: 0.06575 on 3 degrees of freedom
-0.074558 0.048485 0.005498 0.059374 -0.038800	Multiple R-squared: 0.2637, Adjusted R-squared: 0.01821
	F-statistic: 1.074 on 1 and 3 DF, *p*-value: 0.3762
Fig. 3.7.S3a	Coefficients:
lm(formula = DivarcT6Eau ~ NaCl, data = dataset2)	Estimate Std. Error t value Pr(>|t|)
	(Intercept) 2.93444 0.08358 35.109 5.08e-05 ***
Residuals:	NaCl -0.04982 0.04847 -1.028 0.38
1 2 3 4 5	Residual standard error: 0.1294 on 3 degrees of freedom
0.15294 -0.06791 -0.14323 0.03399 0.02421	Multiple R-squared: 0.2605, Adjusted R-squared: 0.01395
	F-statistic: 1.057 on 1 and 3 DF, *p*-value: 0.3796
Fig. 3.7.S3b	Coefficients:
lm(formula = DivarcT3Sed ~ NaCl, data = dataset2)	Estimate Std. Error t value Pr(>|t|)
	(Intercept) 2.54298 0.11823 21.509 0.00022 ***
Residuals:	NaCl -0.01118 0.06856 -0.163 0.88079
1 2 3 4 5	Residual standard error: 0.1831 on 3 degrees of freedom
0.14112 0.06532 -0.24273 -0.07351 0.10980	Multiple R-squared: 0.008791, Adjusted R-squared: -0.3216
	F-statistic: 0.02661 on 1 and 3 DF, *p*-value: 0.8808
Fig. 3.7.S3b	Coefficients:
lm(formula = DivarcT6Sed ~ NaCl, data = dataset2)	Estimate Std. Error t value Pr(>|t|)
	(Intercept) 2.71908 0.08468 32.111 6.64e-05 ***
Residuals:	NaCl -0.08827 0.04910 -1.798 0.17
1 2 3 4 5	Residual standard error: 0.1311 on 3 degrees of freedom
-0.01765 0.12768 -0.17806 0.05582 0.01220	Multiple R-squared: 0.5186, Adjusted R-squared: 0.3581
	F-statistic: 3.231 on 1 and 3 DF, *p*-value: 0.1701
Fig. 3.7.S4a	Coefficients:
lm(formula = DivbacT3Eau ~ NaCl, data = dataset2)	Estimate Std. Error t value Pr(>|t|)
	(Intercept) 3.73505 0.18943 19.717 0.000285 ***
Residuals:	NaCl -0.03976 0.10985 -0.362 0.741382
1 2 3 4 5	Residual standard error: 0.2933 on 3 degrees of freedom

0.16174 -0.27567 0.28940 -0.25634 0.08086	Multiple R-squared: 0.04184, Adjusted R-squared: -0.2775 F-statistic: 0.131 on 1 and 3 DF, *p*-value: 0.7414
Fig. 3.7.S4a lm(formula = DivbacT6Eau ~ NaCl, data = dataset2) Residuals: 1 2 3 4 5 -0.16664 0.08233 0.07490 0.08443 -0.07503	Coefficients: Estimate Std. Error t value Pr(>|t|) (Intercept) 4.01085 0.08576 46.767 2.15e-05 *** NaCl -0.29131 0.04973 -5.858 0.00992 ** Residual standard error: 0.1328 on 3 degrees of freedom Multiple R-squared: 0.9196, Adjusted R-squared: 0.8928 F-statistic: 34.31 on 1 and 3 DF, *p*-value: 0.00992
Fig. 3.7.S4b lm(formula = DivbacT3Sed ~ NaCl, data = dataset2) Residuals: 1 2 3 4 5 0.13447 -0.09569 0.01098 -0.12423 0.07447	Coefficients: Estimate Std. Error t value Pr(>|t|) (Intercept) 5.83506 0.08197 71.185 6.11e-06 *** NaCl -0.02578 0.04753 -0.542 0.625 Residual standard error: 0.1269 on 3 degrees of freedom Multiple R-squared: 0.08932, Adjusted R-squared: -0.2142 F-statistic: 0.2942 on 1 and 3 DF, *p*-value: 0.6252
Fig. 3.7.S4b lm(formula = DivbacT6Sed ~ NaCl, data = dataset2) Residuals: 1 2 3 4 5 0.20670 -0.12866 -0.02387 -0.16297 0.10881	Coefficients: Estimate Std. Error t value Pr(>|t|) (Intercept) 5.869079 0.116862 50.222 1.74e-05 *** NaCl 0.002414 0.067767 0.036 0.974 Residual standard error: 0.181 on 3 degrees of freedom Multiple R-squared: 0.0004228, Adjusted R-squared: -0.3328 F-statistic: 0.001269 on 1 and 3 DF, *p*-value: 0.9738
Fig. 3.7.S10a lm(formula = DiveucT3Eau ~ NaCl, data = dataset2) Residuals: 1 2 3 4 5 0.08921 -0.26913 0.11441 0.20845 -0.14295	Coefficients: Estimate Std. Error t value Pr(>|t|) (Intercept) 3.53894 0.14790 23.928 0.00016 *** NaCl -0.14346 0.08576 -1.673 0.19297 Residual standard error: 0.229 on 3 degrees of freedom Multiple R-squared: 0.4826, Adjusted R-squared: 0.3101 F-statistic: 2.798 on 1 and 3 DF, *p*-value: 0.193
Fig. 3.7.S10a lm(formula = DiveucT6Eau ~ NaCl, data = dataset2) Residuals: 1 2 3 4 5 0.64714 0.06201 -1.75600 1.32892 -0.28207	Coefficients: Estimate Std. Error t value Pr(>|t|) (Intercept) 2.6842 0.8625 3.112 0.0528 . NaCl -0.5795 0.5002 -1.159 0.3305 Residual standard error: 1.336 on 3 degrees of freedom Multiple R-squared: 0.3091, Adjusted R-squared: 0.07886 F-statistic: 1.342 on 1 and 3 DF, *p*-value: 0.3305
Fig. 3.7.S10b lm(formula = DiveucT3Sed ~ NaCl, data = dataset2) Residuals: 1 2 3 4 5 -0.25010 0.16420 0.21374 -0.14326 0.01542	Coefficients: Estimate Std. Error t value Pr(>|t|) (Intercept) 2.97342 0.14724 20.195 0.000265 *** NaCl -0.03167 0.08538 -0.371 0.735316 Residual standard error: 0.228 on 3 degrees of freedom Multiple R-squared: 0.04386, Adjusted R-squared: -0.2749

F-statistic: 0.1376 on 1 and 3 DF, *p*-value: 0.7353

Fig. 3.7.S10b

lm(formula = DiveucT6Sed ~ NaCl, data = dataset2)

Residuals:

1	2	3	4	5
-0.284612	0.170482	0.244315	-0.126934	-0.003252

Coefficients:

	Estimate	Std. Error	t value	Pr(>|t|)	
(Intercept)	3.04892	0.16074	18.968	0.00032	***
NaCl	-0.12429	0.09321	-1.333	0.27459	

Residual standard error: 0.2489 on 3 degrees of freedom

Multiple R-squared: 0.3721, Adjusted R-squared: 0.1628

F-statistic: 1.778 on 1 and 3 DF, *p*-value: 0.2746

RÉFÉRENCES

Abbas, T., Lavadiya, D. N., & Kiran, R. (2021). Exploring the Use of Polyols, Corn, and Beet Juice for Decreasing the Freezing Point of Brine Solution for Deicing of Pavements. *Sustainability, 13*(11), 57-65. https://doi.org/10.3390/su13115765.

Aladin, N. V., Plotnikov, I. S., Micklin, P., & Ballatore, T. (2009). Aral Sea: Water level, salinity and long-term changes in biological communities of an endangered ecosystem-past, present and future. *Natural Resources and Environmental Issues, 15*(1), 36. https://digitalcommons.usu.edu/nrei/vol15/iss1/36.

Alonso, C., Warnecke, F., Amann, R., & Pernthaler, J. (2007). High local and global diversity of Flavobacteria in marine plankton. *Environmental Microbiology, 9*(5), 1253-1266. https://doi.org/10.1111/j.1462-2920.2007.01244.x.

Anderson, O. R. (2018). Evidence for coupling of the carbon and phosphorus biogeochemical cycles in freshwater microbial communities. *Frontiers in Marine Science, 5*(20). https://doi.org/10.3389/fmars.2018.00020.

Angelidaki, I., Karakashev, D., Batstone, D. J., Plugge, C. M., & Stams, A. J. (2011). Biomethanation and its potential. Dans A. Rosenzweig et S. Ragsdale (Dir.) *Methods in enzymology - Methods in Methane Metabolism, Part A* (Vol. 494. 1ere edition, p.338-339). Academic Press. https://doi.org/10.1016/B978-0-12-385112-3.00016-0.

ATC - Association des Transports du Canada (2003). *Synthèses des meilleures pratiques de gestion des sels de voirie*. Gouvernement du Canada. http://www.tacatc.ca/francais/centredesressources/syntheses.cfm.

Astorg, L., Gagnon, J. C., Lazar, C. S., & Derry, A. M. (2022). Effects of freshwater salinization on a salt-naïve planktonic eukaryote community. *Limnology and Oceanography Letters. 8*(1), 38-47 https://doi.org/10.1002/lol2.10229.

Baldwin, D. S., Rees, G. N., Mitchell, A. M., Watson, G., & Williams, J. (2006). The short-term effects of salinization on anaerobic nutrient cycling and microbial community structure in sediment from a freshwater wetland. *Wetlands*, *26*(2), 455-464. https://doi.org/10.1672/0277-5212(2006)26[455:TSEOSO]2.0.CO;2.

Bandh, Suhaib A. (2019) *Freshwater Microbiology: Perspectives of Bacterial Dynamics in Lake Ecosystems*. Academic Press, 229-230.

Bari, M. L., & Yeasmin, S. (2022). Microbes culture methods. Dans Rezaei, N. (dir.), *Encyclopedia of infection and immunity.(Vol. 4, p.77-98).* Elsevier. https://doi.org/10.1016/B978-0-12-818731-9.09976-6.

Bartolomé, M. C., D'ors, A., & Sánchez-Fortún, S. (2009). Toxic effects induced by salt stress on selected freshwater prokaryotic and eukaryotic microalgal species. *Ecotoxicology, 18*(2), 174-179. https://doi.org/10.1007/s10646-8-269-y.

Bertrand, J. C., Caumette, P., Lebaron, P., Matheron, R., Normand, P., & Ngando, T. S. (2015). *Environmental microbiology: fundamentals and applications*. Springer. Dordrecht, The Netherlands, 3-7.

Bianchi, T. S., & Bauer, J. E. (2011). Particulate organic carbon cycling and transformation. *Treatise on Estuarine and Coastal Science, 5*, 69-117. https://doi.org/69-117.10.1016/B978-0-12-374711-2.00503-9.

Boehm, B. (2011). The Impact of an Alternative Deicing Product on Urban Storm Basin Salinity. *Environmental Science: Water & Life*, 1–31.

Boehrer, B., & Schultze, M. (2008). Stratification of lakes. *Reviews of Geophysics, 46*(2). https://doi.org/10.1029/2006RG000210.

Bouvier, T. C., & del Giorgio, P. A. (2002). Compositional changes in free- living bacterial communities along a salinity gradient in two temperate estuaries. *Limnology and oceanography, 47*(2), 453-470. https://doi.org/10.4319/lo.2002.47.2.0453.

Bridgeman, T. B., Wallace, C. D., Carter, G. S., Carvajal, R., Schiesari, L. C., Aslam, S.,… & Yurista, P. M. (2000). A limnological survey of Third Sister Lake, Michigan with historical comparisons. *Lake and Reservoir Management, 16*(4), 253-267. https://doi.org/10.1080/07438140009354234.

Campbell, B. J., & Kirchman, D. L. (2013). Bacterial diversity, community structure and potential growth rates along an estuarine salinity gradient. *The ISME journal, 7*(1), 210-220. https://doi.org/10.1038/ismej.2012.93.

Cañedo-Argüelles, M., Hawkins, C. P., Kefford, B. J., Schäfer, R. B., Dyack, B. J., Brucet, S., ... & Coring, E. (2016). Saving freshwater from salts. *Science, 351*(6276), 914-916. https://doi.org/10.1126/science.aad3488.

Cañedo-Argüelles, M., Kefford, B. J., Piscart, C., Prat, N., Schäfer, R. B., & Schulz, C. J. (2013). Salinisation of rivers: an urgent ecological issue. *Environmental pollution, 173*, 157-167. https://doi.org/10.1016/j.envpol.2012.10.011.

Capo, E., Debroas, D., Arnaud, F., Guillemot, T., Bichet, V., Millet, L.,… & Domaizon, I. (2016). Long-term dynamics in microbial eukaryotes communities: A palaeolimnological view based on sedimentary DNA. *Molecular Ecology, 25*(23), 5925-5943. https://doi.org/10.1111/mec.13893.

Carignan, R., Crago, C., & Van Leeuwen, H. (2003). *État des lacs de la Municipalité de Saint-Hippolyte et de deux lacs de la Municipalité de Prévost en 2001 et 2002. Montréal,*

Station de biologie des Laurentides, Université de Montréal [Rapport]. https://www.saint-hippolyte.ca/wp-content/uploads/2013/04/tude-Carignan-%C3%89tats-des-lacs-2003.pdf.

Cavin, L. (2017). *Freshwater fishes: 250 million years of evolutionary history*. Elsevier.

CCME- Canadian Council of Ministers of the Environment. (2011). *Scientific Criteria Document for the Development of the Canadian Water Quality Guidelines for the Protection of Aquatic Life: Chloride ion*. Canadian Council of Ministers of the Environment. Gouvernement du Canada. https://ccme.ca/fr/res/2011-chloride-ceqg-scd-1460-en.pdf.

Chapra, S. C., Dove, A., & Warren, G. J. (2012). Long-term trends of Great Lakes major ion chemistry. *Journal of Great Lakes Research, 38*(3), 550-560. https://doi.org/10.1016/j.jglr.2012.06.010.

Chen, S., & He, Q. (2015). Persistence of Methanosaeta populations in anaerobic digestion during process instability. *Journal of Industrial Microbiology and Biotechnology, 42*(8), 1129-1137. https://doi.org/10.1007/s10295-015-1632-7.

Chen, S., Wang, P., Liu, H., Xie, W., Wan, X. S., Kao, S. J., ... & Zhang, C. (2020). Population dynamics of methanogens and methanotrophs along the salinity gradient in Pearl River Estuary: implications for methane metabolism. *Applied microbiology and biotechnology, 104*(3), 1331-1346. https://doi.org/10.1007/s00253-019-10221-6.

Clarke, K. R., & Gorley, R. N. (2006). PRIMER v6. User manual/tutorial. Plymouth routine in mulitvariate ecological research. *Plymouth Marine Laboratory*.

Clarke, K. R., & Green, R. H. (1988). Statistical design and analysis for a 'biological effects' study. *Marine Ecology Progress Series, 46*(1), 213-226. https://www.jstor.org/stable/24827586.

Clarke, K. R., Somerfield, P. J., & Gorley, R. N. (2008). Testing of null hypotheses in exploratory community analyses: similarity profiles and biota-environment linkage. *Journal of experimental marine biology and ecology, 366*(1-2), 56-69. https://doi.org/10.1016/j.jembe.2008.07.009.

Coci, M., Riechmann, D., Bodelier, P. L., Stefani, S., Zwart, G., & Laanbroek, H. J. (2005). Effect of salinity on temporal and spatial dynamics of ammonia-oxidising bacteria from intertidal freshwater sediment. *FEMS Microbiology Ecology, 53*(3), 359-368. https://doi.org/10.1016/j.femsec.2005.01.016.

Coldsnow, K. D., Mattes, B. M., Hintz, W. D. et Relyea, R. A. (2017). Rapid evolution of tolerance to road salt in zooplankton. *Environmental Pollution, 222*, 367-373. https://doi.org/10.1016/j.envpol.2016.12.024.

Cooper, J. I. (2012). . *Viruses and the Environment*. Science & Business Media. Springer.

Corsi, S. R., Graczyk, D. J., Geis, S. W., Booth, N. L., & Richards, K. D. (2010). A fresh look at road salt: aquatic toxicity and water-quality impacts on local, regional, and national scales. *Environmental Science & Technology, 44(*19), 7376-7382. https://doi.org/10.1021/es101333u.

Cottingham, K. L., & Schindler, D. E. (2000). Effects of grazer community structure on phytoplankton response to nutrient pulses. *Ecology, 81*(1), 183-200. https://doi.org/10.1890/0012-9658(2000)081[0183:EOGCSO]2.0.CO;2.

Cottrell, M. T., & Kirchman, D. L. (2004). Single-cell analysis of bacterial growth, cell size, and community structure in the Delaware estuary. *Aquatic Microbial Ecology, 34*(2), 139-149. https://doi.org/10.3354/ame034139.

Daley, M. L., Potter, J. D., & McDowell, W. H. (2009). Salinization of urbanizing New Hampshire streams and groundwater: effects of road salt and hydrologic variability. *Journal of the North American Benthological Society, 28*(4), 929-940. https://doi.org/10.1899/09-052.1.

Dang, C., Morrissey, E. M., Neubauer, S. C., & Franklin, R. B. (2019). Novel microbial community composition and carbon biogeochemistry emerge over time following saltwater intrusion in wetlands. *Global Change Biology, 25*(2), 549-561. https://doi.org/10.1111/gcb.14486.

Decho, A. W. (2000). Microbial biofilms in intertidal systems: an overview. *Continental Shelf Research, 20*(10-11), 1257-1273. https://doi.org/10.1016/S0278-4343(00)00022-4.

DeVilbiss, S. E., Steele, M. K., Brown, B. L., & Badgley, B. D. (2022). Stream bacterial diversity peaks at intermediate freshwater salinity and varies by salt type. *Science of The Total Environment, 840*(156690). https://doi.org/10.1016/j.scitotenv.2022.156690.

Dickman, M. D., & Gochnauer, M. B. (1978). Impact of sodium chloride on the microbiota of a small stream. *Environmental Pollution, 17*(2), 109-126. https://doi.org/10.1016/0013-9327(78)90044-7.

Dugan, H. A., Bartlett, S. L., Burke, S. M., Doubek, J. P., Krivak-Tetley, F. E., Skaff, N. K.,… & Roberts, D. C. (2017). Salting our freshwater lakes. *Proceedings of the National Academy of Sciences, 114*(17), 4453-4458. https://doi.org/10.1073/pnas.1620211114.

Edmonds, J. W., Weston, N. B., Joye, S. B., Mou, X., & Moran, M. A. (2009). Microbial community response to seawater amendment in low-salinity tidal sediments. *Microbial Ecology, 58*(3), 558-568. https://doi.org/10.1007/s00248-009-9556-2.

Elliott, M., & Whitfield, A. K. (2011). Challenging paradigms in estuarine ecology and management. Estuarine, *Coastal and Shelf Science, 94*(4), 306-314. https://doi.org/10.1016/j.ecss.2011.06.016.

Environment Canada, (1994). *Cadmium and its compounds - PSL1*. Government of Canada. https://publications.gc.ca/collections/collection_2018/eccc/En40-215-40-eng.pdf.

Environnement Canada. (2001). *Priority Substances List Assessment Report: Road Salts*. *Canadian Environmental Protection Act, 1999*. Gouvernement du Canada https://www.canada.ca/content/dam/hc-sc/migration/hc-sc/ewh-semt/alt_formats/hecs-sesc/pdf/pubs/contaminants/psl2-lsp2/road_salt_sels_voirie/road_salt_sels_voirie-eng.pdf.

Environnement Canada. (2004). *Code de pratique : Pour la gestion environnementale des sels de voirie. Canada Environmental Protection Ser. Report. Environmental protection series. Report.* Gouvernement du Canada. https://canadagazette.gc.ca/rp-pr/p1/2004/2004-04-03/pdf/g1-13814.pdf.

Etzel, H. W., & Maurer, R. J. (1950). The concentration and mobility of vacancies in sodium chloride. *The Journal of Chemical Physics, 18*(8), 1003-1007. https://doi.org/10.1063/1.1747844.

Fenchel, T., King, G. M., & Blackburn, T. H. (2012). Aquatic sediments. Dans Fenchel, T., King, G. M., & Blackburn, T. H., *2012, Bacterial biogeochemistry (3^{e} edition, p.121-142),* Academic Press.

Filion, M, (2012) *Microbiologie BIOL 3253 —Les bactéries : les protéobactéries*. [Notes de cours et illustrations]. Université de Moncton. http://www8.umoncton.ca/umcmfilion_martin/cours/microbiologie/Chapitre%2022.pdf.

Fischer, P. Q., Sánchez-Andrea, I., Stams, A. J., Villanueva, L., & Sousa, D. Z. (2021). Anaerobic microbial methanol conversion in marine sediments. *Environmental Microbiology, 23*(3), 1348-1362. https://doi.org/10.1111/1462-2920.15434.

Fournier, I. B., Lovejoy, C., & Vincent, W. F. (2021). Changes in the Community Structure of Under-Ice and Open-Water Microbiomes in Urban Lakes Exposed to Road Salts. *Frontiers in Microbiology, 12*(660719). https://doi.org/10.3389/fmicb.2021.660719.

Franceschini, J. (2019). *Exploring the impacts of increased salinity on zooplankton communities in Sturgeon Lake*. [Thèse de bacchalauréat, Université Wilfrid Laurier].

Freitag, T. E., Chang, L., & Prosser, J. I. (2006). Changes in the community structure and activity of betaproteobacterial ammonia-oxidizing sediment bacteria along a freshwater–marine gradient. *Environmental Microbiology, 8*(4), 684-696. https://doi.org/10.1111/j.1462-2920.2005.00947.x.

Gagliano, M. C., Ismail, S. B., Stams, A. J., Plugge, C. M., Temmink, H., & Van Lier, J. B. (2017). Biofilm formation and granule properties in anaerobic digestion at high salinity. *Water research, 121*(6), 61-71. https://doi.org/10.1016/j.watres.2017.05.016.

Gagliano, M. C., Sudmalis, D., Pei, R., Temmink, H., & Plugge, C. M. (2020). Microbial community drivers in anaerobic granulation at high salinity. *Frontiers in Microbiology, 11*(235). https://doi.org/10.3389/fmicb.2020.00235.

Gagnon, J. C., Astorg, L., Derry, A. M., & Lazar, C. S. (2022). Response of Prokaryotic Communities to Freshwater Salinization. *Applied Microbiology, 2*(2), 330-346. https://doi.org/10.3390/applmicrobiol2020025.

Galella, J. G., Kaushal, S., Wood, K. L., & Reed, L. (2019). Freshwater Salinization Syndrome: Anthropogenic effects of road salting over land use and time. In *AGU Fall Meeting Abstracts*. https://ui.adsabs.harvard.edu/abs/2019AGUFM.H43Q2319G.

Gao, J., Hou, L., Zheng, Y., Liu, M., Yin, G., Yu, C., & Gao, D. (2018). Shifts in the Community Dynamics and Activity of Ammonia-Oxidizing Prokaryotes Along the Yangtze Estuarine Salinity Gradient. *Journal of Geophysical Research: Biogeosciences, 123*(11), 3458-3469. https://doi.org/10.1029/2017JG004182.

Gerbino-Bevins, B. M., Tuan, C. Y., & Mattison, M. (2012). Evaluation of ice-melting capacities of deicing chemicals. *Journal of Testing and Evaluation, 40*(6), 952-960. https://doi.org/10.1520/JTE104460.

Goecke, F., Thiel, V., Wiese, J., Labes, A., & Imhoff, J. F. (2013). Algae as an important environment for bacteria–phylogenetic relationships among new bacterial species isolated from algae. *Phycologia, 52*(1), 14-24. https://doi.org/10.2216/12-24.1.

Golubkov, S. M., Shadrin, N. V., Golubkov, M. S., Balushkina, E. V., & Litvinchuk, L. F. (2018). Food chains and their dynamics in ecosystems of shallow lakes with different water salinities. *Russian Journal of Ecology, 49*(5), 442-448. https://doi.org/10.1134/S1067413618050053.

Gonzalez, J. M., Sherr, E. B., & Sherr, B. F. (1990). Size-selective grazing on bacteria by natural assemblages of estuarine flagellates and ciliates. Applied and *Environmental Microbiology, 56*(3), 583-589. https://doi.org/10.1128/aem.56.3.583-589.1990.

Government of Canada (2018) *Code de pratique de la gestion environnementale des sels de voirie*. Gouvernement du Canada. https://www.canada.ca/fr/environnement-changement-climatique/services/polluants/sels-voirie/code-pratique-gestion-environnementale.html.

Groffman, P. M., Gold, A. J., & Howard, G. (1995). Hydrologic tracer effects on soil microbial activities. *Soil Science Society of America Journal, 59*(2), 478-481. https://doi.org/10.2136/sssaj1995.03615995005900020030x.

Guo, C., Zhang, G., Sun, J., Leng, X., Xu, W., Wu, C., ... & Pujari, L. (2020). Seasonal responses of nutrient to hydrology and biology in the southern Yellow Sea. *Continental Shelf Research, 206* (104207). https://doi.org/10.1016/j.csr.2020.104207.

Hammer, Ø. (2020). PAST PAleontological STatistics ver. 4.03—Reference Manual. *Natural History Museum. University of Oslo*. https://www.nhm.uio.no/english/research/infraestructure/past.

He, S., Stevens, S. L., Chan, L. K., Bertilsson, S., del Rio, T. G., Tringe, S. G., ... & McMahon, K. D. (2017). Ecophysiology of freshwater Verrucomicrobia inferred from metagenome-assembled genomes. *mSphere, 2*(5), e00277-17. https://doi.org/10.1128/mSphere.00277-17.

Henriques, I. S., Alves, A., Tacão, M., Almeida, A., Cunha, Â., & Correia, A. (2006). Seasonal and spatial variability of free-living bacterial community composition along an estuarine gradient (Ria de Aveiro, Portugal). *Estuarine, Coastal and Shelf Science, 68*(1-2), 139-148. https://doi.org/10.1016/j.ecss.2006.01.015.

Herlemann, D. P., Labrenz, M., Jürgens, K., Bertilsson, S., Waniek, J. J., & Andersson, A. F. (2011). Transitions in bacterial communities along the 2000 km salinity gradient of the Baltic Sea. *The ISME journal, 5*(10), 1571. https://doi.org/10.1038/ismej.2011.41.

Hintz, W. D., & Relyea, R. A. (2017). Impacts of road deicing salts on the early-life growth and development of a stream salmonid: salt type matters. *Environmental Pollution, 223*(44), 409-415. https://doi.org/10.1016/j.envpol.2017.01.040.

Hintz, W. D., Jones, D. K., & Relyea, R. A. (2019). Evolved tolerance to freshwater salinization in zooplankton: life-history trade-offs, cross-tolerance and reducing cascading effects. *Philosophical Transactions of the Royal Society B, 374*(1764), 20180012. https://doi.org/10.1098/rstb.2018.0012.

Hu, Y., Bai, C., Cai, J., Shao, K., Tang, X., & Gao, G. (2018). Low recovery of bacterial community after an extreme salinization-desalinization cycle. *BMC Microbiology, 18*(1), 1-12. https://doi.org/10.1186/s12866-18-1333-2.

Hugenholtz, P., Chuvochina, M., Oren, A., Parks, D. H., & Soo, R. M. (2021). Prokaryotic taxonomy and nomenclature in the age of big sequence data. *the ISME Journal, 15*(7), 1879-1892. https://doi.org/10.1038/s41396-021-00941-x.

Hunt, M., Herron, E., & Green, L. (2012). Chlorides in fresh water. *The University of Rhode Island Watershed Watch, 4*. http://cels.uri.edu/docslink/ww/water-quality-factsheets/Chlorides.pdf.

Ikeda, T. (1977). The effect of laboratory conditions on the extrapolation of experimental measurements to the ecology of marine zooplankton. IV. Changes in respiration and excretion rates of boreal zooplankton species maintained under fed and starved conditions. *Marine Biology, 41*(3), 241-252. https://doi.org/10.1007/BF00390777.

Ikenaga, M., Guevara, R., Dean, A. L., Pisani, C., & Boyer, J. N. (2010). Changes in community structure of sediment bacteria along the Florida coastal everglades marsh–mangrove–

seagrass salinity gradient. *Microbial Ecology, 59*(2), 284-295. https://doi.org/10.1007/s00248-009-9572-2.

Ishika, T., Bahri, P. A., Laird, D. W., & Moheimani, N. R. (2018). The effect of gradual increase in salinity on the biomass productivity and biochemical composition of several marine, halotolerant, and halophilic microalgae. *Journal of Applied Phycology, 30*(3), 1453-1464. https://doi.org/10.1007/s10811-17-1377-y.

Jackrel, S. L., Gilbert, J. A., & Wootton, J. T. (2019). The origin, succession, and predicted metabolism of bacterial communities associated with leaf decomposition. *MBio, 10*(5). https://doi.org/10.1128/mBio.01703-19.

Jackson, C. R., & Vallaire, S. C. (2009). Effects of salinity and nutrients on microbial assemblages in Louisiana wetland sediments. *Wetlands*, *29*(1), 277-287. https://doi.org/10.1672/08-86.1.

Jarrell, K. F. & Albers, S. J., (2019). Archaellum. Dans Schmidt, T. (Dir.), *Encyclopedia of Microbiology* (4e édition, p. 253-261), Academic Press.

Jezbera, J., Horňák, K., & Šimek, K. (2005). Food selection by bacterivorous protists: insight from the analysis of the food vacuole content by means of fluorescence in situ hybridization. *FEMS Microbiology Ecology, 52*(3), 351-363. https://doi.org/10.1016/j.femsec.2004.12.001.

Jiang, H., Dong, H., Zhang, G., Yu, B., Chapman, L. R., & Fields, M. W. (2006). Microbial diversity in water and sediment of Lake Chaka, an athalassohaline lake in northwestern China. *Applied and Environmental Microbiology, 72*(6), 3832-3845. https://doi.org/10.1128/AEM.02869-05.

John, E. S., & Reysenbach, A. L. (2019). Nanoarchaeota. Dans Schmidt, T. (Dir.) *Encyclopedia of Microbiology* (4e édition, p. 274-279). Academic Press.

Jousset, A. (2012). Ecological and evolutive implications of bacterial defences against predators. *Environmental Microbiology, 14*(8), 1830-1843. https://doi.org/10.1111/j.1462-2920.2011.02627.x.

Judd, J. H. (1970). Lake stratification caused by runoff from street deicing. *Water Research, 4*(8), 521-532. https://doi.org/10.1016/0043-1354(70)90002-3.

Judd, K. E., Adams, H. E., Bosch, N. S., Kostrzewski, J. M., Scott, C. E., Schultz, B. M., ... & Kling, G. W. (2005). A case history: effects of mixing regime on nutrient dynamics and community structure in Third Sister Lake, Michigan during late winter and early spring 2003. *Lake and Reservoir Management, 21*(3), 316-329. https://doi.org/10.1080/07438140509354437.

Kalita, E., & Baruah, J. (2020). Environmental remediation. *In Colloidal Metal Oxide Nanoparticles. Chap. 16.. Elsevier.* 525-576. https://doi.org/10.1016/B978-0-12-813357-6.00014-0.

Kan, J., Evans, S. E., Chen, F., & Suzuki, M. T. (2008). Novel estuarine bacterioplankton in rRNA operon libraries from the Chesapeake Bay. *Aquatic Microbial Ecology, 51*(1), 55-66. https://doi.org/10.3354/ame01177.

Kansman, H. (2015). The effects of salinity on the stratification and nutrient dynamics of inland lakes in southeast Michigan. [Senior Honors Theses and Projects, Eastern Michigan University] https://commons.emich.edu/honors/457.

Karakashev, D., Batstone, D. J., Trably, E., & Angelidaki, I. (2006). Acetate oxidation is the dominant methanogenic pathway from acetate in the absence of Methanosaetaceae. *Applied and Environmental Microbiology, 72*(7), 5138-5141. https://doi.org/10.1128/AEM.00489-06.

Karp, G., Isawa, J., & Marshall, W. (2018). *Biologie cellulaire et moléculaire*. De Boeck Supérieur.

Kartal, B., Koleva, M., Arsov, R., van der Star, W., Jetten, M. S., & Strous, M. (2006). Adaptation of a freshwater anammox population to high salinity wastewater. *Journal of Biotechnology, 126*(4), 546-553. https://doi.org/10.1016/j.jbiotec.2006.05.012.

Kaushal, S.S. (2016). Increased salinization decreases safe drinking water. *Environ. Sci. Technol., 50*(5). 2765-2766. https://doi.org/10.1021/acs.est.6b00679.

Kaushal, S. S., Groffman, P. M., Likens, G. E., Belt, K. T., Stack, W. P., Kelly, V. R., ... & Fisher, G. T. (2005). Increased salinization of fresh water in the northeastern United States. *Proceedings of the National Academy of Sciences, 102*(38), 13517-13520. https://doi.org/10.1073/pnas.0506414102.

Kaushal, S. S., Likens, G. E., Pace, M. L., Utz, R. M., Haq, S., Gorman, J., & Grese, M. (2018). Freshwater salinization syndrome on a continental scale. *Proceedings of the National Academy of Sciences, 115*(4), E574-E583. https://doi.org/10.1073/pnas.17112341.

Kaushal, S., Likens, G., Pace, M., Haq, S., Wood, K. L., Galella, J. G., ... & Raike, A. (2018). Freshwater Salinization Syndrome: Causes, Consequences, and Management. *AGUFM*, H23E-10. https://doi.org/10.1007/s10533-021-00784-w.

Kelly, V. R., Findlay, S. E. G., & Weathers, K. C. (2019). Road salt: the problem, the solution, and how to get there. *Cary Institute of Ecosystem Studies*. https://www.caryinstitute.org/sites/default/files/downloads/report_road_salt.pdf.

Khandeparker, L., Eswaran, R., Gardade, L., Kuchi, N., Mapari, K., Naik, S. D., & Anil, A. C. (2017). Elucidation of the tidal influence on bacterial populations in a monsoon

influenced estuary through simultaneous observations. *Environmental Monitoring and Assessment, 189*(1), 41. https://doi.org/10.1007/s10661-16-5687-3.

Kimbrough, D. R. (2006). Salting roads: The solution for winter driving. *ChemMatters, February 2006*(3), 14-16. https://www.acs.org/content/dam/acsorg/education/resources/highschool/chemmatters/articlesbytopic/solutions/chemmatters-feb2006-salting-roads.pdf.

Kirchman, D. L. (2002). The ecology of Cytophaga–Flavobacteria in aquatic environments. FEMS *Microbiology Ecology, 39*(2), 91-100. https://doi.org/10.1111/j.1574-6941.2002.tb00910.x.

Kirillin, G., & Shatwell, T. (2016). Generalized scaling of seasonal thermal stratification in lakes. *Earth-Science Reviews, 161*(5), 179-190. https://doi.org/10.1016/j.earscirev.2016.08.008.

Klein-Paste, A., & Dalen, R. (2018). The fundamentals of plowing, anti-icing, de-icing and sanding. *Sustainable Winter Road Operations, John Wiley & Sons Ltd.,* 6, 82-100. https://doi.org/10.1002/9781119185161.ch6.

Ladwig, R., Rock, L. A., & Dugan, H. A. (2021). Impact of salinization on lake stratification and spring mixing. *Limnology and Oceanography Letters, 8*(1), 93-102. https://doi.org/10.1002/lol2.10215.

Laskar, F., Das Purkayastha, S., Sen, A., Bhattacharya, M. K., & Misra, B. B. (2018). Diversity of methanogenic archaea in freshwater sediments of lacustrine ecosystems. *Journal of Basic Microbiology, 58*(2), 101-119. https://doi.org/10.1002/jobm.201700341.

Lavergne, C. (2014). *Rôle (structure et fonction) des communautés procaryotes (bactéries et archées) dans le cycle de l'azote d'une vasière littorale du Pertuis Charentais : influence des facteurs biotiques et abiotiques par une approche multi-échelle.* [Dissertation doctorale. Sciences agricoles. Université de La Rochelle]. HAL Id: tel-01334705.

Lazar, C. S., Stoll, W., Lehmann, R., Herrmann, M., Schwab, V. F., Akob, D. M., ... & Küsel, K. (2017). Archaeal diversity and CO2 fixers in carbonate-/siliciclastic-rock groundwater ecosystems. *Archaea, 2017*, 1-13. https://doi.org/10.1155/2017/2136287.

Lemos, L. N., de Carvalho, F. M., Gerber, A., Guimarães, A. P. C., Jonck, C. R., Ciapina, L. P., & de Vasconcelos, A. T. R. (2021). Genome-centric metagenomics reveals insights into the evolution and metabolism of a new free-living group in Rhizobiales. *BMC Microbiology*, *21*(1), 1-10. https://doi.org/10.1186/s12866-21-2354-4.

Lennon, J. T., & Jones, S. E. (2011). Microbial seed banks: the ecological and evolutionary implications of dormancy. *Nature Reviews Microbiology, 9*(2), 119-130. https://doi.org/10.1038/nrmicro2504.

Leoni, C., Volpicella, M., Fosso, B., Manzari, C., Piancone, E., Dileo, M. C., ... & Ceci, L. R. (2020). A differential metabarcoding approach to describe taxonomy profiles of bacteria

and archaea in the saltern of margherita di savoia (Italy). *Microorganisms, 8*(6), 936. https://doi.org/10.3390/microorganisms8060936.

Lerman, A., & Weiler, R. R. (1970). Diffusion and accumulation of chloride and sodium in Lake Ontario sediment. *Earth and Planetary Science Letters, 10*(1), 150-156. https://doi.org/10.1016/0012-821X(70)90077-4.

Li, H., Barber, M., Lu, J., & Goel, R. (2020). Microbial community successions and their dynamic functions during harmful cyanobacterial blooms in a freshwater lake. *Water Research, 185* (116292). https://doi.org/10.1016/j.watres.2020.116292.

Lide, D. R. (1995). *CRC handbook of chemistry and physics: a ready-reference book of chemical and physical data*. CRC press.

Lin, Q., Xu, L., Hou, J., Liu, Z., Jeppesen, E., & Han, B. P. (2017). Responses of trophic structure and zooplankton community to salinity and temperature in Tibetan lakes: Implication for the effect of climate warming. *Water Research, 124*(1), 618-629. https://doi.org/10.1016/j.watres.2017.07.078.

Ling, Z., Thakur, N., El-Dalatony, M. M., Salama, E. S., & Li, X. (2022). Protein biomethanation: insight into the microbial nexus. *Trends in Microbiology, 30*(1), 69-78. https://doi.org/10.1016/j.tim.2021.06.004.

Lionard, M., Muylaert, K., Gansbeke, D. V., & Vyverman, W. (2005). Influence of changes in salinity and light intensity on growth of phytoplankton communities from the Schelde river and estuary (Belgium/The Netherlands). *Hydrobiologia, 540*(1), 105-115. https://doi.org/10.1007/s10750-4-7123-x.

Liu, J., Yang, H., Zhao, M., & Zhang, X. H. (2014). Spatial distribution patterns of benthic microbial communities along the Pearl Estuary, *China. Systematic and Applied Microbiology, 37*(8), 578-589. https://doi.org/10.1016/j.syapm.2014.10.005.

Liu, X., Li, M., Castelle, C. J., Probst, A. J., Zhou, Z., Pan, J., ... & Gu, J. D. (2018). Insights into the ecology, evolution, and metabolism of the widespread Woesearchaeotal lineages. *Microbiome, 6* (1), 1-16. https://doi.org/10.1186/s40168-018-0488-2.

Liu, Y., Priscu, J. C., Xiong, J., Conrad, R., Vick-Majors, T., Chu, H., & Hou, J. (2016). Salinity drives archaeal distribution patterns in high altitude lake sediments on the Tibetan Plateau. *FEMS Microbiology Ecology, 92*(3). https://doi.org/10.1093/femsec/fiw033.

Louca, S., Mazel, F., Doebeli, M., & Parfrey, L. W. (2019). A census-based estimate of Earth's bacterial and archaeal diversity. *PLoS Biology, 17*(2), e3000106. https://doi.org/10.1371/journal.pbio.3000106.

Lv, J., Niu, Y., Yuan, R., & Wang, S. (2021). Different Responses of Bacterial and Archaeal Communities in River Sediments to Water Diversion and Seasonal Changes. *Microorganisms, 9*(4), 782. https://doi.org/10.3390/microorganisms9040782.

Ma, X. C., Li, X. K., Wang, X. W., Liu, G. G., Zuo, J. L., Wang, S. T., & Wang, K. (2020). Impact of salinity on anaerobic microbial community structure in high organic loading purified terephthalic acid wastewater treatment system. *Journal of Hazardous Materials, 383*(121132). https://doi.org/10.1016/j.jhazmat.2019.121132.

Mani, K., Taïb, N., Hugoni, M., Bronner, G., Bragança, J. M., & Debroas, D. (2020). Transient Dynamics of Archaea and Bacteria in Sediments and Brine Across a Salinity Gradient in a Solar Saltern of Goa, India. *Frontiers in Microbiology, 11*(1891). https://doi.org/10.3389/fmicb.2020.01891.

Marquis, R. E. (1968). Salt-induced contraction of bacterial cell walls. *Journal of Bacteriology, 95*(3), 775-781. https://doi.org/10.1128/jb.95.3.775-781.1968.

Marriott, J. F. (2010). *Pharmaceutical compounding and dispensing*. Pharmaceutical Press.

Martin, D. D., Ciulla, R. A., & Roberts, M. F. (1999). Osmoadaptation in archaea. *Appl. Environ. Microbiol., 65* (5), 1815-1825. https://doi.org/10.1128/AEM.65.5.1815-1825.1999.

Mayer, T., Snodgrass, W. J., & Morin, D. (1999). Spatial characterization of the occurrence of road salts and their environmental concentrations as chlorides in Canadian surface waters and benthic sediments. *Water Quality Research Journal, 34*(4), 545-574. https://doi.org/10.2166/wqrj.1999.028.

McMurdie, P. J., & Holmes, S. (2013). phyloseq: an R package for reproducible interactive analysis and graphics of microbiome census data. *PloS One, 8*(4), e61217. https://doi.org/10.1371/journal.pone.0061217.

Micklin, P. (2007). The Aral sea disaster. *Annu. Rev. Earth Planet. Sci., 35*(3), 47-72. https://doi.org/10.1146/annurev.earth.35.031306.140120.

Micklin, P., & Aladin, N. V. (2008). Reclaiming the Aral Sea. *Scientific American, 298* (4), 64-71.

MTQ. Ministère des transports du Québec (2019) *Stratégie québécoise pour une gestion environnementale des sels de voirie*. Direction de l'Environnement et de la Recherche. Gouvernement du Québec. https://www.transports.gouv.qc.ca/fr/gestion-environnementale-sels-voirie/bilan-quebecois/Documents/strategie-gestion-env-sels-voirie-mai-2019.pdf.

Nielsen, D. L., Brock, M. A., Rees, G. N., & Baldwin, D. S. (2003). Effects of increasing salinity on freshwater ecosystems in Australia. *Australian Journal of Botany, 51*(6), 655-665. https://doi.org/10.1071/BT02115.

Nielsen, D. L., Brock, M. A., Vogel, M., & Petrie, R. (2008). From fresh to saline: a comparison of zooplankton and plant communities developing under a gradient of salinity with communities developing under constant salinity levels. *Marine and Freshwater Research, 59*(7), 549-559. https://doi.org/10.1071/MF07166.

Novotny, E. V., Murphy, D., & Stefan, H. G. (2008). Increase of urban lake salinity by road deicing salt. *Science of the Total Environment, 406*(1-2), 131-144. https://doi.org/10.1016/j.scitotenv.2008.07.037.

Novotny, E. V., & Stefan, H. G. (2012). Road salt impact on lake stratification and water quality. *Journal of Hydraulic Engineering, 138*(12), 1069-1080. https://doi.org/10.1061/(ASCE)HY.1943-7900.0000590.

Oksanen, J. (2007). Multivariate analysis of ecological communities in R: vegan tutorial. *Univ. of Oulu, Oulu*.

Oksanen, J., Blanchet, F. G., Kindt, R., Legendre, P., Minchin, P. R., O'hara, R. B.,… & Wagner, H. (2013). Community ecology package. R package version, 2-0.

Oren, A. (1999). Bioenergetic aspects of halophilism. *Microbiology and Molecular Biology Reviews, 63*(2), 334-348. https://doi.org/10.1128/MMBR.63.2.334-348.1999.

Ortiz-Reyes, E., & Anex, R. P. (2018). A life cycle impact assessment method for freshwater eutrophication due to the transport of phosphorus from agricultural production. *Journal of cleaner production, 177*, 474-482. https://doi.org/10.1016/j.jclepro.2017.12.255.

Pan, J., Zhou, Z., Béjà, O., Cai, M., Yang, Y., Liu, Y., ... & Li, M. (2020). Genomic and transcriptomic evidence of light-sensing, porphyrin biosynthesis, Calvin-Benson-Bassham cycle, and urea production in Bathyarchaeota. *Microbiome, 8*(1), 1-12. https://doi.org/10.1186/s40168-020-00820-1.

Paver, S. F., Muratore, D., Newton, R. J., & Coleman, M. L. (2018). Reevaluating the salty divide: phylogenetic specificity of transitions between marine and freshwater systems. *Msystems, 3*(6), e00232-18. https://doi.org/10.1128/mSystems.00232-18.

Pavlostathis, S.G., (2011). Kinetics and Modeling of Anaerobic Treatment and Biotransformation Processes. Dans Moo-young, M. (Dir.), *Comprehensive Biotechnology* (2e Édition, Vol. 6, p.385-397), *Academic Press*. https://doi.org/10.1016/B978-0-08-088504-9.00385-8.

Pedrós-Alió, C., Calderón-Paz, J. I., & Gasol, J. M. (2000). Comparative analysis shows that bacterivory, not viral lysis, controls the abundance of heterotrophic prokaryotic plankton. *FEMS Microbiology Ecology, 32*(2), 157-165. https://doi.org/10.1111/j.1574-6941.2000.tb00709.x.

Pernthaler, J. (2005). Predation on prokaryotes in the water column and its ecological implications. Nature *Reviews Microbiology, 3*(7), 537-546. https://doi.org/10.1038/nrmicro1180.

Pernthaler, J., Posch, T., Simek, K., Vrba, J., Amann, R., & Psenner, R. (1997). Contrasting bacterial strategies to coexist with a flagellate predator in an experimental microbial assemblage. *Applied and Environmental Microbiology, 63*(2), 596-601. https://doi.org/10.1128/aem.63.2.596-601.1997.

Pernthaler, J., Rosenberg, E., DeLong, E., & Lory, S. (2013). Freshwater microbial communities. In: *Rosenberg, Eugene; DeLong, Edward; Lory, Stefan. The Prokaryotes. Berlin Heidelberg: Springer*, 97-112.https://doi.org/10.1007/978-3-642-30123-0_40.

Pester, M., Bittner, N., Deevong, P., Wagner, M., & Loy, A. (2010). A 'rare biosphere'microorganism contributes to sulfate reduction in a peatland. *The ISME Journal, 4*(12), 1591-1602. https://doi.org/10.1038/ismej.2010.75.

Pfaff, J. D. (1993). Method 300.0 Determination of inorganic anions by ion chromatography. US Environmental Protection Agency, Office of Research and Development, *Environmental Monitoring Systems Laboratory, 28*.

Phillips, K. N., Godwin, C. M., & Cotner, J. B. (2017). The effects of nutrient imbalances and temperature on the biomass stoichiometry of freshwater bacteria. *Frontiers in Microbiology, 8*(1692). https://doi.org/10.3389/fmicb.2017.01692.

Pierangeli, G. M. F., Domingues, M. R., Jesus, T. A. D., Coelho, L. H. G., Hanisch, W. S., Pompêo, M. L. M., ... & Benassi, R. F. (2021). Higher abundance of sediment methanogens and methanotrophs do not predict the atmospheric methane and carbon dioxide flows in eutrophic tropical freshwater reservoirs. *Frontiers in Microbiology, 12*(647921). https://doi.org/10.3389/fmicb.2021.647921.

Pinard, D., Sérodes, J. B., & Côté, P. A. (1989). Charactérisation des eaux de fonte d'un depot à neiges usées. *Sci. Tech. Eau, 22*(3), 211-215.

Planas, D., Vanier, C., & Lavirotte, E. (2014). *Le programme de recherche sur les cyanobactéries au lac Bromont*. Université du Québec à Montréal. https://sac.uqam.ca/upload/files/publications/communautaire/Bromont_Cahier_2_Connaissances_et_concepts.pdf.

Poolman, B., & Glaasker, E. (1998). Regulation of compatible solute accumulation in bacteria. *Molecular Microbiology, 29*(2), 397-407. https://doi.org/10.1046/j.1365-2958.1998.00875.x.

Prescott, L. M., Willey, J. M., Sherwood, L. M., & Woolverton, C. J. (2018). *Microbiologie 5th ed.*. De Boeck Supérieur.

Prosser J. I., Nicol G. W. (2016). "Candidatus Nitrosotalea" Dans M.E Trujillo, S. Dedysh, P. DeVos, B. Hedlund, P. Kämpfer, F.A. Rainey, et al. *Bergey's Manual of Systematics of Archaea and Bacteria. eds*. (p.1-7). John Wiley & Sons ltd. https://doi.org/10.1002/9781118960608.gbm01292.

Ren, Z., Qu, X., Peng, W., Yu, Y., & Zhang, M. (2019). Functional properties of bacterial communities in water and sediment of the eutrophic river-lake system of Poyang Lake, China. *PeerJ, 7*, e7318.

Robitaille, J. P. (2011). *Les sels de voirie au Québec : proposition d'une démarche de gestion environnementale spécifique aux zones vulnérables*. [Mémoire de maîtrise, Université de Sherbrooke]. http://hdl.handle.net/11143/7434.

Rocca, J. D., Simonin, M., Bernhardt, E. S., Washburne, A. D., & Wright, J. P. (2020). Rare microbial taxa emerge when communities collide: freshwater and marine microbiome responses to experimental mixing. *Ecology*, *101*(3), e02956. https://doi.org/10.1101/550756.

Roeßler, M., & Müller, V. (2001). Osmoadaptation in bacteria and archaea: common principles and differences. *Environmental Microbiology, 3*(12), 743-754. https://doi.org/10.1046/j.1462-2920.2001.00252.x.

Rowe, G. T. (2001). Seasonal hypoxia in the bottom water off the Mississippi River delta. *Journal of Environmental Quality, 30*(2), 281-290. https://doi.org/10.1016/j.conbuildmat.2020.121527.

Sajid, H. U., Naik, D. L., & Kiran, R. (2021). Improving the ice-melting capacity of traditional deicers. *Construction and Building Materials, 271*(121527). https://doi.org/10.1016/j.conbuildmat.2020.121527.

Santoro, A. E. (2010). Microbial nitrogen cycling at the saltwater–freshwater interface. *Hydrogeology Journal, 18*(1), 187-202. https://doi.org/10.1007/s10040-009-0526-z.

Schloss, P. D., Westcott, S. L., Ryabin, T., Hall, J. R., Hartmann, M., Hollister, E. B., ... & Weber, C. F. (2009). Introducing mothur: open-source, platform-independent, community-supported software for describing and comparing microbial communities. *Applied and Environmental Microbiology, 75*(23), 7537-7541. https://doi.org/10.1128/AEM.01541-9.

Schuler, M. S., Cañedo-Argüelles, M., Hintz, W. D., Dyack, B., Birk, S., & Relyea, R. A. (2019). Regulations are needed to protect freshwater ecosystems from salinization. *Philosophical Transactions of the Royal Society B, 374*(1764), 20180019. https://doi.org/10.1098/rstb.2018.0019.

Shabarova, T., Salcher, M. M., Porcal, P., Znachor, P., Nedoma, J., Grossart, H. P., ... & Šimek, K. (2021). Recovery of freshwater microbial communities after extreme rain events is mediated by cyclic succession. *Nature Microbiology, 6*(4), 479-488. https://doi.org/10.1038/s41564-20-852-1.

Shambaugh, A. (2008). *Environmental Implications of Increasing Chloride Levels in Lake Champlain and Other Basin Waters.* Vermont Agency of Natural Resources, Department of Environmental Conservation. https://winooskinrcd.org/wp-content/uploads/Schambaugh2008-1.pdf.

Shenhav, L.; Thompson, M.; Joseph, T.A.; Briscoe, L.; Furman, O.; Bogumil, D.; Mizrahi, I.; Pe'er, I.; Halperin, E. FEAST: fast 778 expectation-maximization for microbial source tracking. Nat. *Methods 2019*(16) 627–632. https://doi.org/10.1038/s41592-19-431-779 x.

Shurigin, V., Hakobyan, A., Panosyan, H., Egamberdieva, D., Davranov, K., & Birkeland, N. K. (2019). A glimpse of the prokaryotic diversity of the Large Aral Sea reveals novel extremophilic bacterial and archaeal groups. *MicrobiologyOpen*, *8*(9), e00850. https://doi.org/10.1002/mbo3.850.

Smith, K. S., & Ingram-Smith, C. (2007). Methanosaeta, the forgotten methanogen?. *Trends in Microbiology*, *15*(4), 150-155. https://doi.org/10.1016/j.tim.2007.02.002.

Smith, S. (2019). Phylosmith: an R-package for reproducible and efficient microbiome analysis with phyloseq-objects. *Journal of Open Source Software*, *4*(38). https://doi.org/10.21105/joss.01442.

Statistics Canada (2020). *Canada's Core Public Infrastructure Survey: Interactive Dashboard, 2018.* Gouvernement du Canada. https://www150.statcan.gc.ca/n1/pub/71-607-x/71-607-x2021002-eng.htm.

Stefanidou, N., Genitsaris, S., Lopez-Bautista, J., Sommer, U., & Moustaka-Gouni, M. (2018). Unicellular eukaryotic community response to temperature and salinity variation in mesocosm experiments. *Frontiers in Microbiology*, *9*(2444). https://doi.org/10.3389/fmicb.2018.02444.

Steinberger, A. (2020). seq-scripts release v. 1.1. Published online, 10. http://doi.org/10.5281/zenodo.4270481.

Sudmalis, D., Gagliano, M. C., Pei, R., Grolle, K., Plugge, C. M., Rijnaarts, H. H. M., ... & Temmink, H. (2018). Fast anaerobic sludge granulation at elevated salinity. *Water Research*, *128*, 293-303. https://doi.org/10.1016/j.watres.2017.10.038.

Sun, Y., Zhong, S., Deng, B., Jin, Q., Wu, J., Huo, J., ... & Li, Y. (2020). Impact of Phellinus gilvus mycelia on growth, immunity and fecal microbiota in weaned piglets. *PeerJ*, *8*, e9067. https://doi.org/10.7717/peerj.9067.

Takeshita, K., Yamada, T., Kawahara, Y., Narihiro, T., Ito, M., Kamagata, Y., & Shinzato, N. (2019). Tripartite symbiosis of an anaerobic scuticociliate with two hydrogenosome-associated endosymbionts, a Holospora-related alphaproteobacterium and a methanogenic archaeon. *Applied and Environmental Microbiology*, *85*(24), e00854-19. https://doi.org/10.1128/AEM.00854-19.

Tang, B. L., Yang, J., Chen, X. L., Wang, P., Zhao, H. L., Su, H. N., ... & Zhang, Y. Z. (2020). A predator-prey interaction between a marine Pseudoalteromonas sp. and Gram-positive bacteria. *Nature Communications*, *11*(1), 1-14. https://doi.org/10.1038/s41467-19-14-133-x.

Tavsanoglu, U. N., Maleki, R., & Akbulut, N. (2015). Effects of Salinity on the Zooplankton Community Structure in Two Maar Lakes and One Freshwater Lake in the Konya Closed Basin, Turkey. *Ekoloji Dergisi, 24*(94). https://doi.org/10.5053/ekoloji.2015.944.

Team, R. (2020). RStudio: integrated development for R. RStudio, Inc., Boston, MA. *42*(14), 84. http://www.rstudio.com.

Tee, H. S., Waite, D., Lear, G., & Handley, K. M. (2021). Microbial river-to-sea continuum: gradients in benthic and planktonic diversity, osmoregulation and nutrient cycling. *Microbiome, 9*(1), 1-18. https://doi.org/10.1186/s40168-021-01145-3.

Thajudeen, J., Yousuf, J., Veetil, V. P., Varghese, S., Singh, A., & Abdulla, M. H. (2017). Nitrogen fixing bacterial diversity in a tropical estuarine sediments. *World Journal of Microbiology and Biotechnology, 33*(2), 1-11. https://doi.org/10.1007/s11274-017-2205-x.

ThermoFisher Scientific (2014). Target quantification using SYBR® Green I dye on the QuantStudio™ 3D Digital PCR System. Demonstrated protocol. *Applied Biosystem*.

ThermoFisher Scientific, (N.D). QuantStudio™ 3D Digital PCR System user manual, PN MAN0007720. *Applied Biosystem*.

Tian, H., Fotidis, I. A., Kissas, K., & Angelidaki, I. (2018). Effect of different ammonia sources on aceticlastic and hydrogenotrophic methanogens. *Bioresource Technology, 250*(20), 390-397. https://doi.org/10.1016/j.biortech.2017.11.081.

Tockner, K., & Likens, G. E. (2009). *Encyclopedia of inland waters*. Academic Press.

Tomas, C. R. (1980). Olisthodiscus luteus (chrysophyceae). V. Its occurrence, abundance and dynamics in narragansett bay, rhode island 1. *Journal of Phycology, 16*(2), 157-166. https://doi.org/10.1111/j.1529-8817.1980.tb03012.x.

Tong, C., Cadillo-Quiroz, H., Zeng, Z. H., She, C. X., Yang, P., & Huang, J. F. (2017). Changes of community structure and abundance of methanogens in soils along a freshwater–brackish water gradient in subtropical estuarine marshes. *Geoderma,* 299(12), 101-110. https://doi.org/10.1016/j.geoderma.2017.03.026.

Varnam, A., & Evans, M. (2000). Environmental microbiology. *CRC Press*. https://doi.org/10.1201/9781840765489.

Vidal-Durà, A., Burke, I. T., Mortimer, R. J., & Stewart, D. I. (2018). Diversity patterns of benthic bacterial communities along the salinity continuum of the Humber estuary (UK). *Aquatic Microbial Ecology, 81*(3), 277-291. https://doi.org/10.3354/ame01875.

Vreeland, R. H., Anderson, R., & Murray, R. G. (1984). Cell wall and phospholipid composition and their contribution to the salt tolerance of Halomonas elongata. *Journal of Bacteriology, 160*(3), 879-883. https://doi.org/10.1128/jb.160.3.879-883.1984.

Walsh, E. A., Kirkpatrick, J. B., Rutherford, S. D., Smith, D. C., Sogin, M., and D'Hondt, S. (2016). Bacterial diversity and community composition from seasurface to subseafloor. *ISME J. 10*, 979–989. https://doi.org/10.1038/ismej.2015.175.

Wang, B., Liu, N., Yang, M., Wang, L., Liang, X., & Liu, C. Q. (2021). Co-occurrence of planktonic bacteria and archaea affects their biogeographic patterns in China's coastal wetlands. *Environmental Microbiome*, *16*(1), 1-12." https://doi.org/10.1186/s40793-021-00388-9.

Wang, X., Xia, K., Yang, X., & Tang, C. (2019). Growth strategy of microbes on mixed carbon sources. *Nature Communications*, *10*(1), 1-7. https://doi.org/10.1038/s41467-019-09261-3.

Webster, G., O'Sullivan, L. A., Meng, Y., Williams, A. S., Sass, A. M., Watkins, A. J.,… & Weightman, A. J. (2015). Archaeal community diversity and abundance changes along a natural salinity gradient in estuarine sediments. *FEMS Microbiology Ecology*, *91*(2), 1-18. https://doi.org/10.1093/femsec/fiu004.

Wetzel R.G. and G.E. Likens. (2000). *Limnological Analyses 3rd edition*. Springer Press. 97-98.

Weynberg, K. D. (2018). Viruses in Marine Ecosystems. *Environmental Virology and Virus Ecology*, *101*(1). https://doi.org/10.1016/bs.aivir.2018.02.001.

WSS – Water Science School, 2018. Saline Water and Salinity. USGS. https://www.usgs.gov/special-topics/water-science-school/science/saline-water-and-salinity#overview.

Wisnoski, N. I., & Lennon, J. T. (2021). Stabilizing role of seed banks and the maintenance of bacterial diversity. *bioRxiv*, *24*(11) 2328-2338. https://doi.org/10.1111/ele.13853.

WHO - World Health Organization & International Programme on Chemical Safety. (1996). Guidelines for drinking-water quality. Vol. 2, Health criteria and other supporting information, 2nd ed. World Health Organization. https://apps.who.int/iris/handle/10665/38551.

Wyman, D. A., & Koretsky, C. M. (2018). Effects of road salt deicers on an urban groundwater-fed kettle lake. *Applied Geochemistry*, *89*, 265-272. https://doi.org/10.1016/j.apgeochem.2017.12.023.

Yan, N., Marschner, P., Cao, W., Zuo, C., & Qin, W. (2015). Influence of salinity and water content on soil microorganisms. *International Soil and Water Conservation Research*, *3*(4), 316-323. https://doi.org/10.1016/j.iswcr.2015.11.003.

Yancey, P. H. (2005). Organic osmolytes as compatible, metabolic and counteracting cytoprotectants in high osmolarity and other stresses. *Journal of Experimental Biology, 208*(15), 2819-2830. https://doi.org/10.1242/jeb.01730.

Yang, J., Ma, L. A., Jiang, H., Wu, G., & Dong, H. (2016). Salinity shapes microbial diversity and community structure in surface sediments of the Qinghai-Tibetan Lakes. *Scientific Reports, 6*(1), 1-6. https://doi.org/10.1038/srep25078.

Yeo, A. (1998). Molecular biology of salt tolerance in the context of whole-plant physiology. *Journal of Experimental Botany, 49*(323), 915-929. https://doi.org/10.1093/jxb/49.323.915.

Yu, T., Liang, Q., Niu, M., & Wang, F. (2017). High occurrence of Bathyarchaeota (MCG) in the deep-sea sediments of South China Sea quantified using newly designed PCR primers. *Environmental Microbiology Reports, 9*(4), 374-382. https://doi.org/10.1111/1758-2229.12539.

Zhang, L., Gao, G., Tang, X., & Shao, K. (2014). Can the freshwater bacterial communities shift to the "marine-like" taxa?. *Journal of Basic Microbiology, 54*(11), 1264-1272. https://doi.org/10.1002/jobm.201300818.

Zheng, P. F., Wei, Z., Zhou, Y., Li, Q., Qi, Z., Diao, X., & Wang, Y. (2022). Genomic Evidence for the Recycling of Complex Organic Carbon by Novel Thermoplasmatota Clades in Deep-Sea Sediments. *Msystems, 7*(3), e00077. https://doi.org/10.1128/msystems.00077-22.

Zhou, Z., Pan, J., Wang, F., Gu, J. D., & Li, M. (2018). Bathyarchaeota: globally distributed metabolic generalists in anoxic environments. *FEMS Microbiology Reviews, 42*(5), 639-655.

Zhu, C., Zhang, J., Nawaz, M. Z., Mahboob, S., Al-Ghanim, K. A., Khan, I. A., ... & Chen, T. (2019). Seasonal succession and spatial distribution of bacterial community structure in a eutrophic freshwater Lake, Lake Taihu. *Science of the Total Environment, 669*, 29-40. https://doi.org/10.1016/j.scitotenv.2019.03.087.

Zou, D., Liu, H., & Li, M. (2020). Community, Distribution, and Ecological Roles of Estuarine Archaea. *Frontiers in Microbiology, 11*(2060). https://doi.org/10.3389/fmicb.2020.02060.

Zou, D., Pan, J., Liu, Z., Zhang, C., Liu, H., & Li, M. (2020). The distribution of Bathyarchaeota in surface sediments of the Pearl river estuary along salinity gradient. *Frontiers in Microbiology, 11*(285). https://doi.org/10.3389/fmicb.2020.00285.